NIHR | Innovation Observatory

Newcastle University

Horizon Scanning Report: Identification of innovations for PET radiopharmaceuticals in the context of the Welsh Health Service

Authors: Sarah Khan, Sonia Garcia Gonzalez Moral, Anjum Jahan, Andrew Mkwashi

Date: November 2023

Professor Dawn Craig
Director

T: +44(0) 191 208 2259
E: info@io.nihr.ac.uk
www.io.nihr.ac.uk

NIHR | Innovation Observatory

Newcastle University

Contents

List of abbreviations

177-Lu	Lutetium-177
18F	Fluorine-18
64CuCl2	Copper (II)-64 chloride
AI	Artificial Intelligence
ARSAC	Administration of Radioactive Substances Advisory Committee
ATSM	Copper(II)-diacetyl-bis(N(4)-methylthiosemicarbazone)
CT	Computed Tomography
CTR1	Copper Transporter 1
Cu	Copper
DFO	Deferoxamine
EMBASE	Excerpta Medica Database
ESCC	Esophageal Squamous Cell Carcinoma
FDG	Fludeoxyglucose
Ga-68	Gallium-68
ID	Identification
IO	Innovation Observatory
ISTR	International Symposium on Trends in Radiopharmaceuticals
MDT	Metastasis Directed Therapy
MM	Multiple Myeloma
MPI	Myocardial Perfusion Imaging
MR	Magnetic Resonance
MRI	Magnetic Resonance Imaging
MRS	Magnetic Resonance Spectroscopy

N-13	Nitrogen-13
NICE	National Institute of Health and Care Excellence
O-15	Oxygen-15
PD-L1	Programmed Cell Death Ligand 1
PET	Positron Emission Tomography
PSMA	Prostate-Specific Membrane Antigen
RAM	Ramucirumab
Rb-82	Rubidium-82
RIS	Research Information Systems
ROW	Rest of World
Sc	Scandium
SPECT	Single Photon Emission Computed Tomography
TFR1	Transferrin Receptor Protein 1
URL	Uniform Resource Locator
VEGFR2	Vascular Endothelial Growth Factor Receptor 2
VOSViewer	Visualisation of Similarities Viewer
WHSSC	Welsh Health Specialised Services Committee
Zr	Zirconium

Glossary

Positron emission tomography (PET): is a form of nuclear imaging technology which is based on the particular properties of positron emitter radionuclides (also called 'beta plus rays')

Radiopharmaceutical: is a radioactive compound used for diagnosis and therapeutic treatment of human diseases. A radiopharmaceutical consists of two components: a radionuclide and a pharmaceutical

Computed Tomography: sometimes called "computerised tomography" or "computed axial tomography" (CAT), is a non-invasive medical examination or procedure that uses specialized X-ray equipment to produce cross-sectional images of the body.

Radionuclide: is a substance that degrades in a very constant manner over time and emits one or several radiations. This degradation or decay is defined by a constant, the period (or half-life) corresponding to the time it takes for half of the remaining substance to disappear. This half-life is specific for each radionuclide.

Nuclear medicine: is a specialized field of medicine covering all aspects of the use of radioactive substances that are either injected in or ingested by humans with the aim to diagnose or treat a disease.

Introduction

Positron emission tomography (PET) radiopharmaceutical is composed of a biologically active pharmacophore and a positron-emitting radionuclide and belongs to a unique species in the pharmaceutical field.[1] PET is a non-invasive molecular imaging technique used to study and visualise human physiology with the detection of probes labelled by positron-emitting radionuclides.[2] It is permissible in most countries worldwide to manufacture and prepare PET radiopharmaceuticals on a commercial scale within the radiopharmaceutical industries and in hospitals' radio pharmacies. However, PET radiopharmaceuticals are potentially hazardous. The level of risk depends on the types of radiation emitted and the half-lives of radioactive isotopes. In addition, because of the short half-lives of PET radiopharmaceuticals, quality control tests prior to human administration within such a short period are extremely challenging.

The most common radionuclides for PET radiopharmaceuticals include carbon-11 (C-11), oxygen-15 (O-15), nitrogen-13 (N-13), fluorine-18 (F-18), gallium-68 (Ga-68), and rubidium-82 (Ru-82). F-18 (t ½ = 110 min) is the most widely used radionuclide in PET, and it is often referred to as the "radionuclide of choice" because of its favourable physical and nuclear characteristics.[2] It is the first PET radiopharmaceutical to be included in the United States Pharmacopoeia USP 1989.[3] F-18 has a half-life of only two hours. The advantage of this very short half-life means that the radioactivity in the patient completely disappears by the end of the day. However, it is also the most constraining property influencing the manufacturing and application of Fludeoxyglucose (FDG).[4]

In addition to providing multidisciplinary functionality and molecular diagnostic information, PET offers enhanced morphological features when combined with structural imaging modalities such as computed tomography (CT). As a result of improved diagnostic performance and guidance of clinicians toward better patient management, PET/CT has gained wide acceptance among nuclear medicine practitioners and the scientific community.[5] The application of PET in clinical oncology is increasing since many molecular targets relevant to cancer can be labelled with positron emitter radionuclides.[4]

Identifying PET radiopharmaceuticals early in the development process is imperative in order to make informed decisions and to prepare for the future development of these innovations. Traditionally, clinical studies of drugs proceed through phase 1, phase 2 and phase 3 before regulatory approval. However, with PET radiopharmaceuticals an initial step called Phase 0, pre-phase 1, microdosing (Europe) or exploratory Investigational New Drug (IND, USA) is often employed.[1] It is commonly known that phase 1 studies are typically carried out in small numbers, phase 2 studies are proof of principle studies to demonstrate that the proposed treatment targets the intended organ or disease process, and phase 3 studies are the definitive efficacy studies required to receive marketing authorization.

Regulation of PET radiopharmaceuticals

PET radiopharmaceuticals are a special class of medicinal formulations used in nuclear medicine for the diagnosis of specific diseases.[2] The formulations contain both a radionuclide and a drug. From the regulatory standpoint, this distinctive character may pose a challenge due to the need

to balance pharmaceutical good manufacturing practices (GMP) and radiation safety concerns.[6] Furthermore, there are a variety of other regulations, some of which are conflicting, which need to be addressed. Among them are the protection of workers, patients, and the general public from the effects of radiation and the handling of radioactive waste.

In the USA, the Food and Drug Administration (FDA) regulates the production of PET radiopharmaceuticals, while the Nuclear Regulatory Commission (NRC) regulates the use of PET radiopharmaceuticals. Therefore, manufacturers must ensure compliance with both sets of regulations. In consideration of the unique nature of PET radiopharmaceuticals, FDA instituted specific current good manufacturing practice (CGMP) requirements in 21 Code of Federal Regulations (CFR) part 212.[4] These requirements ensure that the PET radiopharmaceuticals are manufactured, processed and stored in a safe and appropriate manner. These requirements also cover the labelling, packaging and distribution of the PET radiopharmaceuticals. According to Section 212.30(a), PET drug production facilities must provide adequate facilities for maintaining orderly handling of materials and equipment, preventing mix-ups, and preventing contamination of equipment or product caused by substances, personnel, or environmental conditions which could adversely affect the quality of the product.[7] In order to verify compliance with relevant regulations, the FDA inspects manufacturers or processors of FDA-regulated products. An FDA inspection typically focuses on activities that end at the point of final release of a PET drug product in order to ensure compliance with CGMPs.[4]

In Europe, radiopharmaceuticals have been recognized as a special group of medicines. Thus, the preparation and clinical use of PET radiopharmaceuticals have been regulated and variously adopted by member states.[6] A manufacturing authorisation may be issued by the EMA or by a national authority. Additionally, "in-house" small-scale preparation of PET radiopharmaceuticals is allowed without the requirements of a marketing authorization based on various national laws of European countries. The first official recognition of the special status of radiopharmaceuticals came in the EU Clinical Trials Regulations of 2014, wherein it was acknowledged the clinical trials of diagnostic radiopharmaceuticals did not fall within the regulations.[1] Clinical trials are therefore conducted according to the guidelines of the International Conference on Harmonisation (ICH) for pharmaceutical trials. Trials must also be conducted according to good clinical practice (GCP), which ensures the quality of data obtained from the trial and ensures the safety of trial subjects.[8] According to Nuclear Medicine Europe (NMEU) "current regulatory guidelines do not take account of the particular needs of radiopharmaceuticals (microdoses, half-lives, production specificities) when it comes to developing new products. These regulatory obstacles delay Europe's market access to radiopharmaceuticals (compared to the US), and result in a) fewer new product approvals in recent years, and b) many EU patients lacking access to new diagnoses, therapies and treatments for unmet medical needs.[9] The United Kingdom is unique in having a "specials" licence under which a wide range of products that are not commercially viable can be manufactured.[4]

In recognition of this background and to best inform future developments in service provision, the all-Wales PET Programme within the Welsh Health Specialised Services Committee (WHSSC) requested that the NIHR Innovation Observatory (IO) conduct horizon scanning

activities to identify PET radiopharmaceuticals that meet stakeholder requirements. Table 1 details the inclusion criteria for this scan.

Table 1. PET Radiopharmaceuticals in scope

Technology name	Technology use or application	Technology stage of development	Regulatory status and region
18F pharmaceuticals Fluorine-18 pharmaceuticals Fluorine-18 radionuclides N-13 pharmaceuticals O-15 pharmaceuticals Ga-68 pharmaceuticals Rb-82 pharmaceuticals Zr radiopharmaceuticals Cu radiopharmaceuticals Sc radiopharmaceuticals	Diagnostic (PET; PET CT)	Preclinical Phase 2 Phase 3	Not approved Unable to find Investigational Medicinal Product Special License

Methods

Horizon Scanning for PET Radiopharmaceutical Technologies

The horizon scanning methodologies developed by the IO to identify the pipeline of PET radiopharmaceutical technologies currently in clinical trials and at pre-clinical stage, involved the identification of information sources that detected 'signals' for PET radiopharmaceuticals technologies. The collection of primary and secondary sources was systematically scanned using a combination of traditional scanning methods (manual), automated and novel AI/machine learning techniques.

Search Strategy and Sources

For the scans performed, specific search strategies were developed, and key terms were combined with Boolean operators (where applicable). This allowed the searches to be more precise and targeted, which in turn yielded higher quality results. By using Boolean operators, it was possible to exclude irrelevant results and find more relevant information. A comprehensive list of keywords was compiled by the IO Team, based on project proposal terminology and further reading on the topic. In addition, members of the IO Team attended

the International Symposium on Trends in Radiopharmaceuticals (ISTR-2023) to gain an insight of the pipeline of emerging radiopharmaceuticals in April 2023 which led to the identification of main manufacturers in this field globally.

Information sources used as part of these scans included:

- Clinicaltrials.gov trial registry, used to identify clinical trials in development largely in the US but also in global trial locations
- ScanMedicine[a],the IO's clinical trial database containing information from 11 registries across the globe (e.g. UK, Europe, USA) was used to identify European trials
- BiomedTracker
- Embase
- MHRA products database
- EMA website

Clinical trials

Following an agreed project proposal in May 2023, we undertook searches for clinical trials in early phase 1[b], phase 2 and 3 in the US clinical trial register and IO's searching system, ScanMedicine. Our searches identified 5,816 clinical trials which were downloaded for screening as an Excel spreadsheet. Through the sifting process we identified 818 relevant clinical trials investigating PET radiopharmaceutical technologies mentioned in figure 1 in development for diagnostic purposes. After consultation with the stakeholders, early phase 1 were excluded. The final analysis included 644 relevant clinical trials. Search strategy for the clinical trial searches is presented in Appendix 2. For the purpose of analysis, clinical trials that were investigating more than one radionuclide or radiopharmaceutical, were split into rows. 644 rows based on unique clinical trial IDs after splitting clinical trials based on radionuclides led to a row count of 663. A further splitting of rows based on radiopharmaceuticals led to a row count of 699.

News

News scanning is a method for capturing recent most up-to-date events in the field of study. News sources also provide an opportunity to gather a variety of perspectives on the topic, which can inform the research findings. A search on BiomedTracker, a third-party database provided by Informa[10], was used to search for soft intelligence in 'radiopharmaceuticals' emerged within the last year (August 2022 – August 2023). The searches were undertaken by one information specialist on 15 August 2023 and results were downloaded into a spreadsheet for further analysis. An overview of recent activity captured through news scanning is presented in the results section of this report.

[a] https://scanmedicine.com/

[b] Early phase 1 clinical trials are conducted before phase 1 clinical trials and after preclinical studies. These were included in the first instance as preclinical studies were in remit.

Preclinical studies

The process of PET radiopharmaceutical development can be broadly divided into two stages: preclinical and clinical. Preclinical stage involves synthesizing the radionuclide, testing its characteristics and stability, and evaluating its safety and dosimetry. The clinical stage involves testing the safety and efficacy of the product in humans. A bibliographic database search strategy for pre-clinical studies in the radioisotopes of interest was devised and run on Embase (Ovid). The search strategy was designed by one information specialist and checked by a second information specialist. No date, language or publication type limits were imposed. The search was designed to identify research activity at pre-clinical stage, broadly defined as the pharmaceutical development stages before entering in human clinical trials. The searches were run on 29th of August 2023 and records were exported into a reference management system (EndNote 20, Clarivate Analytics, US) for de-duplication. The full Embase search strategy is provided in Appendix 1.

A total of 2,620 records were retrieved and used for the final analysis. A total of nine subgroups were generated from searching the name of the radioisotope of interest in the title of the record. The following subgroups were created for records that contained any of the radioisotopes of interest in title (F18=885, 13N=8, 15O=22, 68G=264, 82Rb=4, Cu=91, Sc=9, Zr=51), the remaining 1,289 records that did not contain any of the radioisotopes names in title but may contain relevant key words in the abstracts or key word fields, were grouped together for analysis.

The analysis of pre-clinical research activity was conducted using VOSViewer, an open access software developed by van Eck and Waltman of Leiden University that employs the visualisation of similarities (VOS) method to cluster terms based on their frequency counts and their relationships.[11] As a result, we have produced network visualisations for each of the following subgroups of records: F-18, Ga-68, Cu and Zr. It was determined that it would not be appropriate to perform network analyses for the remaining sub groups (Rb-82, Sc, O-15, N-13) due to the small number of records. A list of records is included in Appendix 4 for reference. The remaining group of records, those without relevant radioisotopes in the title, were analysed using a density map to determine high term aggregation and emerging research areas in the periphery of the map. More information can be found in the results section.

Inclusion criteria

All radiopharmaceutical technologies included in the scan had to meet the criteria outlined in table 1. All technologies were further classified, and a pilot data extraction form was shared with stakeholders for approval in June 2023. This was done to ensure that the data extraction form would accurately capture the different technologies to be evaluated and that stakeholders would have the opportunity to review and provide feedback.

Classification of PET radiopharmaceutical technologies:

- General information: trial title and trial status (as agreed on project proposal)

- Product information: name of intervention, name of radioisotope, and classification of radiopharmaceutical
- Patient group: indication, therapeutic area (NICE categories), cancer or non-cancer, gender and age of participants
- Trial information: trial ID, phase, availability of trial results, outcome measures, N of enrolled participants or target, further study design information, date of start and end of trial, sponsor, funding organisations, location of trial recruitment and URL.
- Regulatory information of technology in trial, later enriched with information gathered from MHRA and EMA websites.

Results

Product Pipeline

Out of the 644 clinical trials identified, a large majority were investigating F-18 (521, ~81%) for diagnostic purposes (Figure 1). This is likely due to the fact that F-18 is the most widely used radionuclide for PET imaging in clinical setting for several indications. This was followed by Ga-68 (84, ~13%) and Zr-89 (32, ~5%), which are used in lower quantities in clinical settings. Cu-64 (21, 3%), O-15 (2, 0.3%), N-13 (2, 0.3%), and Rb-82 (1, 0.1%) are used in much lower quantities, hence the small number of trials involving these radionuclides. No clinical trials were identified for scandium. This may be because there is a lack of scientific evidence that this element has beneficial effects on human health. Additionally, scandium may be too expensive or difficult to obtain for use in clinical trials. Furthermore, our scan identified 151 radiopharmaceuticals being investigated in clinical trials which have been categorised according to radionuclides in figure 2-5.

Figure 1: Volume of ongoing trial activity for radiopharmaceutical technologies Cu-64, F-18, Ga-68, N-13, O-15, Rb-82, Zr-89

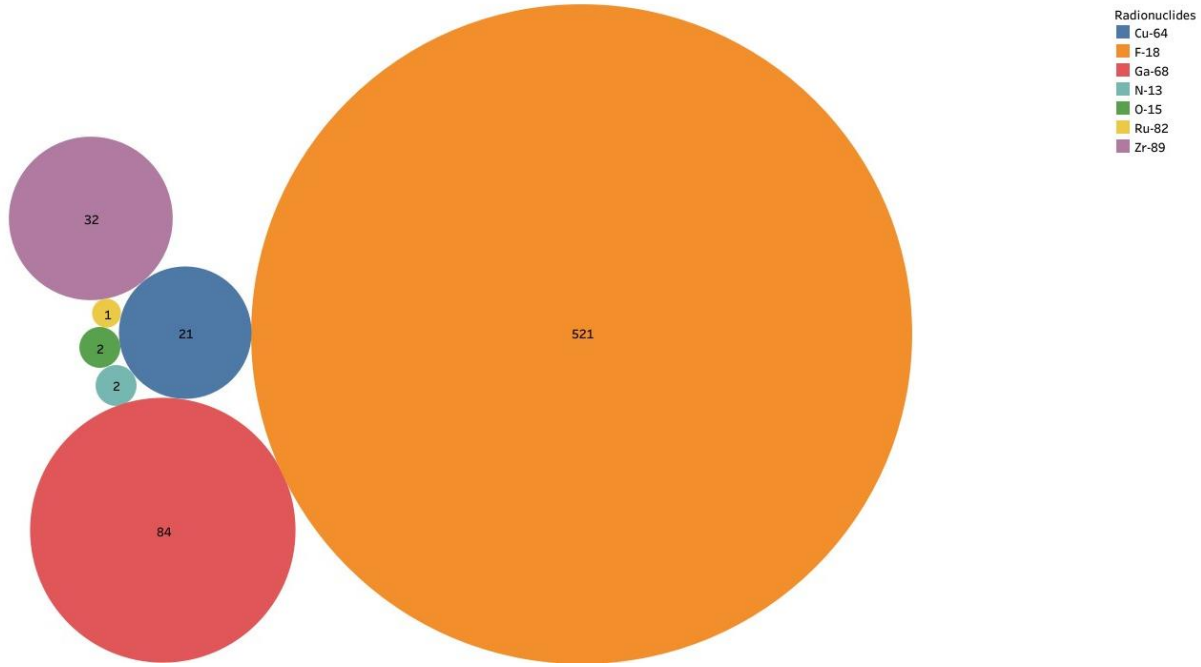

F-18

We found 521 clinical trials investigating radiopharmaceuticals when radiolabelled with F-18. Majority of those clinical trials (359) included radiopharmaceuticals that were not licensed for the indications being investigated. Certain licensed radiopharmaceuticals such as fluorodeoxyglucose (FDG), florbetapir, fluorocholine, piflufolastat, fluoromisonidazole and fluoroestradiol showed a higher volume of clinical trials. Several of the indications that they are being investigated in are already licensed by the MHRA/EMA, however, the scan identified some new indications in clinical development. A few of these new indications include, cervical cancer, stomach cancer and renal cancer for FDG; neurological conditions, diabetes and endocrine disorders and mental health conditions for florbetapir; and thyroid cancer, liver cancer, breast cancer and cardiovascular conditions for fluorocholine. Other new indications for already licensed or unlicensed radiopharmaceuticals radiolabelled with F-18 identified in this scan can be seen in figure 2.

Figure 2: Indications in clinical trials for F-18

Radiopharmaceuticals	Indications	Regulatory authority	Regulatory status: Licensed	Regulatory status: Not licensed
92 probe	Neurological conditions	N/A		1
A-85380	Neurological conditions	N/A		1
AlF-NOTA-neurotensin	Prostate cancer	N/A		1
AlF-NOTA-octreotide	Others	N/A		2
APN-1607	Neurological conditions	N/A		3
Arabinosyl guanine	Mulitple cancers	N/A		1
	Lung cancer	N/A		1
AZD4694	Neurological conditions	N/A		1
C-SNAT4	Lung cancer	N/A		1
CETO	Diabetes and other endocrinal, nutritio..	N/A		1
Choline	Prostate cancer	MHRA	1	
		N/A		4
	N/A	N/A		1
	Mulitple cancers	N/A		1
	Diabetes and other endocrinal, nutritio..	N/A		1
	Cardiovascular conditions	N/A		1
	Brain cancer	N/A		1
	Bladder cancer	N/A		1
CTT1057	Prostate cancer	N/A		2
DCFBC	Prostate cancer	N/A		1
	Metastases	N/A		1
Dota-noc	Respiratory conditions	N/A		1
DPA-714	Neurological conditions	N/A		7
	Infections	N/A		2
	Breast cancer	N/A		2
	Brain cancer	N/A		1
DTBZ	Neurological conditions	N/A		7
Durvalumab	Head and neck cancer	N/A		1
EF5	Head and neck cancer	N/A		1
Fallypride	N/A	N/A		1
FAPI-74	Mulitple cancers	N/A		1
FAZA	Renal cancer	N/A		1
	Others	N/A		1
	Lung cancer	N/A		1
	Brain cancer	N/A		1
FB-IL2	Neurological conditions	N/A		1
FCPHA	Cardiovascular conditions	N/A		1
FDDNP	Neurological conditions	N/A		2
FDHT	Metastases	N/A		5
	Breast cancer	N/A		1
FE-PE2I	Neurological conditions	N/A		1
FHBG	Neurological conditions	N/A		1
Florastamin	Prostate cancer	N/A		1
Florbenazine	Neurological conditions	N/A		3
	N/A	N/A		1
Florbetaben	Neurological conditions	MHRA	10	
	Cardiovascular conditions	N/A		3
Florbetapir	Neurological conditions	MHRA	24	
		N/A		7
	Mental health, behavioural and neurod..	N/A		1
	Diabetes and other endocrinal, nutritio..	N/A		1
Florilglutamic acid	Brain cancer	N/A		1

Number of clinical tri.. 1 – 24

Flortaucipir	Neurological conditions	MHRA	5	
		N/A		11
	N/A	N/A		2
Fluciclatide	Mulitple cancers	N/A		5
	Renal cancer	N/A		1
Fluciclovine	Prostate cancer	EMA	9	
		MHRA	4	
	Metastases	EMA	2	
		N/A		4
	Brain cancer	N/A		4
Fludeoxyglucose	Lung cancer	EMA	1	
Fluorochlorine	Prostate cancer	N/A		1
Fluorocholine	Prostate cancer	EMA	5	
		N/A		8
	Diabetes and other endocrinal, nutritional and metabolic conditions	EMA	1	
		N/A		4
	Thyroid cancer	N/A		2
	Multiple conditions	EMA	1	
		N/A		1
	Metastases	N/A		2
	Liver cancer	N/A		2
	Blood and bone marrow cancers	N/A		2
	Cardiovascular conditions	N/A		1
	Breast cancer	N/A		1
Fluorodeoxyglucose	Mulitple cancers	MHRA	9	
		N/A		3
	Lung cancer	MHRA	11	
	Breast cancer	MHRA	9	
	Blood and bone marrow cancers	MHRA	6	
		N/A		3
	Metastases	MHRA	6	
		N/A		1
	Respiratory conditions	MHRA	2	
		N/A		4
	Neurological conditions	MHRA	4	
		N/A		1
	Head and neck cancer	MHRA	4	
	Cervical cancer	MHRA	1	
		N/A		3
	Others	EMA	1	
		N/A		2
	Cardiovascular conditions	N/A		3
	Skin cancer	MHRA	2	
	Renal cancer	N/A		2
	Musculoskeletal conditions	MHRA	1	
		N/A		1
	Multiple conditions	N/A		2
	Gynaecological conditions	N/A		2
	Bladder cancer	MHRA	1	
		N/A		1
	Thyroid cancer	MHRA	1	
	Stomach cancer	N/A		1
	Penile and testicular cancer	N/A		1
	Ovarian cancer	MHRA	1	
	Digestive tract conditions	N/A		1
	Diabetes and other endocrinal, nutritio..	N/A		1
	Colorectal cancer	MHRA	1	
	Brain cancer	MHRA	1	
	Blood and immune system conditions	N/A		1

Fluorodopa	Diabetes and other endocrinal, nutritional and metabolic conditions	EMA	4	
		N/A		1
	Brain cancer	N/A		5
	Others	EMA	2	
		N/A		2
	Thyroid cancer	EMA	1	
		N/A		1
	Multiple conditions	EMA	2	
	Neurological conditions	EMA	1	
	Mulitple cancers	EMA	1	
	Metastases	N/A		1
Fluoroerytronitroimidazole	Cervical cancer	N/A		1
Fluoroestradiol	Breast cancer	EMA	4	
		MHRA	2	
		N/A		6
	Metastases	EMA	2	
		N/A		4
	Ovarian cancer	N/A		2
	Gynaecological conditions	EMA	1	
Fluoroethoxybenzovesami..	Mental health, behavioural and neurod..	N/A		2
	Neurological conditions	N/A		1
Fluoroethylcholine	Prostate cancer	N/A		4
Fluoroethyltyrosine	Brain cancer	N/A		4
Fluorofuranylnorprogeste..	Gynaecological conditions	N/A		1
	Breast cancer	MHRA	1	
Fluoromisonidazole	Brain cancer	EMA	7	
	Mulitple cancers	EMA	3	
		N/A		1
	Head and neck cancer	EMA	3	
	Prostate cancer	EMA	1	
		N/A		1
	Lung cancer	EMA	2	
	Liver cancer	EMA	1	
		N/A		1
	Neurological conditions	N/A		1
	Cervical cancer	EMA	1	
Fluoropivalate	Mulitple cancers	N/A		1
Fluorothymidine	Breast cancer	N/A		4
	Blood and bone marrow cancers	N/A		3
	Mulitple cancers	N/A		2
	Lung cancer	MHRA	1	
		N/A		1
	Brain cancer	N/A		2
	Renal cancer	N/A		1
	Pancreatic cancer	N/A		1
	Metastases	N/A		1
Fluorthanatrace	Breast cancer	N/A		1
Flurpiridaz	Cardiovascular conditions	N/A		4
Flutematamol	Cardiovascular conditions	N/A		1
Flutemetamol	Neurological conditions	MHRA	13	
		N/A		2
	N/A	N/A		1
	Mental health, behavioural and neurod..	MHRA	1	
	Diabetes and other endocrinal, nutritio..	MHRA	1	
	Cardiovascular conditions	MHRA	1	
	Breast cancer	MHRA	1	
FPCIT	Neurological conditions	N/A		1
FPPRGD2	Mulitple cancers	N/A		1
FPyGal	Mulitple cancers	N/A		1
FSPG	Mulitple cancers	N/A		1
	Lung cancer	MHRA	1	
	Digestive tract conditions	N/A		1
	Cardiovascular conditions	N/A		1

FTC 146	Blood and bone marrow cancers	N/A		1
GEH120714	Neurological conditions	N/A		1
Gozetotide	Prostate cancer	N/A		4
	Thyroid cancer	N/A		2
GP1	Cardiovascular conditions	N/A		1
GTP1	Neurological conditions	N/A		1
HBED-CC PSMA	Thyroid cancer	N/A		1
HX4	Mulitple cancers	N/A		3
	Head and neck cancer	N/A		1
	Cervical cancer	N/A		1
Hydroxyl Dendrimer	Neurological conditions	N/A		1
JK-PSMA-7	Prostate cancer	N/A		1
K5-RGD	Metastases	N/A		1
LBT-999	Neurological conditions	N/A		1
lortaucipir	Neurological conditions	MHRA	1	
MC225	Neurological conditions	N/A		1
Meta-fluorobenzylguanidi..	Others	N/A		4
	Cardiovascular conditions	N/A		1
mFBG	Others	N/A		1
MFES	Breast cancer	N/A		1
MK-6240	Neurological conditions	N/A		3
	Diabetes and other endocrinal, nutritio..	N/A		1
ML-10	Metastases	N/A		2
	Mulitple cancers	N/A		1
NAV4694	Neurological conditions	N/A		3
PBR06	Neurological conditions	N/A		4
PEG folate	Ovarian cancer	N/A		1
	Neurological conditions	N/A		1
PI-2620	Neurological conditions	N/A		6
Piflufolastat	Prostate cancer	EMA	21	
	Metastases	EMA	2	
		N/A		1
	Liver cancer	N/A		2
	Pancreatic cancer	N/A		1
	Mulitple cancers	N/A		1
Piflufolastat, PSMA	Prostate cancer	EMA	1	
PM-PBB3	Neurological conditions	N/A		2
PMPBB3	Neurological conditions	MHRA	1	
		N/A		1
PSMA	Prostate cancer	EMA	1	
		N/A		3
	Mulitple cancers	N/A		2
PSMA-617	Prostate cancer	N/A		1
PSMA-1007	Prostate cancer	N/A		14
	Mulitple cancers	N/A		1
	Metastases	N/A		1
	Brain cancer	N/A		1
RGD-K5	Mulitple cancers	N/A		1
rhPSMA-7.3	Prostate cancer	EMA	5	
		N/A		2
RO6958948	Neurological conditions	N/A		1
Sodium fluoride	Metastases	EMA	5	
	Cardiovascular conditions	N/A		3
	Blood and bone marrow cancers	N/A		2
	Renal cancer	N/A		1
	Neurological conditions	N/A		1
	Multiple conditions	N/A		1
SYN2	Cardiovascular conditions	N/A		1
THK-5351	Neurological conditions	MHRA	1	
		N/A		3
	Mental health, behavioural and neurod..	N/A		1
Thretide	Prostate cancer	N/A		1
Triphenylphosphonium	Cardiovascular conditions	N/A		1
Water	Cardiovascular conditions	N/A		1
XTR003	Cardiovascular conditions	N/A		1
XTR004	Cardiovascular conditions	N/A		1

Ga-68

Ga-68 had the second most number of clinical trials identified as shown in figure 1. Only three radiopharmaceuticals namely dotatate, edotreotide, and gozetotide are licensed by MHRA/EMA for certain conditions shown in figure 3. Our scan includes thirty-three radiopharmaceuticals that are not yet licensed for diagnostic purposes when radiolabelled with Ga-68.

Figure 3: Indications in clinical trials for Ga-68

Radiopharmaceuticals	Indications	Regulatory authority	Regulatory status: Licensed	Regulatory status: Not licensed
ABY-025	Mulitple cancers	N/A		1
	Breast cancer	N/A		1
Deferoxamine	Infections	N/A		1
Dolacga	Liver cancer	N/A		1
Dota-E-(cRGDfK)2	Head and neck cancer	N/A		1
Dota-MGS5	Mulitple cancers	N/A		1
Dota-noc	Multiple conditions	N/A		1
Dota-SSTR	Blood and bone marrow cancers	N/A		1
Dotatate	Thyroid cancer	N/A		2
	Others	N/A		1
	Neurological conditions	N/A		1
	Mulitple cancers	N/A		1
	Metastases	N/A		1
	Head and neck cancer	MHRA	1	
	Diabetes and other endocrinal, nutritio..	N/A		1
	Brain cancer	N/A		1
Edotreotide	Mulitple cancers	MHRA	3	
	Diabetes and other endocrinal, nutritio..	N/A		1
	Cardiovascular conditions	N/A		1
FAP-2286	Mulitple cancers	N/A		1
FAP-CHX	Mulitple cancers	N/A		1
FAP-RGD	Mulitple cancers	N/A		1
FAPI	Digestive tract conditions	N/A		1
FAPI-04	Ovarian cancer	N/A		1
FAPI-46	Pancreatic cancer	N/A		2
	Mulitple cancers	N/A		1
	Lung cancer	N/A		1
Gozetotide	Prostate cancer	EMA	3	
		MHRA	17	
	Metastases	MHRA	2	
	Liver cancer	N/A		2
	Lung cancer	MHRA		1
HBED-CC PSMA	Prostate cancer	N/A		10
MAA	Lung cancer	N/A		1
NeoB	Stomach cancer	N/A		1
	Breast cancer	N/A		1
NeoB, PSMA-R2	Prostate cancer	N/A		1
NODAGA-exendin-4	Diabetes and other endocrinal, nutritio..	N/A		1
NODAGA-RGD	Metastases	N/A		1
NOTA-AE105	Bladder cancer	N/A		1
NOTA-Anti-HER2 VHH1	Mulitple cancers	N/A		1
NY104	Metastases	N/A		1
ODAGA-RGD	Cardiovascular conditions	N/A		1
P16-093	Breast cancer	N/A		1
PEG-αvβ3-Integrin Adhesi..	Breast cancer	N/A		1
Pentixafor	Diabetes and other endocrinal, nutritio..	N/A		1
PSMA	Prostate cancer	N/A		2
PSMA-617	Prostate cancer	N/A		1
RGD	Lung cancer	N/A		1
RM2	Prostate cancer	N/A		1

Number of clinical tri.. 1 17

Cu-64

Out of the 21 clinical trials identified for Cu-64, two trials were found to be investigating already licensed radiopharmaceuticals, copper chloride and dotatate. We identified nine new radiopharmaceuticals that are being investigated for diagnostic purposes when radiolabelled with Cu-64 (figure 4).

Figure 4: Indications in clinical trials for Cu-64

Radiopharmaceuticals	Indications	Regulatory authority	Regulatory status	Number of clincial tri..
ATSM	Colorectal cancer	N/A	Not licensed	1
Copper chloride	Diabetes and other endocrinal, nutritional and metabolic conditions	MHRA	Licensed	1
	Metastases	MHRA	Licensed	1
	Penile and testicular cancer	MHRA	Licensed	1
	Prostate cancer	MHRA	Licensed	3
Dota-trastuzumab	Breast cancer	N/A	Not licensed	1
Dotatate	Cardiovascular conditions	MHRA	Licensed	1
	Metastases	N/A	Not licensed	1
	Others	N/A	Not licensed	1
FBP8	Neurological conditions	N/A	Not licensed	1
Fluorodeoxyglucose	Cardiovascular conditions	MHRA	Licensed	1
Granzyme B	Mulitple cancers	N/A	Not licensed	1
PSMA I&T	Metastases	N/A	Not licensed	1
SAR-bisPSMA	Prostate cancer	N/A	Not licensed	3
SAR-Bombesin	Prostate cancer	N/A	Not licensed	2
SARTATE	Others	N/A	Not licensed	1
Thiosemicarbazone	Cardiovascular conditions	N/A	Not licensed	1

N-13, O-15, Ru-82, Zr-89

We performed a combined analysis of N-13, O-15, Ru-82, and Zr-89, since the number of trials investigating these radionuclides were few (figure 5). N-13 ammonia is being trialled for two new indications and has not been licensed for use by MHRA/EMA. O-15 water is being used to diagnose cardiovascular conditions in two clinical trials and is not licensed for any regulatory authority either.

Zr-89 is being investigated for diagnosis in several clinical trials when conjugated with therapeutic drugs like monoclonal antibodies. Some of these drugs have been marked as licensed for use in figure 5. This is because they are licensed for the indications they are in trials for; however, they are not licensed for diagnosis of those conditions.

Figure 5: Indications in clinical trials for N-13, O-15, Ru-82, Zr-89

N-13, O-15, Ru-82, Zr-89

Radionuclides	Radiopharmaceuticals	Indications	Regulatory authority	Regulatory status: Licensed	Regulatory status: Not licensed
N	Ammonia	Respiratory conditions	N/A		1
		Blood and immune system conditions	N/A		1
O	Water	Cardiovascular conditions	N/A		2
Ru	Chloride	Cardiovascular conditions	MHRA	1	
Zr	Atezolizumab	Blood and bone marrow cancers	N/A		1
	Bevacizumab	Neurological conditions	N/A		1
		Cardiovascular conditions	N/A		1
	Crefmirlimab	Skin cancer	N/A		1
		Mulitple cancers	N/A		1
	Crefmirlimab Berdoxam	Mulitple cancers	N/A		1
	Daratumumab	Blood and bone marrow cancers	MHRA	2	
	Df-IAB2M	Prostate cancer	N/A		2
		Metastases	N/A		1
	Df-IAB22M2C	Mulitple cancers	N/A		1
		Infections	N/A		1
	DFO-Atezolizumab	Renal cancer	N/A		1
	DFO-fianlimab	Metastases	N/A		1
	DFO-huJ591	Prostate cancer	N/A		1
	DFO-MSTP2109A	Prostate cancer	N/A		1
	DFO-Nimotuzumab	Mulitple cancers	N/A		1
	Durvalumab	Lung cancer	MHRA	1	
	GC1008	Brain cancer	N/A		1
	Girentuximab	Renal cancer	N/A		3
		Mulitple cancers	N/A		1
		Breast cancer	N/A		1
	Ipilimumab	Skin cancer	MHRA	1	
	Ofatumumab	Blood and bone marrow cancers	N/A		1
	Panitumumab	Head and neck cancer	N/A		1
	Pembrolizumab	Lung cancer	MHRA	1	
	Rituximab	Blood and bone marrow cancers	N/A		1
	Trastuzumab	Metastases	N/A		2
		Breast cancer	MHRA	1	

Number of clinical tri.. 1 3

Therapeutic Area Landscape

A breakdown of the different therapeutic areas for which these technologies are currently being investigated is presented in figure 6. This figure helps to illustrate which areas are receiving the most attention when it comes to advancing the development of these technologies. It also highlights which areas are lagging in terms of research and development.

Figure 6: Therapeutic areas being investigated for each radiopharmaceutical in clinical trials according to NICE categorisation

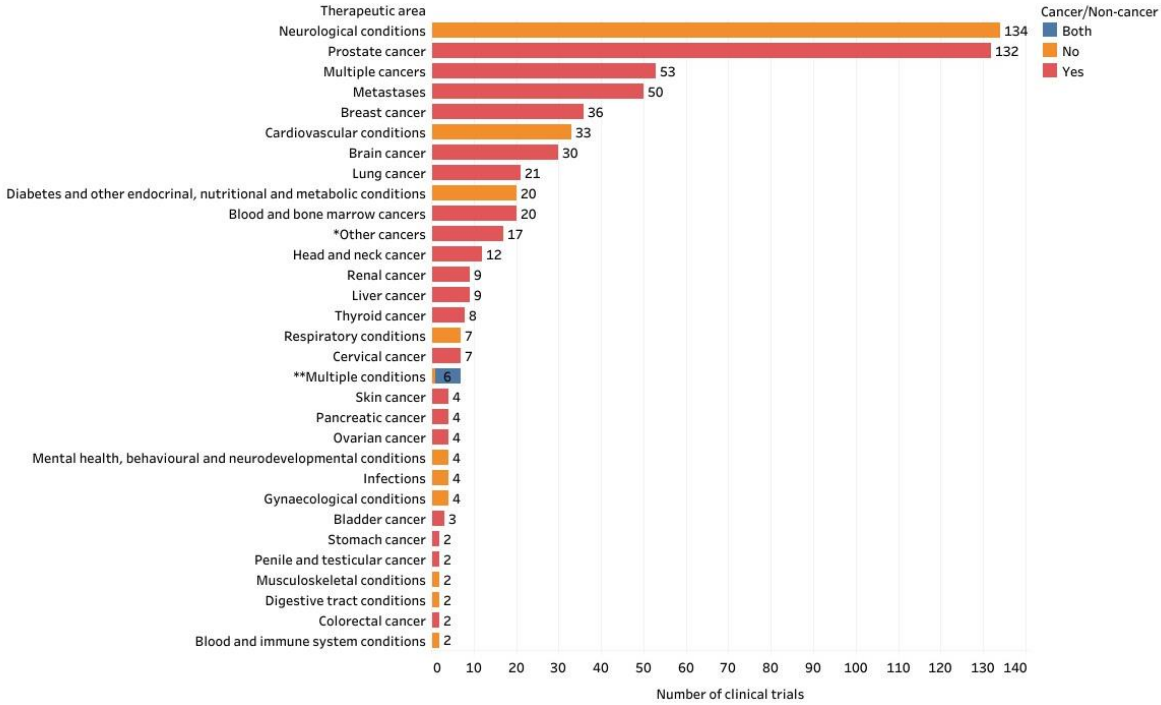

*Others: Trials that included cancer indications that did not appear to fall under the NICE cancer categories; e.g. neuroendocrine tumours, neuroblastomas.
**Multiple conditions: Trials which included both cancer and non-cancer indications or non-cancer indications in more than one organ

Majority of the 644 clinical trials (~66%), were investigating cancer indications while 33% were investigating non-cancer indications (Figure 7). Seven (<1%) clinical trials were found to be investigating both cancer and non-cancer indications.

Figure 7: Number of clinical trials investigating cancer and non-cancer indications

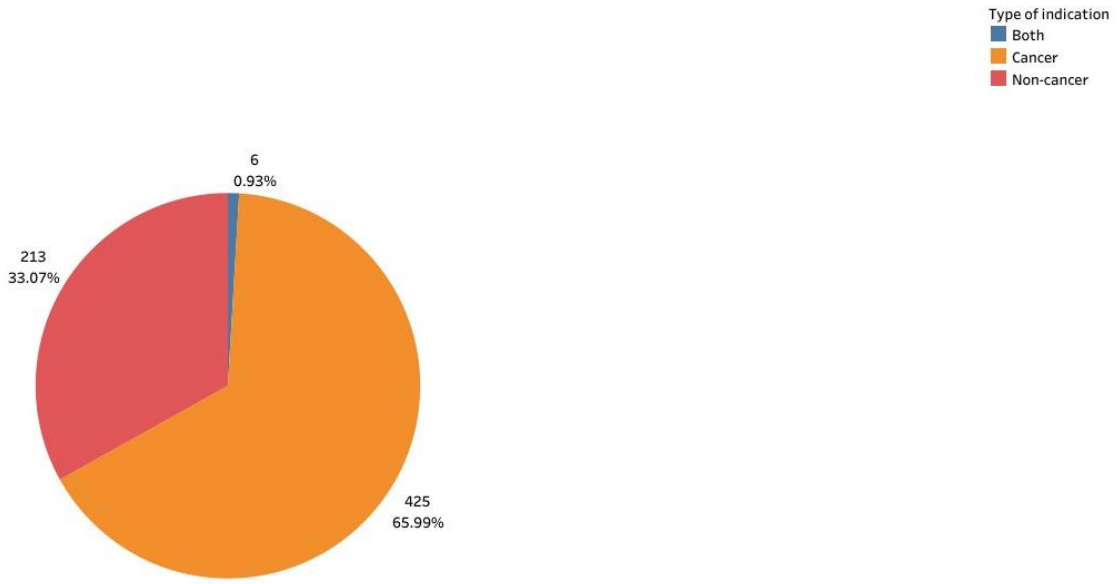

A majority of the clinical trials investigating cancer indications were for prostate cancer, metastatic conditions, multiple cancers, breast cancer, and brain tumours as shown in figure 8. This figure also shows that cancer indications are being diagnosed using radiopharmaceuticals radiolabelled with F-18, Ga-68, Cu-64, and Zr-89. F-18 is the most used radionuclide followed by Ga-68 with very few clinical trials for Cu-64 and Zr-89.

Figure 8: Number of clinical trials for radiopharmaceuticals being investigated for diagnosing cancer indications

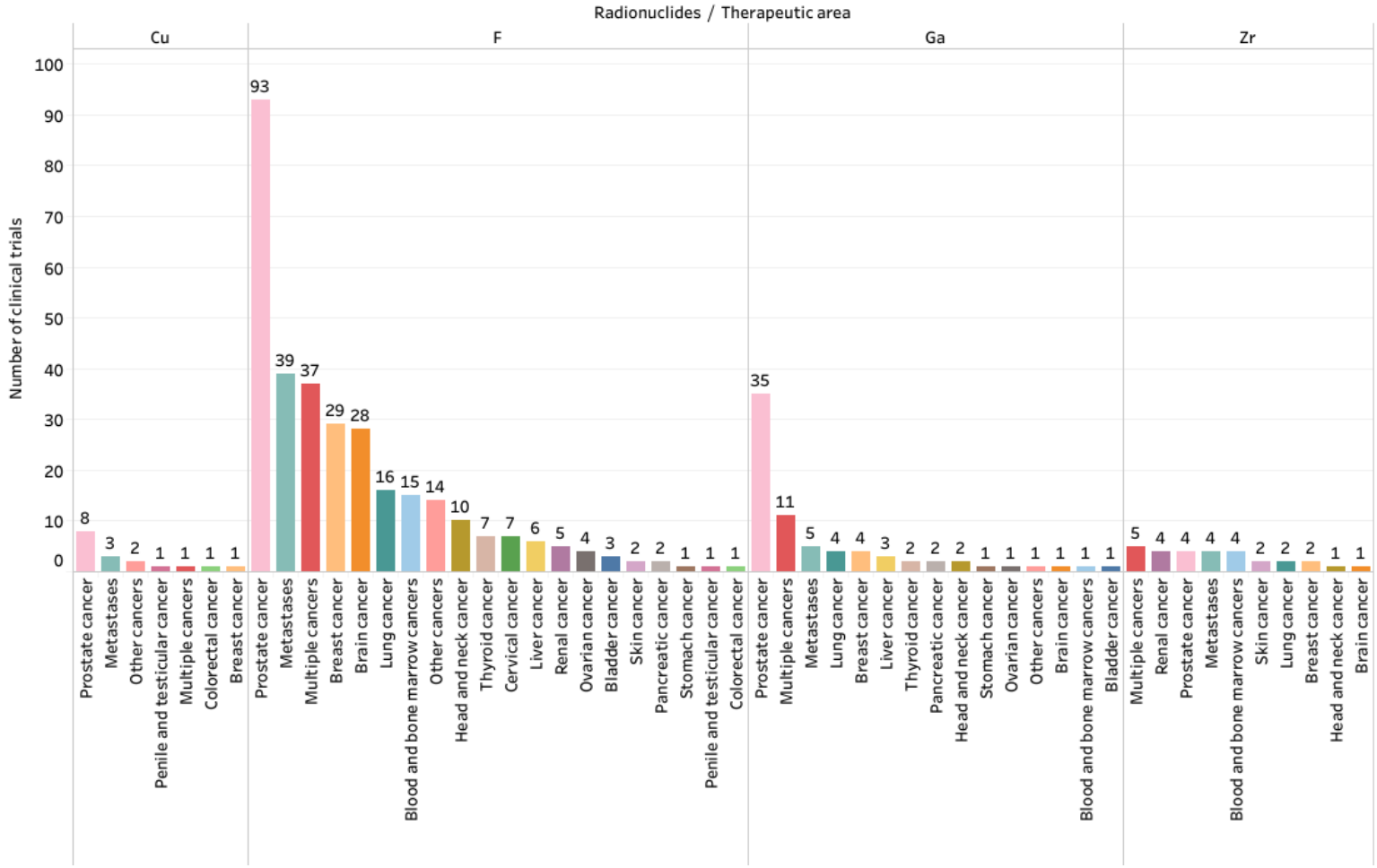

Figure 9: Number of clinical trials for radiopharmaceuticals being investigated for diagnosing non-cancer indications

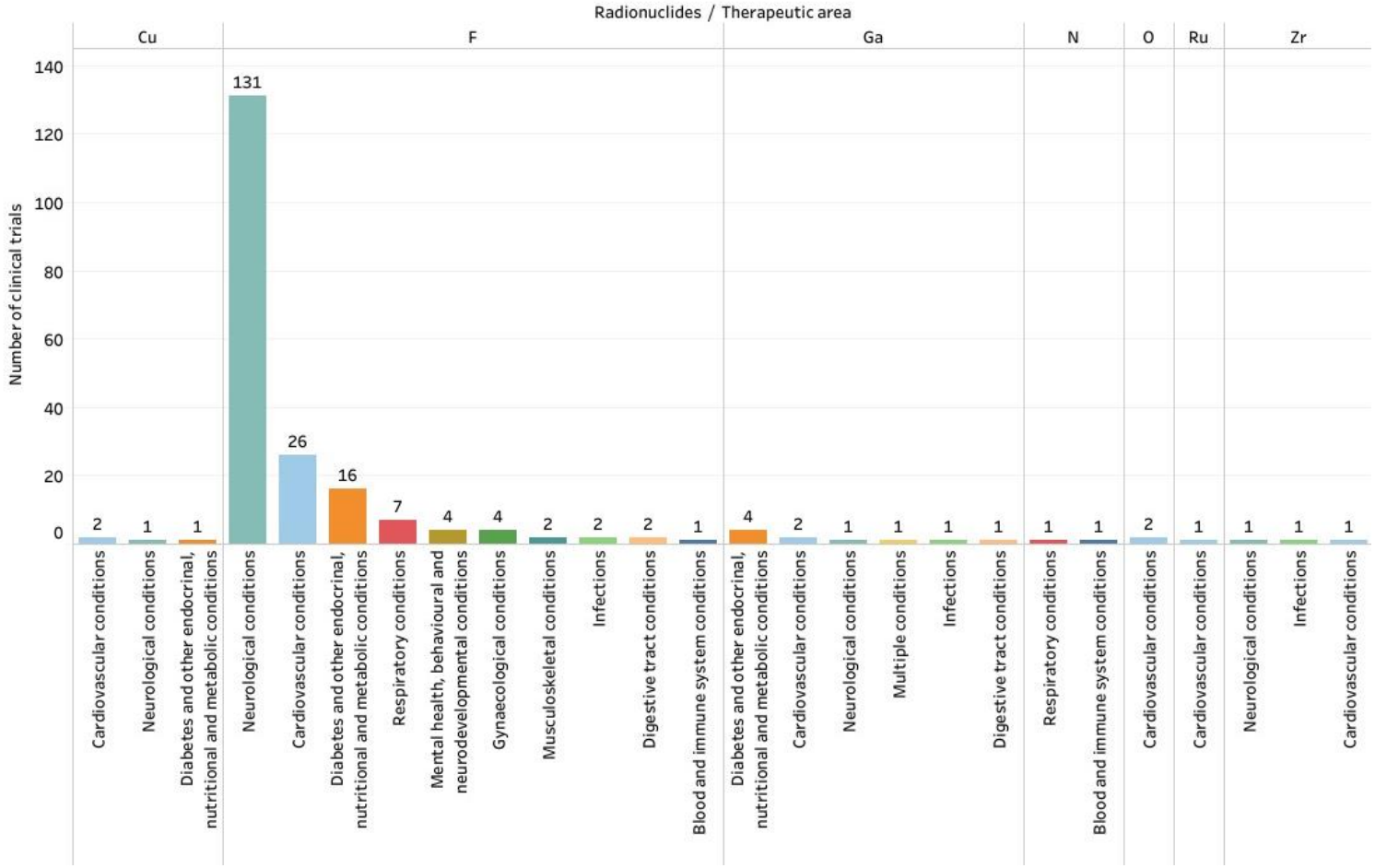

Figure 9 shows non-cancer indications diagnosed with N-13, O-15, and Ru-82, in addition to F-18, Ga-68, Cu-64, and Zr-89, across a wide spread of non-cancer indications. Neurological conditions, cardiovascular conditions, and diabetes and other endocrinal, nutritional and metabolic conditions were the most common non-cancer indications investigated by PET imaging. F-18 was the radiopharmaceutical used the most for diagnosis in the afore-mentioned non-cancer indications, followed by Ga-68, Zr-89 and Cu-64. In fact, F-18 was used the most for imaging for all cancer and non-cancer indication headings.

Clinical Trial Landscape

All radiopharmaceuticals identified have been classified based on their stage of development (phase 1,2 and 2, and phase 2,3 and 3). The majority (401, 62%) of these radiopharmaceuticals were in phase 2 development stage while phase 3 consisted of nearly a quarter of the clinical trials (146, ~23%) (Figure 10).

Figure 10: Number of clinical trials in different stages of development

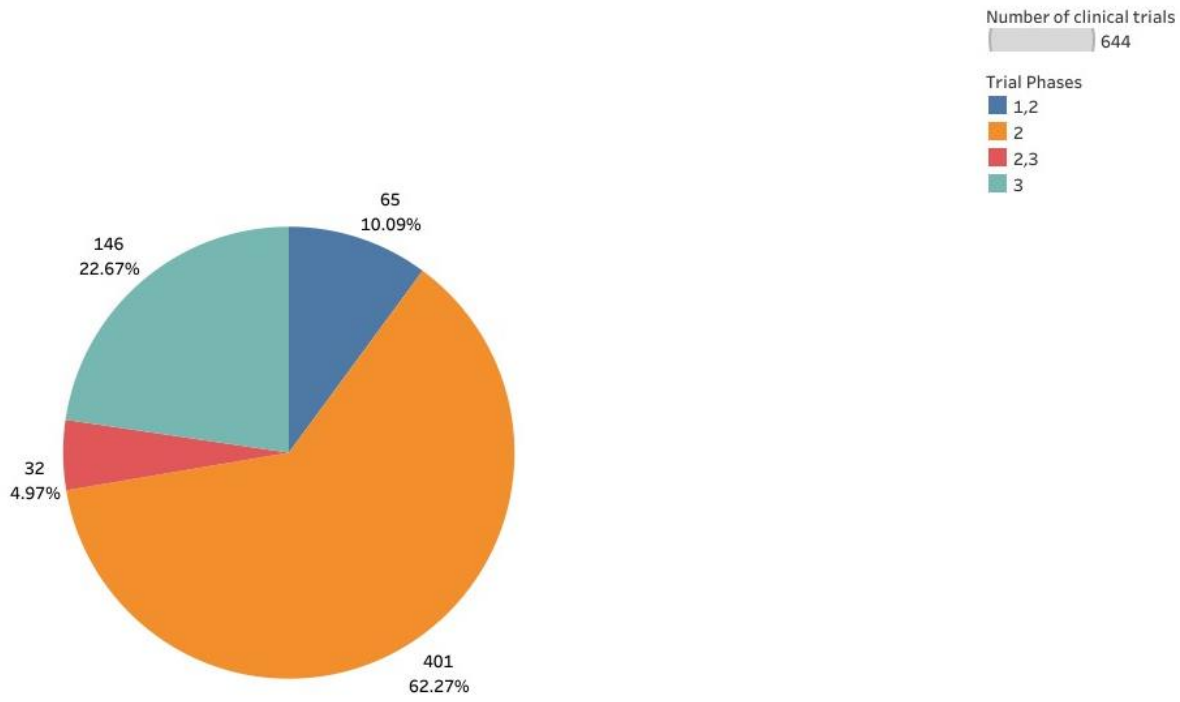

These numbers as illustrated in figure 8,9, and 10 above are important as they reveal the progress being made in terms of clinical trials for new treatments and therapies. They give us an idea of which treatments may be available in the near future and which ones may take longer to develop.

Trial location

An almost equal number of the clinical trials were conducted in locations of US and Canada (271, ~42%), and UK/EU (265, ~41%) while those in ROW (rest of world) locations constituted (56, ~9%) in number (Figure 11). Worldwide locations included trials that had trial locations in more than one of the above location groups and were (27, 4%) in number. The trial locations could not be found for (27, 4%) clinical trials.

Figure 11: Locations of clinical trials

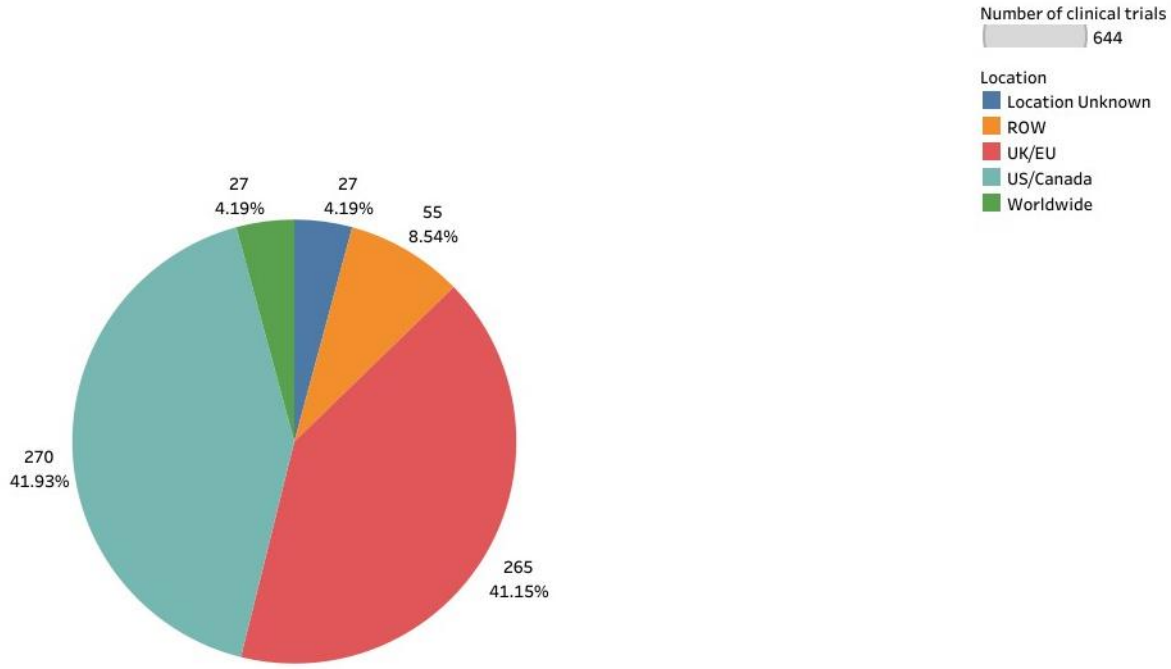

As shown in figure 12, clinical trials being conducted in the UK/EU area are investigating all relevant radiopharmaceuticals.

Figure 12: Locations of clinical trials investigating PET radiopharmaceuticals

Radionuclides	Location Unknown	ROW	UK/EU	US/Canada	Worldwide
Cu-64		2	9	10	
F-18	26	43	217	210	25
Ga-68	3	12	27	41	1
N-13				2	
O-15			1	1	
Ru-82			1		
Zr-89			15	15	2

Location

Number of clinical tri..
1 217

Sponsor Information

Our analysis showed that 446 clinical trials (69%) were sponsored by non-industry sponsors. Industry sponsored 117 (18%) clinical trials while 81 (12.5%) clinical trials involved both

industry and non-industry sponsors (Figure 13). These results suggest that non-industry sponsors are more likely to fund clinical trials, while industry sponsors typically collaborate with other entities to fund clinical trials.

Figure 13: Type of sponsors in clinical trials

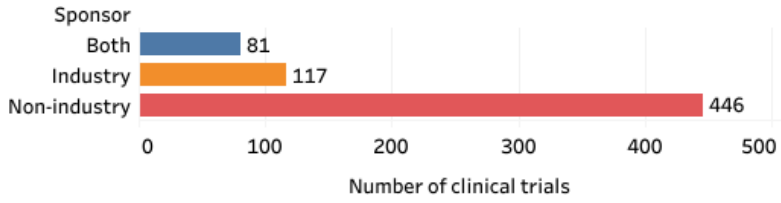

Our analysis also found that non-industry is more involved in testing radiopharmaceuticals that are not currently in use in clinical practice for the purposes of diagnosis such as Cu-64, O-15, Ga-68, and Zr-89 (Figure 14). This is likely due to the fact that industry is more focused on developing products that are already in use, while non-industry researchers are more likely to be interested in exploring new avenues of research and testing new radiopharmaceuticals.

Figure 14: Number of clinical trials investigating radiopharmaceuticals with sponsor

Radionuclides	Sponsor type: Both	Industry	Non-industry
Cu-64	3	10	8
F-18	65	97	359
Ga-8	5	5	74
N-13		1	1
O-15	1		1
Ru-82		1	
Zr-89	10	6	16

Count of Radionuclid.. 1 – 359

Manufacturer landscape

From our analysis we have identified industry sponsors conducting clinical trials investigating radiopharmaceuticals. Avid Radiopharmaceuticals is shown to be a key player in the field, sponsoring the vast majority of industry-led clinical trials, as shown in figure 15. Table 2 further summarises which of the various radionuclides under investigation by industry sponsors, as well as the locations of trials conducted by each industry sponsor.

Figure 15: Top 20 industry sponsors

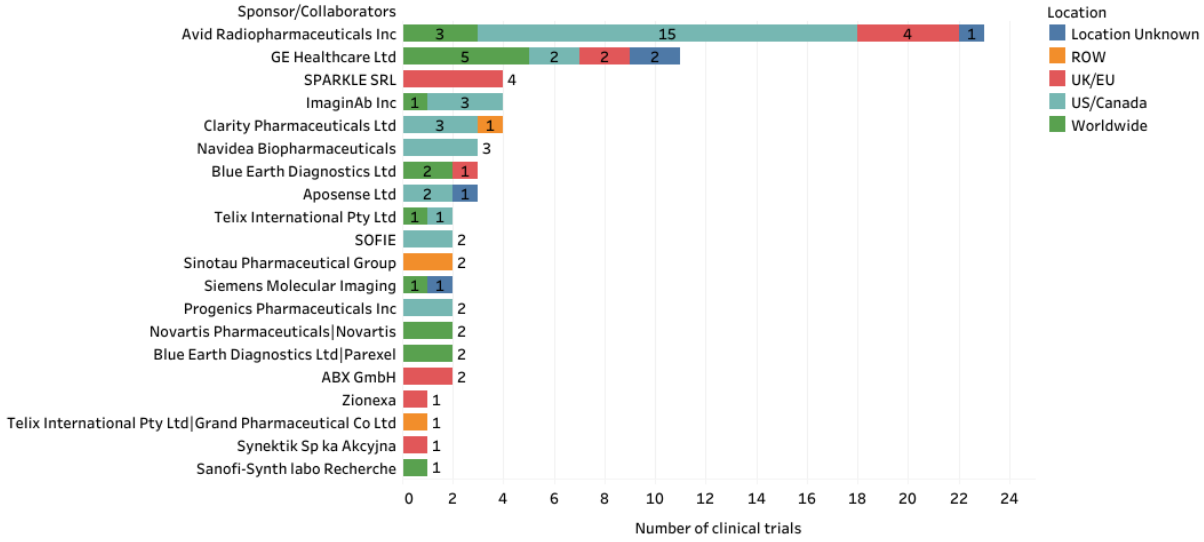

Table 2: List of radionuclides being investigated by industry sponsors identified from clinical trial analysis

Sponsors	Radionuclides	Location	EU or UK
ABX advanced biochemical compounds GmbH	F	Worldwide	
ACR Image Metrix, LLC	F	Worldwide	
Advanced Accelerator Applications	F, Rb	UK/EU	Both
Advanced Imaging Projects, LLC	Ga	ROW	
Advanced Nuclear Medicine Ingredients (acquired by Telix Pharmaceuticals)	F, Ga	UK/EU	EU
Affibody AB	Ga	UK/EU	EU
Amgen	F	US/Canada	
Aposense Ltd.	F	US/Canada	

Sponsors	Radionuclides	Location	EU or UK
APRINOIA Therapeutics	F	Worldwide	
Ashvattha Therapeutics, Inc.	F	US/Canada	
Astellas Pharma Europe Ltd.	F	US/Canada	
AstraZeneca	F, Zr	Worldwide	
Avid Radiopharmaceuticals	F	Worldwide	
Bayer	F, N	US/Canada	
Biokosmos S.A.	F	UK/EU	EU
Blue Earth Diagnostics	F	Worldwide	
Bristol-Myers Squibb	F, Zr	UK/EU	EU
BV Cyclotron VU	F	UK/EU	EU
Cell Point LLC	F	US/Canada	
CellSight Technologies, Inc.	F	US/Canada	
CHU de Bordeaux	F	UK/EU	EU
Cis Bio International	F	UK/EU	EU
Clarity Pharmaceuticals Ltd	Cu	Worldwide	
Curium Pharma	Cu	US/Canada	
Cyclopharma	F	UK/EU	EU
FluoroPharma Medical	F	UK/EU	EU
GE Healthcare	F	Worldwide	
Genentech, Inc.	F, Zr	Worldwide	
Genzyme	F, Zr	Worldwide	
GlaxoSmithKline	F, Zr	Worldwide	
HTA Co., Ltd.	F	ROW	

Sponsors	Radionuclides	Location	EU or UK
IASON GmbH (acquired by Curium Pharma)	F	UK/EU	EU
ICNAS Produção Unipessoal Lda	Ga	UK/EU	EU
ImaginAb, Inc.	Zr	Worldwide	
Innervate Radiopharmaceuticals LLC	F	US/Canada	
Instituto Tecnológico PET	F	UK/EU	EU
IQVIA (formerly Quintiles)	F	US/Canada	
ITEL Telecommunications S.r.l.	F	EU	EU
Janssen Pharmaceuticals	F	UK/EU	EU
Lantheus Medical Imaging, Inc.	F	Worldwide	
Life Molecular Imaging GmbH (formerly Piramal Imaging)	F	Worldwide	
LiteCure LLC	F	US/Canada	
MedTrace Pharma A/S	O	Worldwide	
Merck KGaA	F	UK/EU	EU
Merck Sharp & Dohme LLC	F, Zr	Worldwide	
Navidea Biopharmaceuticals	F	US/Canada	
Novartis Pharmaceuticals	Ga, F	Worldwide	
PETNET Solutions, Inc.	F	UK/EU	UK
Pfizer	F	US/Canada	

Sponsors	Radionuclides	Location	EU or UK
Piramal	F	UK/EU	EU
Pozitron-Diagnostics Ltd.	F	UK/EU	EU
Progenics Pharmaceuticals, Inc.	F	US/Canada	
Proportional Technologies, Inc.	Cu, O	US/Canada	
RadioMedic S.R.O.	F	UK/EU	EU
Radiomedix, Inc.	Cu	US/Canada	
Regeneron Pharmaceuticals	Zr	UK/EU	EU
Roche	F, Zr	Worldwide	
Sanofi	F	Worldwide	
Siemens Molecular Imaging	F	Worldwide	
Sinotau Pharmaceutical Group	F	ROW	
SOFIE	F	US/Canada	
Sparkle SRL	Cu	UK/EU	EU
Synektik SA	F	UK/EU	EU
Telix Pharmaceuticals	F, Zr, Ga	Worldwide	
Threshold Pharmaceuticals (acquired by Molecular Templates)	F	UK/EU	UK
Zionexa	F	UK/EU	EU

Members of the IO team attended the ISTR-2023, which has led to the identification of main manufacturers in this field globally. Table 3 details the list of exhibitors from this conference, along with the radionuclide produced by each exhibitor and the locations in which they operate and/or supply to. It may be important to note that none of the companies from the list of exhibitors have sponsored industry-led clinical trials identified from our scan.

Table 3: List of exhibitors presented at the ISTR-2023 and which radionuclide they produce

Company	Radionuclide Produced	Location
AI4R	N/A	Worldwide
Berthold Technologies GmbH	N/A	EU
Best Cyclotron Systems Inc	^{18}F, ^{13}N, ^{68}Ga, ^{89}Zr, ^{15}O, ^{64}Cu	Worldwide
China Isotope & Radiation Corporation	^{18}F	Worldwide
COMECER	^{82}Rb, Cu, ^{89}Zr, ^{68}Ga, ^{44}Sc,	Worldwide
Eckert & Ziegler Radiopharma GmbH	^{18}F, ^{68}Ga, ^{89}Zr, ^{64}Cu	Worldwide
Eichrom Technologies	^{18}F, ^{68}Ga, ^{44}Sc, ^{89}Zr	Worldwide
Fluidomica Lda.	Other	EU
IBA Radiopharma Solutions	^{18}F, ^{68}Ga, ^{89}Zr, ^{64}Cu, ^{13}N, ^{15}O	Worldwide
Institute of Isotopes Co. Ltd	Other	Worldwide
iPHASE Technologies	^{18}F, ^{68}Ga, ^{89}Zr, ^{64}Cu	Worldwide
Isotopia Molecular Imaging Ltd	^{18}F, ^{68}Ga	Worldwide
Isotope JSC	^{85}Rb, ^{87}Rb, Zr, Cu, ^{68}Ga	Worldwide
ITM Isotope Technologies Munich SE	^{18}F, ^{68}Ga	Worldwide
LabLogic Systems Ltd	N/A	Worldwide
Mediso Medical Imaging Ltd	N/A	Worldwide
MOLECUBES	N/A	Worldwide
Ontario Power Generation	N/A	USA & Canada
Pars Isotope Company	^{18}F, ^{68}Ga, ^{67}Ga	ROW
Ridgeview Instruments AB (Ligand Tracer)	N/A	Worldwide
Rotem GmbH	^{18}F, ^{68}Ga	Worldwide

Scannix	N/A	EU
Shimadzu Handels GmbH	N/A	Worldwide
Sylvia Fedoruk Canadian Centre for Nuclear Innovation Inc.	^{18}F, ^{64}Cu, ^{89}Zr	Canada
Tema Sinergie	^{18}F, ^{68}Ga, ^{64}Cu	Worldwide
TrisKem International	Cu, Sc, Ga, Zr	Worldwide

N/A: company produce instrumentation/hardware for radiopharmaceutical tracing/use

Regulatory information

We identified 151 radiopharmaceuticals in our scan, out of which 126 were not licensed for any indication by MHRA/EMA (Figure 16). Only 25 radiopharmaceuticals identified were licensed. Out of the 25 licensed radiopharmaceuticals, 20 (listed in Figure 16) were licensed by the MHRA, while 5 were only licensed by EMA (Figure 17).

Figure 16: Regulatory status of radiopharmaceuticals

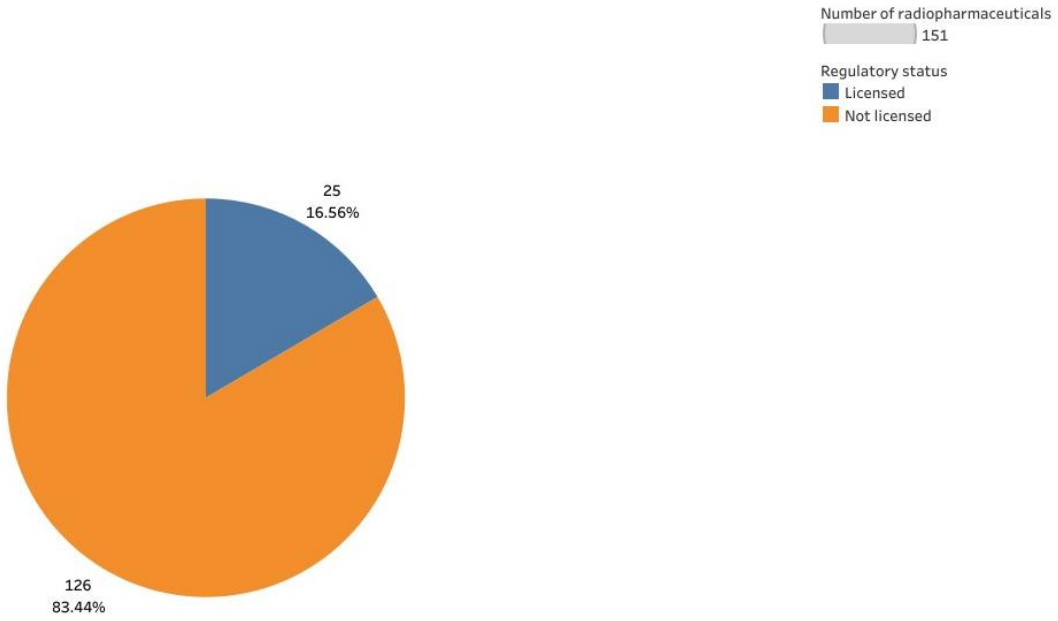

Figure 17a: Regulatory status of radiopharmaceuticals

Regulatory status	Regulatory authority	
Licensed	EMA	5
	MHRA	20
Not licensed	N/A	126

Number of radiophar..
5 126

Figure 17b: Licensed radiopharmaceuticals

Radiopharmaceuticals	Regulatory authority
Chloride	MHRA
Copper chloride	MHRA
Daratumumab	MHRA
Dotatate	MHRA
Edotreotide	MHRA
Florbetaben	MHRA
Florbetapir	MHRA
Flortaucipir	MHRA
Fluciclovine	MHRA
Fludeoxyglucose	MHRA
Fluorodopa	EMA
Fluoroestradiol	EMA
Fluorofuranylnorprogesterone	MHRA
Fluoromisonidazole	EMA
Fluorothymidine	MHRA
Flutemetamol	MHRA
FSPG	MHRA
Gozetotide	MHRA
Ipilimumab	MHRA
Iortaucipir	MHRA
Pembrolizumab	MHRA
Piflufolastat	EMA
PMPBB3	MHRA
PSMA	MHRA
Sodium fluoride	EMA

UK Landscape

Narrowing our analysis down to UK trial locations led to a very small subset of 17 clinical trials. All clinical trials were for adult population. Three clinical trials were investigating female population for cervical and breast cancer. One clinical trial was investigating prostate cancer. All cancer and non-cancer indications are shown in figure 18.

Figure 18: UK Landscape of radiopharmaceuticals and therapeutic areas

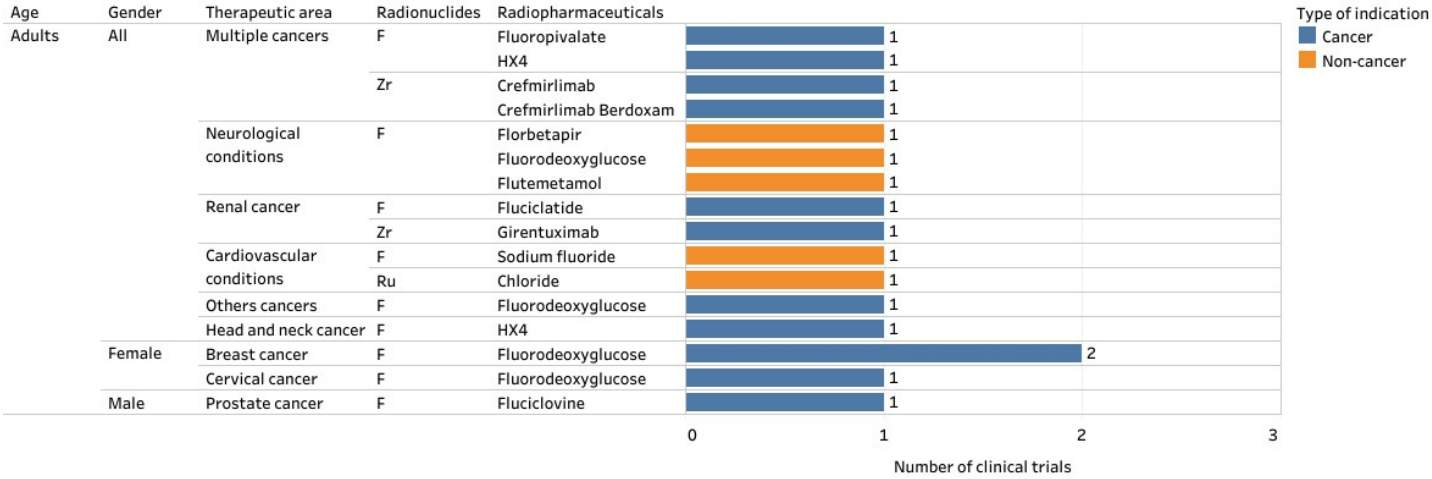

F-18 was the most used radiopharmaceutical in clinical trials while a very small number was using Zr-89 for diagnosis. One trial was identified in the entire scan that was investigating Ru-82 for cardiovascular conditions (Figure 18).

News and events landscape

As part of our news and events scan, we identified activity in radiopharmaceuticals at various stages of development within the last year (August 2022 to August 2023) (preclinical, investigator-initiated studies, and approved products). Most of these events have focused on the announcement of trial progress (publication of results or the initiation of new trials), however, some have also covered new partnerships or company asset acquisitions that will accelerate the global expansion of some of their pipeline products into new markets.

In 2022 there were a total of 17 events for approved (n=13), investigator initiated trials (n=2) and preclinical studies (n=2). Amongst the approved events of note is the positive CHMP (Committee for Medicinal Products for Human Use) opinion gained in October 2022 for Pluvicto (lutetium Lu 177 vipivotide tetraxetan - Novartis Pharmaceuticals) a Breakthrough designated drug for the treatment of prostate cancer, and subsequent regulatory approval for Europe in December 2022 for the treatment of adult patients with prostate-specific membrane antigen (PSMA)–positive metastatic castration-resistant prostate cancer (mCRPC) in combination with androgen deprivation therapy (ADT) with or without androgen receptor (AR) pathway inhibition.[12] In October 2022, Illuccix (68Ga-HBED-CC-PSMA-11 - Telix Pharmaceuticals Limited, Australia) was approved in Canada for prostate cancer imaging.[13] Top line trial results were announced for Pylarify (PYLCLARI, piflufolastat, 18F-DCFPyL PET/CT - Lantheus Holdings, Inc. US) and Xofigo (Radium-223 Dichloride – Bayer AG) an FDA approved

(2013) radiopharmaceutical for the treatment of men with symptomatic late-stage (metastatic) castration-resistant prostate cancer that has spread to bones but not to other organs.

Furthermore, in 2022 Isoray, Inc. (USA) registered two separate phase 1 and phase ½ investigator initiated trials for neuroendocrine tumours – Imaging and two innovative radiopharmaceuticals for solid tumours present data at two international conferences namely CLR-12120 (Phospholipid Ether + 212b, Cellectar Biosciences, Inc. - US) and PNT2001 (177Lu-PNT2001, POINT Biopharma Global Inc. – Canada).

Between January and August 2023 there were a total of 20 events for approved drugs in prostate cancer and prostate cancer imagining. For the treatment of prostate cancer, Pluvicto became the first targeted radioligand therapy for the treatment of PSMA-positive mCRPC in Canada[14] and Xofigo announced the completion of trial recruitment for their on-going phase 3 clinical trial PEACE III (NCT02194842) for asymptomatic or mildly symptomatic castration resistant prostate cancer patients metastatic to bone.

For prostate cancer imaging, Posluma (18F-rhPSMA-7 PET Imaging, flotufolastat F 18 injection– Bracco Spa., Italy), the first radiohybrid PSMA-targeted PET imaging agent, was approved by the US FDA for PET of PSMA positive lesions in men with prostate cancer with suspected metastasis who are candidates for initial definitive therapy or with suspected recurrence based on elevated serum prostate-specific antigen (PSA) level.[15] Pylarify received positive CHMP opinion in May 2023 with subsequent regulatory approval gained in July for the detection of PSMA positive lesions with PET in adults with prostate cancer in primary staging of patients with high-risk PCa prior to initial curative therapy and to localize recurrence of prostate cancer in patients with a suspected recurrence based on increasing serum prostate-specific antigen (PSA) levels after primary treatment with curative intent.[16] In March 2023 Illuccix received an FDA approval for a supplementary New Drug Application to enable its use for the selection of patients with metastatic prostate cancer for whom lutetium-177 PSMA-directed therapy is indicated.[17]

In the preclinical research arena, between January and August 2023, a total of 5 new radiopharmaceuticals announced or demonstrated progress. In summary, two innovative biologics such as AT-02 (Actinium Pharmaceuticals) an anti-HER3 AC225 monoclonal antibody for non-small cell lung cancer that targets ErbB3/HER3[18] and TLX300 (Eli Lilly and Co.) a radiolabelled olaratumab for sarcoma imaging that targets platelet-derived growth factor receptor (PDGFR)[19]; two New Molecular Entities such as FPI-2059 (Fusion Pharmaceuticals Inc.) that targets NT1 (Neurotensin receptor type 1) for colorectal cancer[20] and LNTH-1558 (Lantheus Holdings, Inc.) a small molecule that targets PSMA for prostate cancer imaging[21] and an undisclosed Glypican-3 Targeted Radiopharmaceutical (RayzeBio, Inc.) for Hepatocellular (Liver) Cancer (Including Secondary Metastases).[22]

Preclinical research landscape analysis through network visualisation analyses

A bibliographic database search in Embase (Ovid) was undertaken on 29th August 2023 to identify recent (2020-2023) research activity on radionuclides and PET, no language limits were imposed and conference abstracts were included. A detailed search strategy is included in Appendix 1.

The search identified a total of 2,620 records that were imported into Endnote 20 for further assessment. No screening for inclusion/exclusion was undertaken since the aim of this task was exploratory however, some classification by radioisotope name in title was undertaken by one reviewer and performed in Endnote 20. A total of eight groups were created one per each of the included radioisotopes (F18=885, 13N=8, 15O=22, 68G=264, 82Rb=4, Cu=91, Sc=9, Zr=51). Additionally, one more group was created for all the remaining records (1289) that did not include any of the known radioisotopes in title but included synonymous terms in the abstract and keywords fields. The records were then exported on RIS (Research Information Systems) file format into a visualisation of similarities software (VOSViewer), a free software tool for creating network and density maps based on term co-ocurrence and keyword frequency count. We constructed graphical networks to understand the clustering of the keywords and their degree of dissimilarity to study the connections between keywords in relation to articles that contained the relevant radioisotopes in scope. We excluded *empty* words such as 'article', 'conference abstract' and 'non human'. Figures 19 to 23 present a visual overview of the recent research by radioisotope.

Figure 19: Preclinical research overview for F-18 in title (publication year 2020-2023)

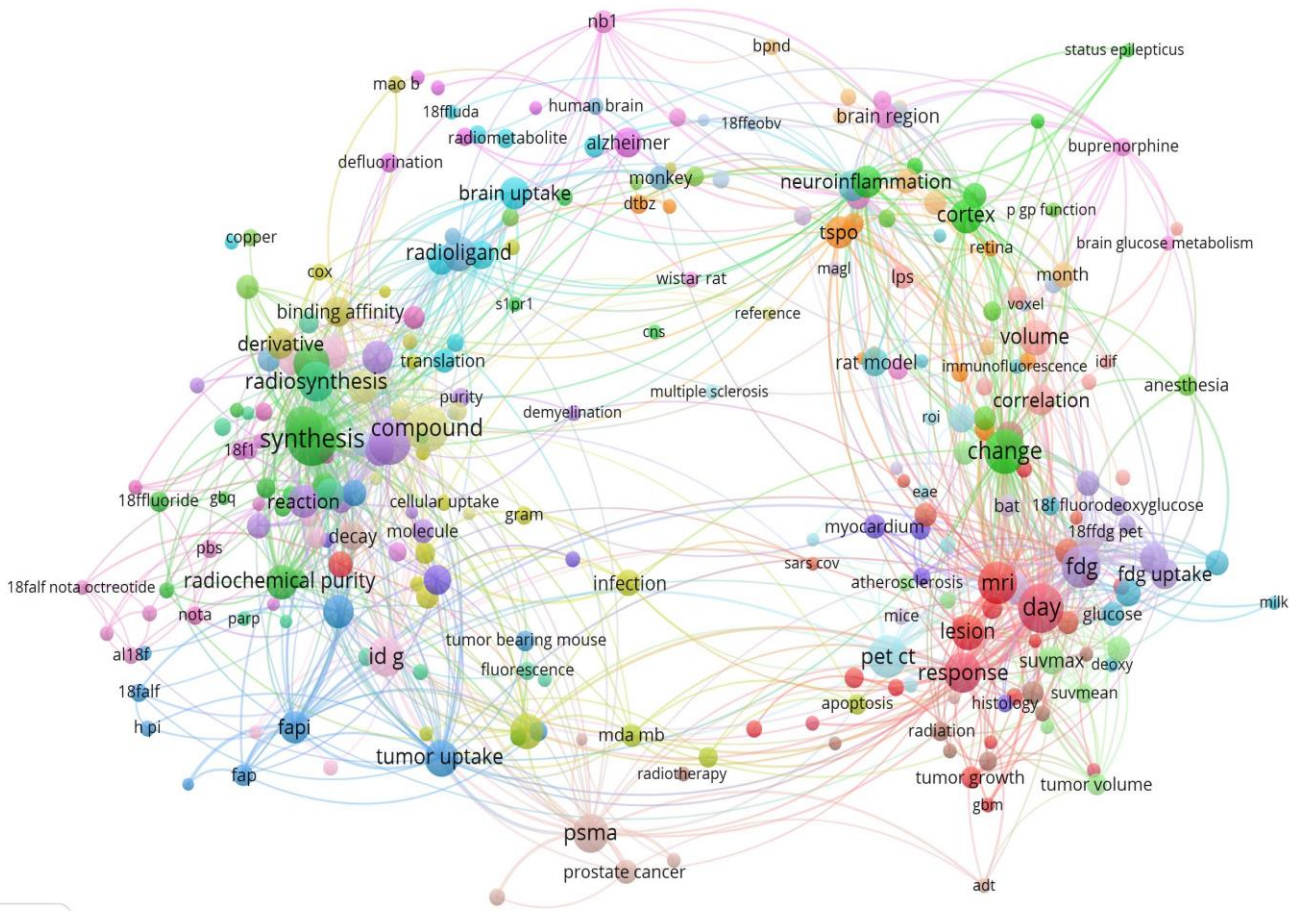

F-18 was included in the title of 885 records retrieved from Embase. A network visualisation analysis of the terms in title and abstract of those records generated thirty-seven different clusters which contained at least 5 terms each. The distance between the clusters represent their relatedness and the size of the labels is determined by the weight of the item. The heavier the weight of an item, the larger the label and the circle of the item. In this instance, the clusters for 'synthesis' and 'radiosynthesis', 'tumour uptake', 'psma', 'lesion' and 'response' appear to have greater weight in the network of related terms. Scattered within the network there are terms with less weight such as 'neuroinflammation' that appears in green in a network with other terms such as 'status epilepticus' and 'cortex' and not distantly related to terms such as 'brain region' which indicates the early research landscape in the field of PET and F-18 for monitoring neuroinflammation.[23-26]

Figure 20: Preclinical research overview of Ga-68 in title (publication year 2020-2023)

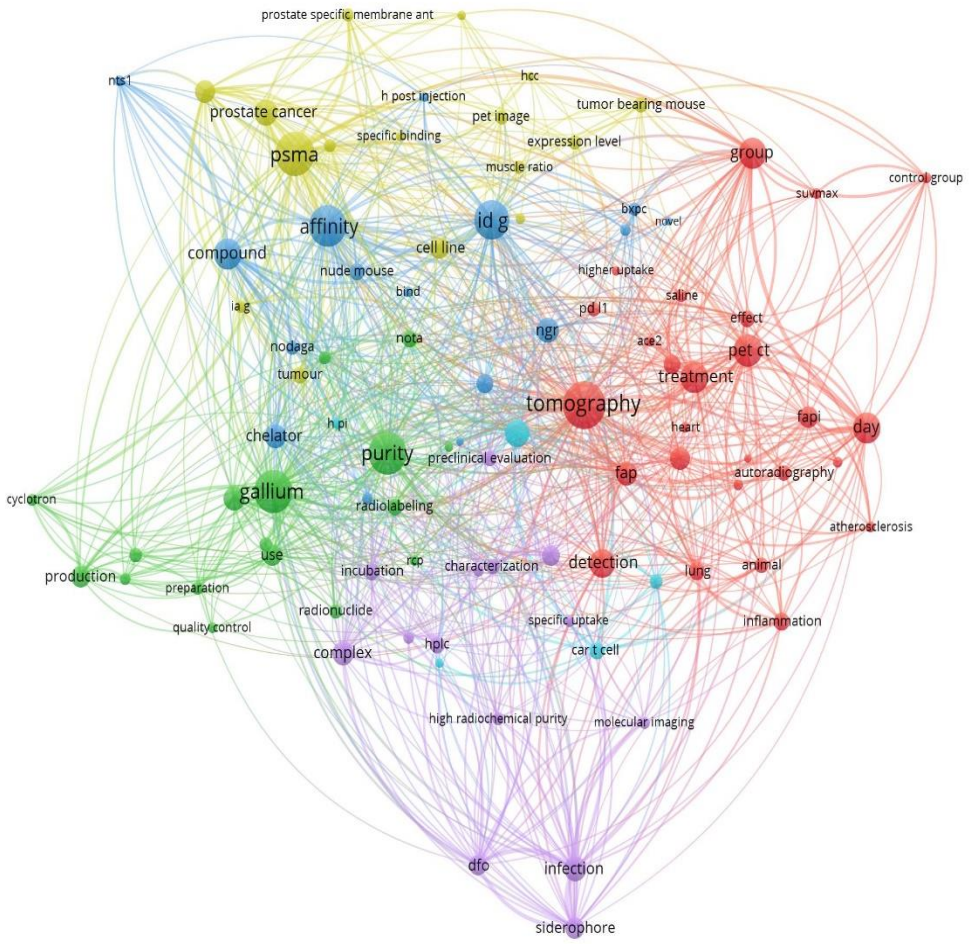

A total of 264 records were identified that included Ga-68 or a synonym in title. The network visualisation for Ga-68 presents 6 clusters with the smaller cluster including at least 5 related terms. The higher weight in the network is for 'tomography', 'gallium', 'affinity', 'psma' and 'purity'. Distant related terms appear in the periphery of the network and present less weight denoted by the size of the labels. The terms 'cyclotron' and 'production' appear in the same network with 'gallium' and 'purity' although distantly related. Of note, the term 'atherosclerosis' appears in the periphery of a network for 'tomography' 'PET-CT' and 'PET ct imaging' (all in red) indicating the relatedness of these terms in the early scientific landscape.[27-31] Further in the network periphery the term 'siderophore' (purple) appears closely related to 'infection' and 'molecular imaging' all on the same network with 'gallium' and 'PET-CT'. This relationship in the network may signal early research in the use of siderophores radiolabelled with Ga-68 for the identification of bacterial infections via molecular imaging by positron emission tomography (PET).[32-39] Bridging these two networks sits the term 'inflammation' closely related to

'detection' and 'PET-CT' and more distant but still within the same network with 'infection' and '68ge 68ga generator' (which cannot be seen in the picture due to size of node).[40,41]

Figure 21: Preclinical research overview of Cu-64 in title (publication year 2020-2023)

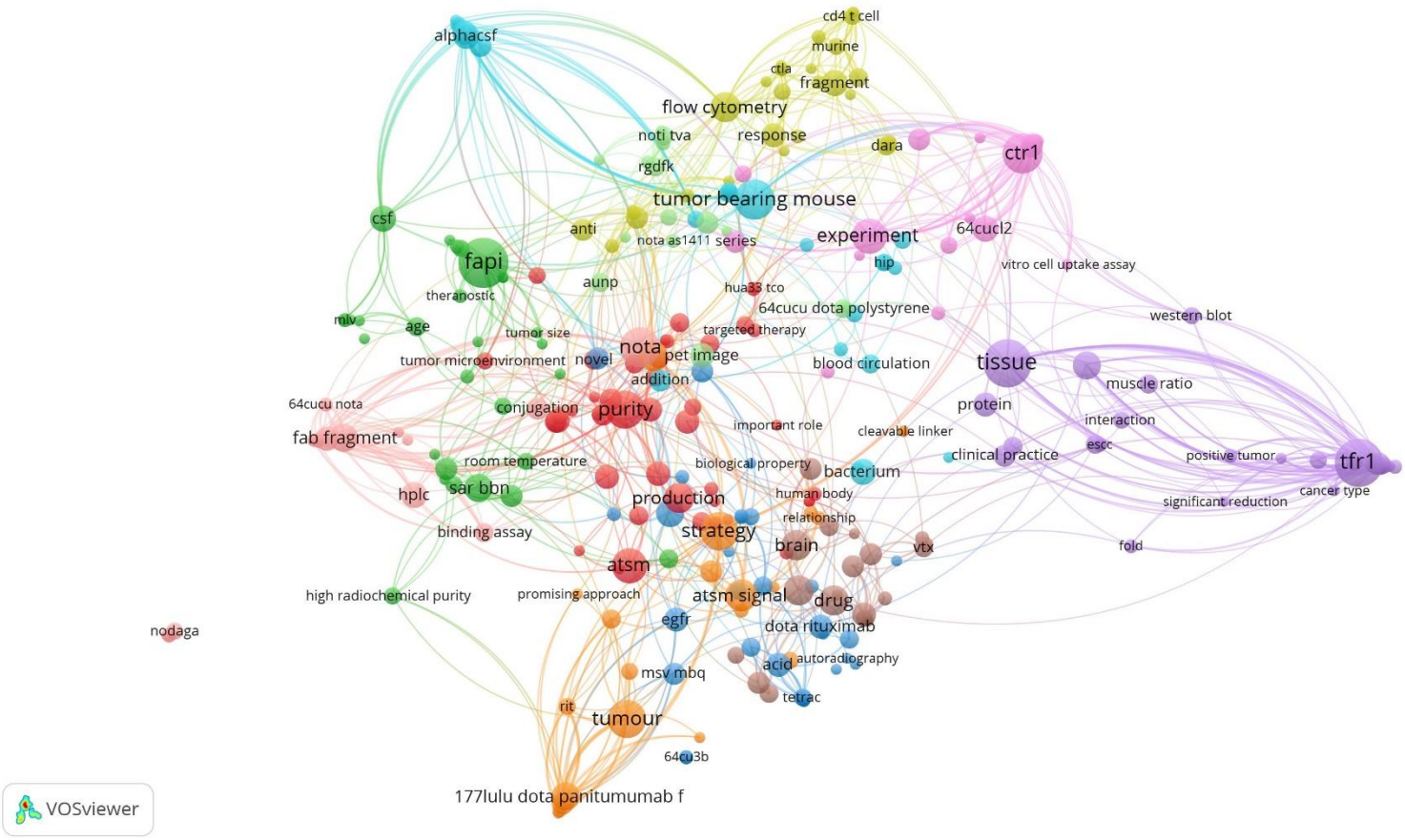

Ninety-one records that contained the word Cu or synonymous terms in title were grouped to be analysed in VOSViewer. Due to the small sample of records the threshold for terms repetition was set at 5 which means that words repeated in the title or abstracts of those ninety-one records less than five times would not appear in the cluster visualisation. A total of four clusters were generated. Lowering the threshold for word repetition has allowed to visualise deeper the content of those records however, the clusters and the weight of those labels in fig 16 are smaller and the network looks more dispersed. Of note are the association of '177Lu-lu panitumumab f' with words such as 'tumour', 'promising approach' and 'atsm signal'.[42] In purple, the term 'tfr1' (transferrin receptor protein 1), appears strongly related with terms such as 'tissue' 'protein', 'escc' (esophageal squamous cell carcinoma), 'clinical practice', 'significant reduction' and 'cancer type' signalling the research field of new applications of Copper-64 in ferroptosis induction.[43,44] The node labelled as 'atsm' (Copper(II)-diacetyl-bis(N(4)-methylthiosemicarbazone)) signals a PET tracer (Cu-ATSM) developed for hypoxia imaging that could potentially be used to identify cancers susceptible to redox-directed

therapies.[45] Furthermore, the relationship with terms such as 'production' and 'purity' reveals research in the field of production and radiosynthesis methods for this candidate for imaging of tumour hypoxia.[46] The node labelled 'ctr1' (copper transporter 1), in pink, shows a strong relationship with other pink terms such as 'experiment' and '64cucl2' (copper (II)-64 chloride) signalling the level of experimental research for 64Copper chloride as PET tracer and/or theragnostic agent for a number of different cancers such as lung, thyroid, prostate and hypoxic tumours.[43,47-52] The green node 'FAPI' (fibroblast activation protein inhibitors) signals research into tumour uptake of 64Cu radiolabelled DOTHA2-FAPI-04 and 64Cu-FAPI-04 for prostate cancer imaging and theranostics applications in pancreatic cancer mouse models respectively.[53,54]

Figure 22: Preclinical research overview of Zr in title (publication year 2020-2023)

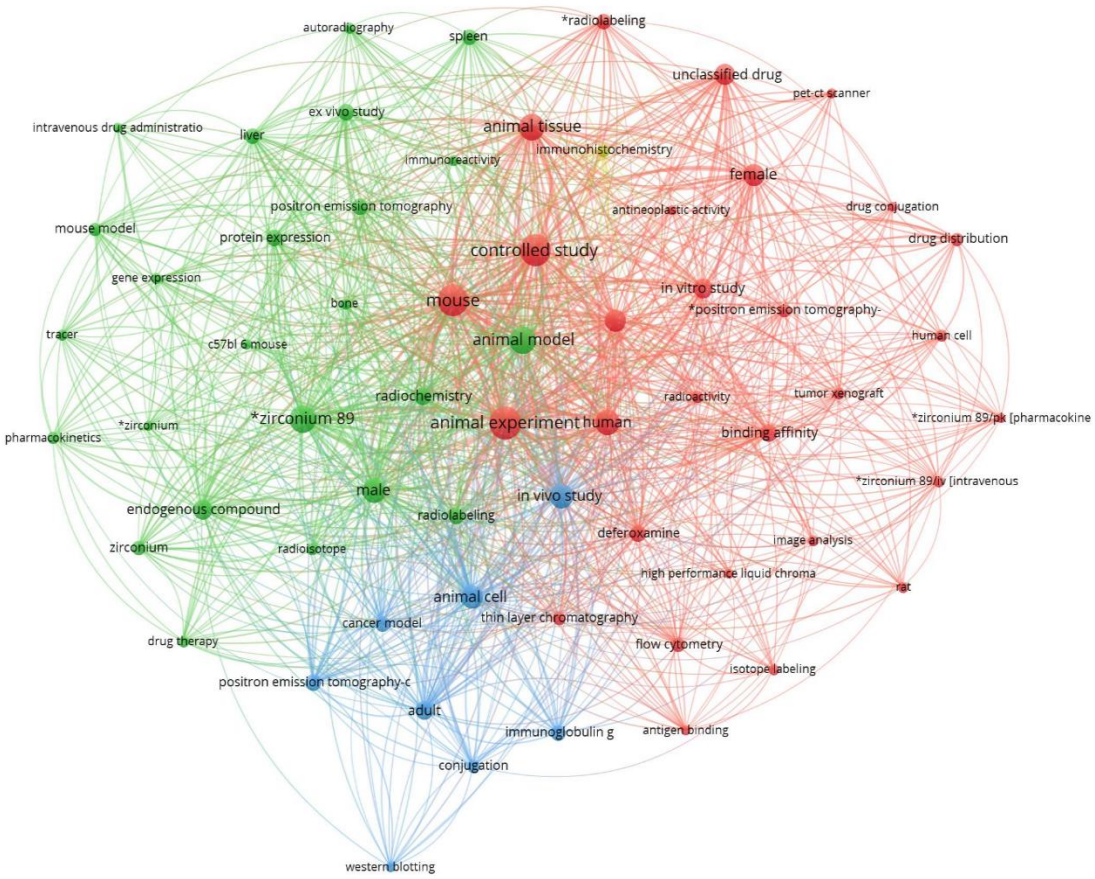

Fifty-one records that included Zr or synonymous terms were grouped and exported into VOSviewer for network visualisation of terms and their relationship within. Minimum term repetition count was set at 5 and four clusters were generated with a minimum of 1 term in cluster 4 'immunohistochemistry'. Of note are frequent terms represented in red such as 'controlled study', 'mouse', 'animal experiment' and 'animal tissue' all of those terms have links across most of the terms in the network signalling the type of animal studies, both 'in vitro' and

'in vivo' studies in 'animal tissue' and 'animal cell'. The term 'Zirconium 89' appears in the network several times. Zirconium radiolabelling studies appear in the relationship with the term 'radiolabelling' indicating preclinical research of novel applications of Zr in PET imaging studies for cancers such as multiple myeloma (MM) where Zr is labelled with elotuzumab as PET imaging agent for MM[55], in the study of ramucirumab radiolabelled with 89Zr ([89Zr]Zr-DFO-RAM) potency to target and image VEGFR2-positive tumours[56], in cancers overexpressing sialic acid-binding immunoglobulin-like lectin 15 (Siglec-15) for which a novel anti-Siglec-15 monoclonal antibody (NC318) was radiolabelled with zirconium-89 to synthesize [89Zr]Zr-DFO-NC318[57], in colorectal cancer PET-imaging and radiotherapy study of a novel anti-DR5 monoclonal antibody CTB006[58] or in chronic kidney disease imaging studies where 89Zr is studied as novel non-invasive method for assessing whole-body alpha-klotho distribution.[59] The immunohistochemistry node reveals pre-clinical research in the field of 89Zr radiolabelling, such as the study of Zr-89 labelled anti-CD11b antibody for evaluating CD11b+ myeloid cells in gastric cancer imaging with PET[60] or the use of [89Zr]DFO-Anti-PDL1, a monoclonal antibody targeting the programmed death-cell ligand (PD-L1) radiolabelled with 89Zr, for non-invasive imaging whole-body mapping of PD-L1 sites to improve the assessment of tumoural PD-L1 expression.[61]

A total of 43 (13N=8, 15O=22, 82Rb=4 and Sc=9) records comprised the group of remaining records for which one of the included radionuclides was mentioned in title. Due to the small number of records per radionuclide a network visualisation was deemed not useful as there were not enough term repetitions to reveal relationship of terms and networks of relevance. Alternatively, a list of these records has been included in Appendix 4.

Figure 23: Density visualisation of preclinical research for all included radioisotopes (in abstract, 2020-2023)

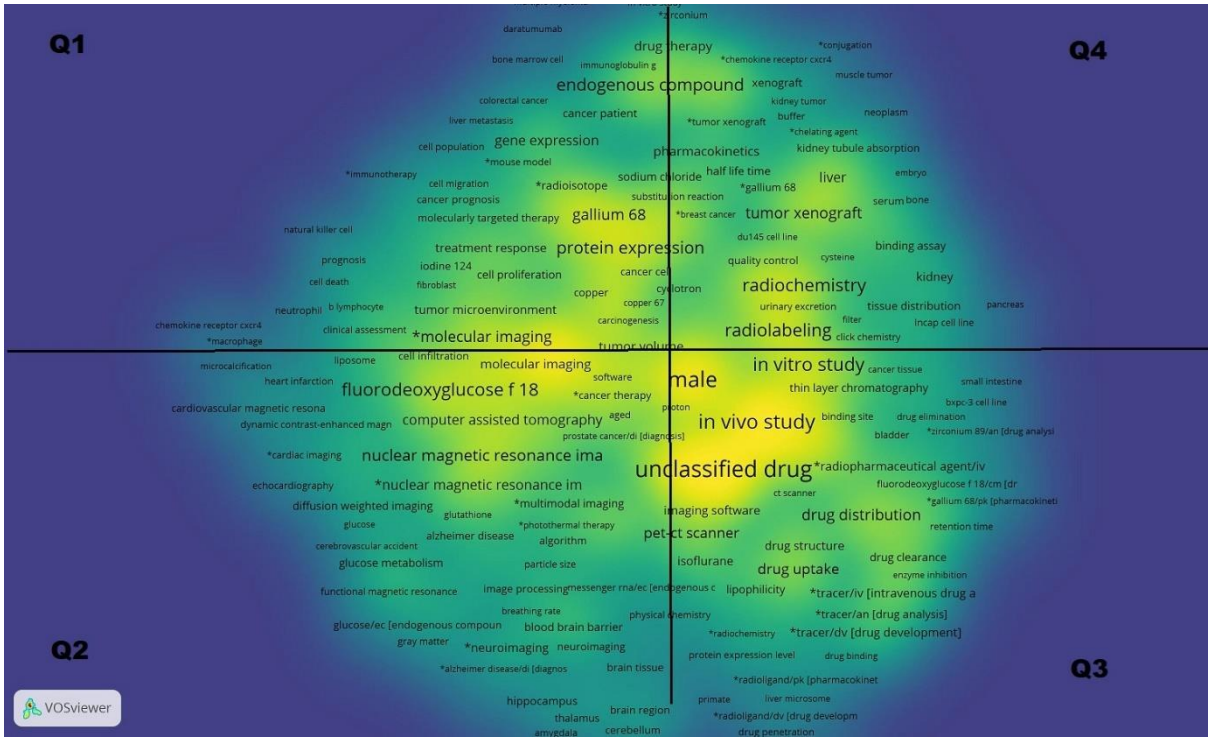

A total of 1,289 records that did not contain any of the included radionuclides of interest in the title but may be included in the abstracts or key word fields were exported into a RIS file to be analysed in VOSviewer. A density visualisation map was generated after removing publication type related keywords such as (conference abstracts, review or preclinical study) and animal and human related tissue or cell related key words. The threshold for word repetition was set at 5 (minimum number of keyword repetition) which produced a total of 974 items distributed across four clusters. The yellow and orange colour designates higher concentration of key words such as 'in vivo' or 'in vitro study', 'fluorodeoxyglucose F18', 'positron emission tomography', 'unclassified drug', 'male', 'protein expression', 'radiolabelling', 'radiochemistry', 'gallium 68' and 'endogenous compound'. Anticlockwise, located in the outer area of the map (Q1) are less frequent terms such as 'multiple myeloma', 'glioblastoma', 'liver metastasis', 'breast carcinoma', 'melanoma' and 'prostate cancer' which could signal early research activity in these cancers. Moving onto Q2 still in the periphery of the map there are terms such as 'microcalcification', 'ischemia', 'heart infarction', 'heart left ventricle ejection', 'heart function', 'brain ischaemia' and 'Alzheimer disease' which could be an indication other non-cancer conditions in which the included radionuclides are being investigated. Q3 includes terms related to the study of pharmacokinetics of some radioligands and 'drug distribution', 'synthesis' and 'uptake' of 'radiopharmaceutical agents'. In Q4 terms such as 'kidney', 'liver', 'pancreas', 'spleen', 'bone', 'muscle', 'heart' and 'stomach' appear alongside other terms such as 'tissue distribution', 'circulation time', 'blood distribution', 'dose response' and 'dosimetry' amongst others.

Discussion

We identified 25 radiopharmaceuticals that were licensed by the MHRA/EMA. Several radiopharmaceuticals like FDG, florbetapir, fluoroclovine are already licensed for use for diagnosis for a number of indications.[62]

FDG is a globally recognised radiopharmaceutical for imaging in several cancer indications. However, there were a few new indications for FDG and other radiopharmaceuticals that this scan was able to identify as shown in figures 2-5. FDG has shown to have limitations in the assessment of a few conditions like prostate cancer. In our analysis, prostate cancer was the cancer indication that was being investigated the most. Some of the non-licensed radiopharmaceuticals that are being investigated for prostate cancer diagnosis identified in this scan include fluorocholine, fluoroethylcholine, and gozetotide when radiolabelled with F-18.[63]

There are several indications mentioned in the 2022 guidance published by the Royal College of Radiologists (RCR)[64], that the radiopharmaceuticals are not licensed for but are recommended for diagnostic purposes for those indications. Some of these indications align with those identified in our scan. For instance, choline is not licensed for any indication, however, it is in clinical trials for diagnosis of prostate cancer and is also mentioned in the RCR guidance as a potential indication and an alternative to other licensed radiopharmaceuticals like gozetotide when radiolabelled with Ga-68.

We identified only one clinical trial investigating Ru-82 for diagnosis of cardiovascular conditions. This appears to be the only indication Ru-82 is licensed for with a recent date of approval from the MHRA in March 2023.[65]

Our scan identified quite a few Ga-68 fibroblast activation protein inhibitors (FAPIs) namely FAPI-2286, FAP-CHX, FAP-RGD, FAPI, FAPI-04, and FAPI-46. They are being investigated for broad cancer indications, and a few specific cancer indications, such as ovarian cancer, pancreatic cancer, and lung cancer. These FAPIs are being considered promising especially for targeted therapy.[66] These appear to be very new in the radiopharmaceutical space. The trials included in this scan for these FAPIs were all posted between 2020 -2023 and none these radiopharmaceuticals are mentioned in the RCR guidance.

Cu-64 is being recognised as a promising radiopharmaceutical in preclinical studies.[67] However, this appears to be a recent development. Most of the trials identified in the scan for Cu-64 were posted after 2020. The RCR guidance does not include any indications recommended for use for Cu-64 as well.

All clinical trials identified for Zr-89, used monoclonal antibodies conjugated with Zr-89, also referred to as radioimmunoconjugates.[68] The use of radioimmunoconjugates in PET imaging allows better understanding of uptake in tumours which can prove vital to determine which patients benefit from treatment. While Zr-89 has been investigated in several clinical trials in the last decade, it is still not licensed by MHRA/EMA or recommended for any indication by RCR. More evidence might be required to understand if Zr-89 is beneficial to patients.

Ammonia as N-13, not licensed for any indication by MHRA/EMA, has been recommended in the RCR guidance for myocardial perfusion imaging.[64] The clinical trials identified in the scan were for respiratory conditions and blood and immune system conditions as shown in figure 5. We can speculate the reasons why ammonia is being investigated albeit in a small number of trials, however, that is beyond the scope of this scan and would need to be investigated separately.

Conclusion

Our scan showed that most of the identified clinical trials were investigating the use of F-18 for diagnosing cancer indications using PET imaging procedures. Ga-68 was also found to have a considerable number of clinical trials, but a relatively small number of clinical trials were testing Rb-82, Cu-64, Zr-89, N-13, and O-15. No clinical trials were found for scandium. Cancer indications were being investigated in a majority of the clinical trials identified. There were more clinical trials at phase 1/2 and 2 stage of clinical development compared to phase 2/3 and 3. Most of the clinical trials are being sponsored by non-industry and most of the clinical trials are being conducted US, Canada, UK/EU areas.

Based on the guidance produced by the UK Health Security Agency for Administration of Radioactive Substances Advisory Committee (ARSAC), which can be considered to be a guide to good clinical practice in the UK for nuclear medicine, there are several indications where radiopharmaceutical technologies are being used in the UK for therapeutic and diagnostic

purposes[3]. Many of these are for diagnostic use for F-18 including imaging for hepatocellular cancer, prostate cancer, neuroendocrine and brain tumours along with a few indications for Ga-68 and one indication for Rb-82. However, there are no indications mentioned against Cu-68, O-15, Zr-89. These could be new radiopharmaceutical technologies for use in diagnosis and would require preparation for adoption into clinical practice.

Our global horizon scan provides not only the all-Wales PET Programme and WHSSC, but also other organisations/bodies, with information on the opportunities for discovering new indications for the radiopharmaceutical technologies of interest. The knowledge of these new and upcoming clinical indications of interest and radiopharmaceuticals could support in future planning for inclusion of radiopharmaceuticals currently in use for other indications. It will also allow health organisations to prepare for the adoption of new radiopharmaceutical technologies in clinical use for the purpose of diagnosis.

The visualisation of similarities technique used to study the preclinical research field for the included radionuclides of interest has provided a relatively rapid approach to understanding the research landscape by aiding with the discovery of some early research applications. Although this method cannot replace the robustness of a systematic literature review, it can support the identification of research leads to follow more systematically in a literature review. As a caveat is worth mentioning that having specialist knowledge in the field would allow for better interpretation of results and study of associations in research field of study.

References

1 Huang Y-Y. An Overview of PET Radiopharmaceuticals in Clinical Use: Regulatory, Quality and Pharmacopeia Monographs of the United States and Europe. *Nuclear Medicine Physics*. 2018.

2 Lodi F, Boschi S. Quality Control of PET Radiopharmaceuticals. In: Khalil MM, ed. *Basic Science of PET Imaging*. Cham: Springer International Publishing; 2017: 105-26.

3 Biricova V, Kuruc J. *Synthesis of the radiopharmaceuticals for positron emission tomography*. International Atomic Energy Agency; 2007. Available from: https://inis.iaea.org/collection/NCLCollectionStore/_Public/38/059/38059371.pdf.

4 Hung JC. Regulatory Aspects of PET Radiopharmaceutical Production in the United States. In: Khalil MM, ed. *Basic Science of PET Imaging*. Cham: Springer International Publishing; 2017: 145-70.

5 Khalil MM. Basics and Advances of Quantitative PET Imaging. In: Khalil MM, ed. *Basic Science of PET Imaging*. Cham: Springer International Publishing; 2017: 303-22.

6 Ballinger JR, Koziorowski J. Regulation of PET Radiopharmaceuticals Production in Europe. In: Khalil MM, ed. *Basic Science of PET Imaging*. Cham: Springer International Publishing; 2017: 127-43.

7 Code of Federal Regulations. *Part 212 - Current good manufacturing practice for positron emission tomography drugs*.

8 European Commission. The rules governing medicinal products in the European Union. *EudraLex - Volume 10*.

9 Nuclear Medicine Europe. *What is nuclear medicine and how can it help Europe beat cancer?*; 2022. Available from: https://nuclearmedicineeurope.eu/wp-

content/uploads/2022/07/What-is-nuclear-medicine-and-how-can-it-help-Europe-beat-cancer.pdf.

10 *BiomedTracker: Pharma Intelligence*. 2023. Available from: https://www.biomedtracker.com/ [Accessed 10/10/2023].

11 Leiden University. *VOSviewer version 1..6.19*. 2023. Available from: https://www.vosviewer.com/ [Accessed 10/10/2023].

12 Novartis. *Novartis receives European Commission approval for Pluvicto® as the first targeted radioligand therapy for treatment of progressive PSMA–positive metastatic castration-resistant prostate cancer*. 2022. Available from: https://www.novartis.com/news/media-releases/novartis-receives-european-commission-approval-pluvicto-first-targeted-radioligand-therapy-treatment-progressive-psma-positive-metastatic-castration-resistant-prostate-cancer [Accessed 10/10/2023].

13 Telix Pharmaceuticals Limited. *Health Canada Approves Illuccix® for Prostate Cancer Imaging*. 2022. Available from: https://www.prnewswire.com/news-releases/health-canada-approves-illuccix-for-prostate-cancer-imaging-301649214.html [Accessed 10/10/2023].

14 Novartis Pharmaceuticals Canada. *PLUVICTO™ receives positive recommendations from CADTH and INESSS for progressive PSMA-positive metastatic castration-resistant prostate cancer*. 2023. Available from: https://www.newswire.ca/news-releases/pluvicto-tm-receives-positive-recommendations-from-cadth-and-inesss-for-progressive-psma-positive-metastatic-castration-resistant-prostate-cancer-864526183.html [Accessed 10/10/2023].

15 Blue Earth Diagnostics. *U.S. FDA Approves Blue Earth Diagnostics' POSLUMA® (Flotufolastat F 18) Injection, First Radiohybrid PSMA-targeted PET Imaging Agent for Prostate Cancer*. 2023. Available from: https://www.businesswire.com/news/home/20230530005180/en/U.S.-FDA-Approves-Blue-Earth-Diagnostics%E2%80%99-POSLUMA%C2%AE-Flotufolastat-F-18-Injection-First-Radiohybrid-PSMA-targeted-PET-Imaging-Agent-for-Prostate-Cancer [Accessed 10/10/2023].

16 Curium. *Curium Receives Marketing Authorization in the EU for PYLCLARI™, an Innovative 18F-PSMA PET Tracer Indicated in Adults With Prostate Cancer*. 2023. Available from: https://www.globenewswire.com/news-release/2023/07/28/2712980/0/en/Curium-Receives-Marketing-Authorization-in-the-EU-for-PYLCLARI-an-Innovative-18F-PSMA-PET-Tracer-Indicated-in-Adults-With-Prostate-Cancer.html [Accessed 10/10/2023].

17 Telix Pharmaceuticals Limited. *FDA Approves Expanded Indication for Telix's Illuccix® to Include Patient Selection for PSMA-Directed Radioligand Therapy*. 2023. Available from: https://www.prnewswire.com/news-releases/fda-approves-expanded-indication-for-telixs-illuccix-to-include-patient-selection-for-psma-directed-radioligand-therapy-301774122.html [Accessed 10/10/2023].

18 Actinium Pharmaceuticals I. *Actinium Highlights First-In-Class HER3 Targeted Radiotherapy Data Demonstrating Potent Anti-Cancer Activity of in Ovarian and Colorectal Cancer Models at the AACR Annual Meeting*. 2023. Available from: https://www.prnewswire.com/news-releases/actinium-highlights-first-in-class-her3-targeted-radiotherapy-data-demonstrating-potent-anti-cancer-activity-of-in-ovarian-and-colorectal-cancer-models-at-the-aacr-annual-meeting-301801356.html [Accessed 10/10/2023].

19 Telix Pharmaceuticals Limited. *Olaratumab Antibody Licensed from Lilly Demonstrates Proof of Concept as a Theranostic Radiopharmaceutical*. 2023. Available from: https://www.prnewswire.com/news-releases/olaratumab-antibody-licensed-from-lilly-demonstrates-proof-of-concept-as-a-theranostic-radiopharmaceutical-301798405.html [Accessed 10/10/2023].

20 Fusion Pharmaceuticals Inc. *Fusion Pharmaceuticals Announces Presentation of Preclinical Data Supporting FPI-2059 and Leading Targeted Alpha Therapy Platform at AACR Annual Meeting*. 2023. Available from: https://www.newswire.ca/news-releases/fusion-pharmaceuticals-announces-presentation-of-preclinical-data-supporting-fpi-2059-and-leading-targeted-alpha-therapy-platform-at-aacr-annual-meeting-870144630.html [Accessed 10/10/2023].

21 Lantheus. *41st Annual JP Morgan Healthcare Conference*. 2023. Available from: https://investor.lantheus.com/static-files/e8903e6a-93d6-4ef8-a58b-d0492b284564.

22 RayzeBio I. *RayzeBio nominates Glypican-3 (GPC3) targeted radiopharmaceutical therapy drug candidate for treatment of liver cancer*. 2023. Available from: https://rayzebio.com/rayzebio-nominates-glypican-3-gpc3-targeted-radiopharmaceutical-therapy-drug-candidate-for-treatment-of-liver-cancer/ [Accessed 10/10/2023].

23 Hu W, Pan D, Wang Y, Bao W, Zuo C, Guan Y, et al. PET Imaging for Dynamically Monitoring Neuroinflammation in APP/PS1 Mouse Model Using [18F]DPA714. *Frontiers in Neuroscience*. 2020;14:810. Available from: https://doi.org/https://dx.doi.org/10.3389/fnins.2020.00810.

24 Kim K, Kim H, Bae SH, Lee SY, Kim YH, Na J, et al. [18F]CB251 PET/MR imaging probe targeting translocator protein (TSPO) independent of its Polymorphism in a Neuroinflammation Model. *Theranostics*. 2020;10(20):9315-31. Available from: https://doi.org/https://dx.doi.org/10.7150/thno.46875.

25 Liu H, Luo Z, Gu J, Jiang H, Joshi S, Shoghi KI, et al. In vivo Characterization of Four 18F-Labeled S1PR1 Tracers for Neuroinflammation. *Molecular Imaging and Biology*. 2020;22(5):1362-9. Available from: https://doi.org/https://dx.doi.org/10.1007/s11307-020-01514-8.

26 Van Camp N, Balbastre Y, Herard AS, Lavisse S, Tauber C, Wimberley C, et al. Assessment of simplified methods for quantification of [18F]-DPA-714 using 3D whole-brain TSPO immunohistochemistry in a non-human primate. *Journal of Cerebral Blood Flow and Metabolism*. 2020;40(5):1103-16. Available from: https://doi.org/https://dx.doi.org/10.1177/0271678X19859034.

27 Chen X, Yang T, Guo F, Wu C, Liang YK, Wang D. Astudy of 68Ga-FAPIin the imaging of atherosclerosis inNew Zealand rabbits. *Journal of Nuclear Medicine*. 2021;62(SUPPL 1)https://jnm.snmjournals.org/content/62/supplement_1/1233

http://ovidsp.ovid.com/ovidweb.cgi?T=JS&PAGE=reference&D=emed22&NEWS=N&AN=635439906.

28 Song W, Song Y, Qin C, Gai Y, Zhang X, Lan X. Early monitoring of the atherosclerosis plaque formationby 68Ga-DOTA-TATE, 68Ga-LLP2A and F-FDG: Apreliminary study by head-to-head comparation. *Journal of Nuclear Medicine*. 2021;62(SUPPL 1)https://jnm.snmjournals.org/content/62/supplement_1/1230

http://ovidsp.ovid.com/ovidweb.cgi?T=JS&PAGE=reference&D=emed22&NEWS=N&AN=635439895.

29 Stahle M, Hellberg S, Virta J, Liljenback H, Metsala O, Li XG, et al. Evaluation of glucagon-like peptide-1 receptor expression in nondiabetic and diabetic atherosclerotic mice using PET tracer 68Ga-NODAGA-exendin-4. *American Journal of Physiology - Endocrinology and Metabolism*. 2021;320(5):E989-E98. Available from: https://doi.org/https://dx.doi.org/10.1152/AJPENDO.00465.2020.

30 Wang D, Chen X, Yang T, Guo F, Wu C, Liang YK. The availability of the fibroblast activation protein receptor in early identification of vulnerable atherosclerotic plaques: A preclinical study using a 68Ga- FAPIPET. *Journal of Nuclear Medicine*. 2021;62(SUPPL 1)https://jnm.snmjournals.org/content/62/supplement_1/1395

http://ovidsp.ovid.com/ovidweb.cgi?T=JS&PAGE=reference&D=emed22&NEWS=N&AN=635438305.

31 Sivapackiam J, Muthukumar K, Zhou D, Gropler R, Gelman A, Sharma V. 68Ga-Galuminox: A PET Tracer for Imaging Mitochondrial ROS Activity. *Molecular Imaging and Biology*. 2022;24(Supplement 2):S455. Available from: https://doi.org/https://dx.doi.org/10.1007/s11307-022-01794-2.

32 Darwesh A, Wellman R, Abbate V, Cooper MS, Hider R, Morais M, et al. Simple radiosynthesis of 68Ga-desferrioxamine B (68Ga DFO) for infection imaging. *European Journal of Nuclear Medicine and Molecular Imaging*. 2020;47(SUPPL 1):S298. Available from: https://doi.org/https://dx.doi.org/10.1007/s00259-020-04988-4.

33 Petrik M, Umlaufova E, Raclavsky V, Palyzova A, Havlicek V, Pfister J, et al. Preclinical evaluation of 68Ga-Desferal for bacterial infection imaging. *European Journal of Nuclear Medicine and Molecular Imaging*. 2020;47(SUPPL 1):S267-S8. Available from: https://doi.org/https://dx.doi.org/10.1007/s00259-020-04988-4.

34 Hubmann I, Mular A, Gumienna-Kontecka E, Misslinger M, Pfister J, Haas H, et al. Preclinical evaluation of 68ga-labelled artificial siderophores of the ferrioxamine type. *European Journal of Nuclear Medicine and Molecular Imaging*. 2021;48(SUPPL 1):S254-S5. Available from: https://doi.org/https://dx.doi.org/10.1007/s00259-021-05547-1.

35 Petrik M, Umlaufova E, Raclavsky V, Palyzova A, Havlicek V, Pfister J, et al. 68Ga-labelled desferrioxamine-B for bacterial infection imaging. *European Journal of Nuclear Medicine and Molecular Imaging*. 2021;48(2):372-82. Available from: https://doi.org/https://dx.doi.org/10.1007/s00259-020-04948-y.

36 Peukert C, Langer LNB, Wegener SM, Tutov A, Bankstahl JP, Karge B, et al. Optimization of Artificial Siderophores as 68Ga-Complexed PET Tracers for in Vivo Imaging of Bacterial Infections. *Journal of Medicinal Chemistry*. 2021;64(16):12359-78. Available from: https://doi.org/https://dx.doi.org/10.1021/acs.jmedchem.1c01054.

37 Darwesh A, Cooper M, Gibson V, Barrington S, Sallam M, Patel A, et al. Targeting microbial siderophore receptors: first GMP formulation of [68Ga]Ga-DFO for PET imaging of microbial infection. *Nuclear Medicine Communications*. 2022;43(5):578. Available from: https://doi.org/https://dx.doi.org/10.1097/MNM.0000000000001555.

38 Petrik M, Palyzova A, Novy Z, Houst J, Havlicek V, Khoylou M, et al. Monitoring Aspergillus fumigatus infection in rats using 68Ga-siderophores. *European Journal of Nuclear Medicine and Molecular Imaging*. 2022;49(Supplement 1):S18. Available from: https://doi.org/https://dx.doi.org/10.1007/s00259-022-05924-4.

39 Petrik M, Bendova K, Palyzova A, Novy Z, Havlicek V, Popper M, et al. 68Ga-siderophores for imaging Escherichia coli infection: selection of suitable candidates. *EJNMMI Radiopharmacy and Chemistry*. 2023;8(Supplement 1). Available from: https://doi.org/https://dx.doi.org/10.1186/s41181-023-00193-4.

40 Pan X, Zhu J, Xu Z, Xiao Q, Zhou X, Xu K, et al. 68Ga-WRWWWW Is a Potential Positron Emission Tomography Probe for Imaging Inflammatory Diseases by Targeting Formyl Peptide Receptor 2. *Molecular Pharmaceutics*. 2022;19(5):1368-77. Available from: https://doi.org/https://dx.doi.org/10.1021/acs.molpharmaceut.1c00922.

41 Puuvuori E, Liggieri F, Velikyan I, Chiodaroli E, Sigfridsson J, Romelin H, et al. PET-CT imaging of pulmonary inflammation using [68Ga]Ga-DOTA-TATE. *EJNMMI Research*. 2022;12(1):19. Available from: https://doi.org/https://dx.doi.org/10.1186/s13550-022-00892-0.

42 Ku A, Kondo M, Cai Z, Meens J, Li MR, Ailles L, et al. Dose predictions for [177Lu]Lu-DOTA-panitumumab F(ab')2 in NRG mice with HNSCC patient-derived tumour xenografts based on [64Cu]Cu-DOTA-panitumumab F(ab')2 - implications for a PET theranostic strategy. *EJNMMI Radiopharmacy and Chemistry*. 2021;6(1):25. Available from: https://doi.org/https://dx.doi.org/10.1186/s41181-021-00140-1.

43 Zhou R, Shen Y, Jin H, Wang Y. Preclinical Evaluation of [64Cu]NOTA-HFn as a PET Imaging Agent for Radioiodine Refractory Differentiated Thyroid Cancer. *European Journal of Nuclear Medicine and Molecular Imaging*. 2022;49(Supplement 1):S423. Available from: https://doi.org/https://dx.doi.org/10.1007/s00259-022-05924-4.

44 Zhou R, Shen Y, Wang Y, Jin H, Bi L. Preclinical Evaluation of [64Cu/67Cu]NOTA-HFn as a Theranostic Agent for Radioiodine Refractory Differentiated Thyroid Cancer. *Molecular Imaging and Biology*. 2022;24(Supplement 2):S465. Available from: https://doi.org/https://dx.doi.org/10.1007/s11307-022-01794-2.

45 Floberg JM, Wang L, Bandara N, Rashmi R, Mpoy C, Garbow JR, et al. Alteration of Cellular Reduction Potential Will Change 64Cu-ATSM Signal With or Without Hypoxia. *Journal of Nuclear Medicine*. 2020;61(3):427-32. Available from: https://doi.org/https://dx.doi.org/10.2967/jnumed.119.230805.

46 Liu T, Redalen KR, Karlsen M. Development of an automated production process of [64Cu][Cu (ATSM)] for positron emission tomography imaging and theranostic applications. *Journal of Labelled Compounds and Radiopharmaceuticals*. 2022;65(7):191-202. Available from: https://doi.org/https://dx.doi.org/10.1002/jlcr.3973.

47 Cantiello F, Crocerossa F, Cascini GL, Russo GI, Ferro M, Cimino S, et al. 64CuCl2 PET/CT as a potential new imaging method in prostate cancer: illusion or reality? *Minerva urologica e nefrologica = The Italian journal of urology and nephrology*. 2020. Available from: https://doi.org/https://dx.doi.org/10.23736/S0393-2249.20.03615-2.

48 Jiang L. PET Imaging of Lung Cancer with 64CuCl2: A Pilot Study. *European Journal of Nuclear Medicine and Molecular Imaging*. 2020;47(SUPPL 1):S643-S4. Available from: https://doi.org/https://dx.doi.org/10.1007/s00259-020-04988-4.

49 Wang Q, Song D, Ma X, Wu X, Jiang L. Preclinical PET imaging study of lung cancer with 64CuCl2. *Annals of Nuclear Medicine*. 2020;34(9):653-62. Available from: https://doi.org/https://dx.doi.org/10.1007/s12149-020-01491-6.

50 Aljammaz I. Synthesis and in vitro and in vivo evaluation of a new 64Cu-semicarbazone complex: potential theranostic radiopharmaceutical for hypoxic tumor. *Nuclear Medicine and Biology*. 2022;108-109(Supplement):S52. Available from: https://doi.org/https://dx.doi.org/10.1016/S0969-8051%2822%2900138-X.

51 Capriotti G, Piccardo A, Giovannelli E, Signore A. Targeting Copper in Cancer Imaging and Therapy: A New Theragnostic Agent. *Journal of Clinical Medicine*. 2023;12(1):223. Available from: https://doi.org/https://dx.doi.org/10.3390/jcm12010223.

52 Kirk FT, Munk DE, Swenson ES, Quicquaro A, Vendelbo MH, Schilsky M, et al. Effects of tetrathiomolybdate on copper distribution and biliary excretion: a controlled 64CuCl2 PET/MRI. *Journal of Hepatology*. 2023;78(Supplement 1):S985. Available from: https://doi.org/https://dx.doi.org/10.1016/S0168-8278%2823%2903042-8.

53 Watabe T, Liu Y, Kaneda-Nakashima K, Shirakami Y, Lindner T, Ooe K, et al. Theranostics targeting fibroblast activation protein in the tumor stroma: 64Cu- And 225Ac-labeled FAPI-04 in pancreatic cancer xenograft mouse models. *Journal of Nuclear Medicine*. 2020;61(4):563-9. Available from: https://doi.org/https://dx.doi.org/10.2967/jnumed.119.233122.

54 Belissant O, Dumulon-Perreault V, Milot M, Ben-Salem I, Croteau E, Ait-Mohand S, et al. Use of the fibroblast activation protein inhibitor [64Cu] Cu-DOTHA2-FAPI-04 to overcome heterogeneity in prostate cancer. *European Journal of Nuclear Medicine and Molecular Imaging*. 2021;48(SUPPL 1):S15-S6. Available from: https://doi.org/https://dx.doi.org/10.1007/s00259-021-05547-1.

55 Ghai A. Immuno PET imaging of CS1/SLAMF7 in multiple myeloma using Zr DFO elotuzumab. *Journal of Nuclear Medicine*. 2020;61(Supplement 1)http://ovidsp.ovid.com/ovidweb.cgi?T=JS&PAGE=reference&D=emed21&NEWS=N&AN=633250958.

56 Novy Z, Janousek J, Barta P, Petrik M, Hajduch M, Trejtnar F. Preclinical evaluation of anti-VEGFR2 monoclonal antibody ramucirumab labelled with zirconium-89 for tumour imaging. *Journal of Labelled Compounds and Radiopharmaceuticals*. 2021;64(7):262-70. Available from: https://doi.org/https://dx.doi.org/10.1002/jlcr.3909.

57 Jagoda EM, Basuli F, Olkowski C, Weiss I, Phelps TE, Wong K, et al. Immuno-PET Imaging of Siglec-15 Using the Zirconium-89-Labeled Therapeutic Antibody, NC318. *Molecular Imaging*. 2023;2023:3499655. Available from: https://doi.org/https://dx.doi.org/10.1155/2023/3499655.

58 Yang Y, Wang J, Liu W, Deng H, Zhao P, Liao W, et al. 89Zr and 177Lu labeling of anti-DR5 monoclonal antibody for colorectal cancer targeting PET-imaging and radiotherapy. *Journal of Radioanalytical and Nuclear Chemistry*. 2021;330(3):997-1005. Available from: https://doi.org/https://dx.doi.org/10.1007/s10967-021-07979-3.

59 Lau WL, Liang C, Liu H, Singh K, Mukherjee J. Development of zirconium-89 PET for in vivo imaging of alpha-klotho. *American Journal of Nuclear Medicine and Molecular Imaging*. 2020;10(2):95-105http://www.ajnmmi.us/files/ajnmmi0110442.pdf

http://ovidsp.ovid.com/ovidweb.cgi?T=JS&PAGE=reference&D=emed21&NEWS=N&AN=2004292965.

60 Zhang Y, Cheng D. Preclinical ImmunoPET Imaging of Gastric cancer- Infiltrating Myeloid Cells Using Zirconium-89 Labeled Anti-CDiib Antibody. *Journal of Nuclear Medicine*. 2021;62(SUPPL 1)https://jnm.snmjournals.org/content/62/supplement_1/1512

http://ovidsp.ovid.com/ovidweb.cgi?T=JS&PAGE=reference&D=emed22&NEWS=N&AN=635438243.

61 Krache A, Fontan C, Pestourie C, Bardies M, Bouvet Y, Payoux P, et al. Preclinical Pharmacokinetics and Dosimetry of an 89Zr Labelled Anti-PDL1 in an Orthotopic Lung

Cancer Murine Model. *Frontiers in Medicine*. 2022;8:741855. Available from: https://doi.org/https://dx.doi.org/10.3389/fmed.2021.741855.

62 Medicines and Healthcare products Regulatory Agency (MHRA). *MetaTrace FDG Solution for Injection Summary of Product Characteristics*.

63 Giammarile F, Castellucci P, Dierckx R, Estrada Lobato E, Farsad M, Hustinx R, et al. Non-FDG PET/CT in Diagnostic Oncology: a pictorial review. *Eur J Hybrid Imaging*. 2019;3(1):20. Available from: https://doi.org/10.1186/s41824-019-0066-2.

64 Royal College of Radiologists. Evidence-based indications for the use of PET-CT in the United Kingdom 2022. London: 2022.

65 Medicines and Healthcare products Regulatory Agency (MHRA). *Cardiogen-82 3.3–5.6 GBq radionuclide generator: SUmmary of Product Characteristics*

66 Giesel FL, Adeberg S, Syed M, Lindner T, Jiménez-Franco LD, Mavriopoulou E, et al. FAPI-74 PET/CT using either 18F-AlF or cold-kit 68Ga labeling: biodistribution, radiation dosimetry, and tumor delineation in lung cancer patients. *Journal of Nuclear Medicine*. 2021;62(2):201-7.

67 Natarajan A. Copper-64-immunoPET imaging: bench to bedside. *The Quarterly Journal of Nuclear Medicine and Molecular Imaging: Official Publication of the Italian Association of Nuclear Medicine (AIMN)[and] the International Association of Radiopharmacology (IAR),[and] Section of the Society of*. 2020;64(4):356-63. Available from: https://doi.org/10.23736/S1824-4785.20.03310-5.

68 Parakh S, Lee ST, Gan HK, Scott AM. Radiolabeled Antibodies for Cancer Imaging and Therapy. *Cancers*. 2022;14(6):1454. Available from: https://doi.org/10.3390/cancers14061454.

Appendix 1. Preclinical studies search strategy

Database: Embase (Ovid) <1974 to 2023 August 28>

Date of search: 29th August 2023

Records retrieved: 2,620

Search strategy:

1	positron emission tomography/ or whole body pet/	171713
2	(((PET or positron*) and (tracer* or tomograph* or imaging)) or positron emi*).mp.	288154
3	copper 62/ or copper 64/ or copper 67/ or fluorine 18/ or gallium 68/ or gallium 68 plus germanium 68/ or nitrogen 13/ or oxygen 15/ or rubidium 82/ or scandium 46/ or zirconium 89/	48943
4	(Cu or Copper* or 62Cu* or 62-Cu* or Cu62 or Cu-62 or 62Copper* or 64Cu* or 64-Cu* or Cu64 or Cu-64 or 64Copper* or 67Cu* or 67-Cu* or Cu67 or Cu-67 or 67Copper*).ti,hw,kf.	217940
5	(Fluori* or 18F* or 18-F* or F18 or F-18 or 18fluori*).ti,hw,kf.	209787
6	(Gallium* or 68Ga* or 68-Ga* or Ga688 or Ga-68 or 68gallium*).ti,hw,kf.	34154
7	(Nitro* or 13N* or 13-N* or N13 or N-13 or 13nitro*).ti,hw,kf.	609272
8	(Oxygen* or 15O* or 15-O* or O15 or O-15 or 15Oxygen*).ti,hw,kf.	962288
9	(Rubidi* or 82Rb* or 82-Rb* or Rb82 or Rb-82 or 82Rubidi*).ti,hw,kf.	11313
10	(Sc or Scandium* or 46Sc* or 46-Sc* or Sc46 or Sc-46 or 46Scandium*).ti,hw,kf.	10970

11	(Zr* or Zircon* or 89Zr* or 89-Zr* or Zr89 or Zr-89 or 89zircon*).ti,hw,kf.	28344
12	(or/3-11) and (1 or 2)	125902
13	limit 12 to yr="2020 -Current"	32539
14	exp *element/	1114812
15	exp *radiopharmaceutical agent/	133138
16	exp *"imaging and display"/	600763
17	exp *isotope labeling/	12542
18	*isotope analysis/	1758
19	exp *radioisotope/	128814
20	or/14-19	1904058
21	20 and 13	16365
22	preclinical study/	56391
23	(preclinical or pre-clinical).ti,hw,kf.	87345
24	"proof of concept"/	21820
25	exploratory research/	34351
26	(developing or development or develop or novel*).ti.	1251979
27	(exp animal/ not (exp human/ or exp human experiment/)) or (exp animal experiment/ or exp animal model/ or nonhuman/)	9506540
28	or/22-27	10347479
29	21 and 28	3199
30	29 not exp clinical study/	2620

Appendix 2. Clinical trials search strategy

Source: Clinicaltrials.gov, ScanMedicine

Date: 19th June 2023

Records retrieved: 5,816

Source	Search terms	Results
Clinicaltrials.gov	18F, Fluorine-18, N-13, O-15, Ga-68, Rb-82, Zr, Cu, Sc	5,214
ScanMedicine	18F, Fluorine-18, N-13, O-15, Ga-68, Rb-82, Zr, Cu, Sc	660
58 behavioural studies were removed from the total 5874 downloaded clinical trials prior to sifting.		

Appendix 3. Non-industry sponsors

Sponsors	Radionuclides	Location	EU or UK
Aarhus University Hospital	Cu	UK/EU	EU
AHS Cancer Control Alberta	F	US/Canada	
AHS Cancer Control Alberta|Cross Cancer Institute	F	US/Canada	
Alan Nichol|British Columbia Cancer Agency	F	US/Canada	
Amsterdam UMC - location VUmc	F	UK/EU	EU
Amsterdam UMC, location VUmc|ZonMw: The Netherlands Organisation for Health Research and Development	F	UK/EU	EU
Amsterdam UMC, VU University Medical Center	F	UK/EU	EU
Amsterdam University Medical Center - location VUmc	F	UK/EU	EU
Andrei Iagaru|Canary Foundation|Boston University|Stanford University	F	US/Canada	
Andrei Iagaru|National Cancer Institute (NCI)|Stanford University	F	US/Canada	
Andrei Iagaru|Stanford University	Zr	US/Canada	
Anna Raciborska|Maria Sklodowska-Curie National Research Institute of Oncology|Åukasiewicz Research Network|WrocÅ‚aw University of Environmental and Life Sciences|Institute of Mother and Child, Warsaw, Poland	F	UK/EU	EU

Antoni van Leeuwenhoek Hospital-Nuclear Medicine department	Zr	UK/EU	EU
Aou Di Bologna Policlinico S.Orsola-Malpighi	Ga	UK/EU	EU
Asan Foundation	F	ROW	
Asan Medical Center	F	ROW	
Assistance Publique - HÃ´pitaux de Paris|Pierre and Marie Curie University	F	UK/EU	EU
Assistance Publique - Hopitaux De PARIS (AP-HP)	F	UK/EU	EU
Assistance Publique Hopitaux De Marseille	F	UK/EU	EU
Azienda Ospedaliera Arcispedale S. Maria Nuova	F	UK/EU	EU
Azienda Ospedaliera Di Bologna Policlinico S. Orsola M. Malpighi	F	UK/EU	EU
Azienda Ospedaliera Ospedali Galliera	F	UK/EU	EU
Azienda Ospedaliera Sant'Andrea	Ga	UK/EU	EU
Azienda Ospedaliera Universitaria Careggi	F	UK/EU	EU
Azienda Ospedaliera Universitaria Integrata Verona	F	UK/EU	EU
Azienda Ospedaliero -Universitaria Pisana	F	UK/EU	EU
Azienda USL Di Forli'	F	UK/EU	EU
Barts Health NHS Trust	F	UK/EU	UK
Brigham and Women's Hospital	Zr	US/Canada	
Brigham and Women's Hospital|U.S. Army Medical Research Acquisition Activity	F	US/Canada	
Brigham and Women's Hospital|U.S. Army Medical Research and Development Command|Boston University	F	US/Canada	
British Columbia Cancer Agency|Canadian Institutes of Health Research (CIHR)	F	US/Canada	
Bundeswehr	F	UK/EU	EU
Cancer Institute and Hospital, Chinese Academy of Medical Sciences	F	ROW	
Canisius Wilhelmina Hospital	F	UK/EU	EU
Catharina Hospital Eindhoven	F	UK/EU	EU
CEA	F	UK/EU	EU
Cedars-Sinai Medical Center	F	US/Canada	
Central Hospital, Nancy, France	Ga	Location Unknown	

Centre de recherche du Centre hospitalier universitaire de Sherbrooke|Canadian Cancer Society (CCS)|UniversitÃ© de Sherbrooke	F	US/Canada	
Centre de recherche du Centre hospitalier universitaire de Sherbrooke|UniversitÃ© de Sherbrooke	F	US/Canada	
Centre Franois Baclesse	F	UK/EU	EU
Centre Francois Baclesse	F	UK/EU	EU
Centre Georges-Franois Leclerc	F	UK/EU	EU
Centre hospitalier de l'UniversitÃ© de MontrÃ©al (CHUM)	F	US/Canada	
Centre Hospitalier Universitaire de Caen Normandie	O	UK/EU	EU
Centre Hospitalier Universitaire de la RÃ©union	F	UK/EU	EU
Chang Gung Memorial Hospital	Ga	ROW	
Chang Gung Memorial Hospital|National Science Council, Taiwan	F	ROW	
Charite University, Berlin, Germany	F	UK/EU	EU
Children's Hospital of Philadelphia|University of Pennsylvania	F	US/Canada	
CHRU de Brest	F	Worldwide	
CHU de Bordeaux	F	UK/EU	EU
CHU de Caen	F	UK/EU	EU
CHU de la R union	F	UK/EU	EU
CHU de N mes	F	UK/EU	EU
CHU Toulouse	F	UK/EU	EU
City of Hope Medical Center|National Cancer Institute (NCI)	Cu	US/Canada	
Cliniques Universitaires Saint Luc	F	UK/EU	EU
Columbia University	F	US/Canada	
Columbia University|Hebrew Home at Riverdale|National Institute on Aging (NIA)	F	US/Canada	
Columbia University|National Institute of Neurological Disorders and Stroke (NINDS)	F	US/Canada	
Consorci Mar Parc de Salut de Barcelona (Parc de Salut MAR)	F	UK/EU	EU
Dae Hyuk Moon|Asan Medical Center	F	ROW	
David M. Schuster, MD|Emory University	F	US/Canada	
Department of Endocrinology, Sahlgrenska University Hospital	Ga	UK/EU	EU

Department of Neurology, Medical University of Vienna	F	UK/EU	EU
Department of Nuclear Medicine and Endocrinology, Paracelsus Medical University Salzburg	F	UK/EU	EU
Department of Nuclear Medicine, Aalborg University Hospital	Ga	UK/EU	EU
Deutsches Krebsforschungszentrum (DKFZ), Stiftung des ffentlichen Rechts	Ga	UK/EU	EU
Dr. Markus Hartenbach|German Federal Armed Forces	F	UK/EU	EU
Eastern Health, Canada	F	Location Unknown	
ECOG-ACRIN Cancer Research Group|Eastern Cooperative Oncology Group	F	US/Canada	
ECOG-ACRIN Cancer Research Group|National Cancer Institute (NCI)|Eastern Cooperative Oncology Group	F	US/Canada	
Edward D Huey, MD|National Institute on Aging (NIA)|Columbia University	F	US/Canada	
Emory University	Ga	US/Canada	
Emory University|National Cancer Institute (NCI)	F	US/Canada	
Ente Ospedaliero Ospedali Galliera	F, Cu	UK/EU	EU
Erasmus Medical Center	F	UK/EU	EU
Eunice Kennedy Shriver National Institute of Child Health and Human Development (NICHD)|National Institute of Diabetes and Digestive and Kidney Diseases (NIDDK)|National Institutes of Health Clinical Center (CC)	F, Ga	US/Canada	
First Affiliated Hospital of Fujian Medical University	F	ROW	
Fondazione IRCCS Ca' Granda Ospedale Maggiore Policlinico Di Milano	F	UK/EU	EU
Fondazione Toscana Gabriele Monasterio	F	UK/EU	EU
Frederick Daniel Grant|Dana-Farber Cancer Institute|Boston Children's Hospital	F	US/Canada	
Fundaci ACE-Institut Catal de Neuroci ncies Aplicades	F	UK/EU	EU
Fundaci Cl nic per a la Recerca Biom dica	F	UK/EU	EU

Fundaci n P blica Andaluza para la Gesti n de la Investigaci n en Salud de Sevilla	F	UK/EU	EU
Fundacion Clinic per a la Recerca BiomÃ©dica	F	Location Unknown	
G.A.P. Hospers|University Medical Center Groningen	F	UK/EU	EU
Geriatric Centre, Ume University hospital	F	UK/EU	EU
German Cancer Research Center|ABX CRO|Friedrich-Alexander-UniversitÃ¤t Erlangen-NÃrnberg|University Hospital Freiburg	Ga	UK/EU	EU
German Oncology Center	F	UK/EU	EU
Ghent University Hospital	F	UK/EU	EU
Glenn Bauman|Western University, Canada|United States Department of Defense|Centre for Probe Development and Commercialization|Lawson Health Research Institute	F	US/Canada	
Gustave Roussy, Cancer Campus, Grand Paris	F	UK/EU	EU
Heike E Daldrup-Link|Stanford University	F	US/Canada	
Hoag Memorial Hospital Presbyterian	F	US/Canada	
Hospices Civils de Lyon	F	UK/EU	EU
Hospital Universitario Dr. Negrin	F	UK/EU	EU
Institut Cancerologie de l'Ouest|Fondation ARC	Cu	UK/EU	EU
Institut Cancerologie de l'Ouest|Siric Iliad	F	UK/EU	EU
Institut Curie	F	UK/EU	EU
Institut de cancerologie Strasbourg Europe	F	Location Unknown	
Institut De Cancerologie De L'ouest	F	UK/EU	EU
Institut de Recerca HSCSP	F	UK/EU	EU
Institute for Neurodegenerative Disorders	F	UK/EU	EU
Institute of Nuclear Energy Research, Taiwan	Ga	ROW	
Istituti Fisioterapici Ospitalieri	F	UK/EU	EU
Istituto Europeo Di Oncologia	F	UK/EU	EU
Istituto Neurologico Mediterraneo Neuromed	F	UK/EU	EU
Istituto Scientifico Romagnolo per lo Studio e la cura dei Tumori	F	UK/EU	EU
Istituto Scientifico Romagnolo Per Lo Studio E La Cura Dei Tumori (IRST) S.R.L. IRCCS	F	UK/EU	EU
Jae Seung Kim|Asan Medical Center	F	ROW	

Jae Seung Kim|Korea Health Industry Development Institute|Samsung Medical Center|Asan Medical Center	F	ROW	
James Brugarolas|University of Texas Southwestern Medical Center	Zr	US/Canada	
James M Noble, MD, MS, CPH, FAAN|National Institute on Aging (NIA)|Columbia University	F	US/Canada	
Joan Albert Barbera Mir|Hospital Clinic of Barcelona	F	Location Unknown	
Jonsson Comprehensive Cancer Center	Ga	US/Canada	
Jonsson Comprehensive Cancer Center|National Cancer Institute (NCI)	Ga	US/Canada	
Jules Bordet Institute	Ga	UK/EU	EU
Karolinska University Hospital	Ga	UK/EU	EU
King's College London	F	UK/EU	UK
KU Leuven	F	UK/EU	EU
Leiden Universitair Medisch Centrum	F	UK/EU	EU
Leiden University Medical Center	Zr	UK/EU	EU
Lek rska fakulta Univerzity Komensk ho v Bratislave	Ga	UK/EU	EU
Lida Jafari|University of California, Los Angeles|VA Greater Los Angeles Healthcare System	F	US/Canada	
M.D. Anderson Cancer Center|National Cancer Institute (NCI)|Trevarx Biomedical, Inc	F	US/Canada	
Maastricht University Medical Center	F	UK/EU	EU
MAASTRO Clinic	F	UK/EU	EU
Marcelo F. Di Carli, MD, FACC|Brigham and Women's Hospital	F	US/Canada	
Masaryk v onkologick stav	F	UK/EU	EU
Massachusetts General Hospital	F	US/Canada	
Massachusetts General Hospital|National Heart, Lung, and Blood Institute (NHLBI)	Cu	US/Canada	
Mayo Clinic	Ga	US/Canada	
Mayo Clinic|National Cancer Institute (NCI)	Ga	US/Canada	
Mayo Clinic|National Cancer Institute (NCI)|United States Department of Defense	Ga	US/Canada	
Medical University Innsbruck	Ga	UK/EU	EU
Medical University of Vienna, Department of Biomedical Imaging and Image-guided Therapy	F	UK/EU	EU

Medizinische Universit t Innsbruck	Ga	UK/EU	EU
Medizinische Universit t Wien, Univ.Klinik f.Radiodiagnostik	F	UK/EU	EU
Memorial Sloan Kettering Cancer Center	F	US/Canada	
Memorial Sloan Kettering Cancer Center|National Cancer Institute (NCI)	F	US/Canada	
Memorial Sloan Kettering Cancer Center|Weill Medical College of Cornell University|Broad Institute	Zr	US/Canada	
Michael Graham PhD, MD|University of Iowa	Ga	US/Canada	
Michael Graham PhD, MD|University of Iowa|Holden Comprehensive Cancer Center	Ga	US/Canada	
Michael Graham|Holden Comprehensive Cancer Center|University of Iowa	Ga	US/Canada	
Michael J. Fox Foundation for Parkinson's Research|Institute for Neurodegenerative Disorders	F	US/Canada	
Miguel Pampaloni|University of California, San Francisco	F	US/Canada	
Mikkel Holm Vendelbo	F	UK/EU	EU
MUW-Medical University of Vienna,Medizinische Universit t Wien	F	UK/EU	EU
Nanjing Medical University	F	ROW	
Nantes University Hospital	F	UK/EU	EU
National Cancer Institute (NCI)	F	US/Canada	
National Cancer Institute (NCI)|National Institutes of Health Clinical Center (CC)	F	US/Canada	
National Cancer Institute (NCI)|NRG Oncology	F	US/Canada	
National Institute of Diabetes and Digestive and Kidney Diseases (NIDDK)|National Institutes of Health Clinical Center (CC)	Ga	US/Canada	
National Institute of Mental Health (NIMH)|National Institutes of Health Clinical Center (CC)	F	US/Canada	
National Institutes of Health Clinical Center (CC)	F	US/Canada	
National Taiwan University Hospital	F	ROW	
Neil M Rofsky, MD, MHA|University of Texas Southwestern Medical Center	F	US/Canada	

Norbert Avril, M.D.|Case Comprehensive Cancer Center	Ga	US/Canada	
Northwestern University|National Cancer Institute (NCI)	F	US/Canada	
Nottingham University Hospitals NHS Trust	F	UK/EU	UK
Odense University Hospital	F	UK/EU	EU
OHSU Knight Cancer Institute|National Cancer Institute (NCI)|Oregon Health and Science University|Weill Cornell University	F	US/Canada	
Ontario Clinical Oncology Group (OCOG)|Ontario Ministry of Health and Long Term Care	F	US/Canada	
Ospedale Classificato Equiparato Sacro Cuore Don Calabria - Presidio Ospedaliero Accreditato	F	UK/EU	EU
Ospedale San Raffaele	F	UK/EU	EU
Oxford University Hospitals NHS Trust	F	UK/EU	UK
Peking Union Medical College Hospital	Ga	ROW	
Peter MacCallum Cancer Centre, Australia	F	ROW	
Policlinico Universitario Agostino Gemelli	F	UK/EU	EU
Princess M xima Center for pediatric oncology	F	UK/EU	EU
Queen's Medical Center|National Cancer Institute (NCI)	F	US/Canada	
Radboud University Medical Center	F	UK/EU	EU
Radboud University Medical Center|Amsterdam UMC, location VUmc|University Medical Center Groningen|MMC Hopsital Veldvoven (Department of Surgery)	F	UK/EU	EU
Radboudumc	F	UK/EU	EU
Rahul Aggarwal|National Cancer Institute (NCI)|U.S. Army Medical Research Acquisition Activity|University of California, San Francisco	Cu	US/Canada	
Region Sk ne	F	UK/EU	EU
Rigshospitalet	Cu	UK/EU	EU
Rigshospitalet, Denmark	F, Cu	UK/EU	EU
Sanjiv Sam Gambhir|National Cancer Institute (NCI)|Stanford University	F	US/Canada	
Shanghai Chest Hospital	F	Location Unknown	
Sidney Kimmel Comprehensive Cancer Center at Johns Hopkins	F	US/Canada	

Sidney Kimmel Comprehensive Cancer Center at Johns Hopkins|National Cancer Institute (NCI)	F	US/Canada	
Sir Mortimer B. Davis - Jewish General Hospital	F	US/Canada	
St. Antonius Hospital	Ga	UK/EU	EU
St. Jude Children's Research Hospital	N	US/Canada	
Stanford University	F	US/Canada	
Stanford University School of Medicine	F	Worldwide	
Stanford University|National Cancer Institute (NCI)	Ga	US/Canada	
Stanford University|National Institutes of Health (NIH)	F	US/Canada	
Stockholm County Council	F	UK/EU	EU
Sue O'Dorisio|National Cancer Institute (NCI)|University of Iowa	Ga	US/Canada	
Sue O'Dorisio|University of Iowa	Ga	US/Canada	
The European Uro-Oncology Group|Centre for Human Drug Research, Netherlands	F	UK/EU	EU
Thomas Hope|Conquer Cancer Foundation|Gateway for Cancer Research|Prostate Cancer Foundation|University of California, San Francisco	Ga	US/Canada	
Thomas Hope|University of California, San Francisco	F	US/Canada	
Tianjin Medical University Cancer Institute and Hospital	F	Location Unknown	
tichting Het Nederlands Kanker Instituut_Antoni van Leeuwenhoek	F	UK/EU	EU
Tim Lau|McGill University|The Royal Ottawa Mental Health Centre	F	Location Unknown	
Turku PET Centre	F	UK/EU	EU
Turku University Hospital	F	UK/EU	EU
UMC Utrecht	F	UK/EU	EU
UMCG	F	UK/EU	EU
Ume University Hospital	F	UK/EU	EU
UNC Lineberger Comprehensive Cancer Center	Ga	US/Canada	
Univ.-Kl.f.Nuklearmedizin Wien	F	UK/EU	EU
Universit del Piemonte Orientale	F	UK/EU	EU

Universit t Heidelberg, Medizinische Fakult t Mannheim	F	UK/EU	EU
Universitair Ziekenhuis Brussel|Kom Op Tegen Kanker|Agentschap voor Innovatie door Wetenschap en Technologie, Project Toegepast Biomedisch onderzoek met een primair Maatschappelijke finaliteit.	Ga	UK/EU	EU
Universitaire Ziekenhuizen KU Leuven|University Hospital, Antwerp|University Hospital, Ghent|Netwerk, Belgium	F	UK/EU	EU
University College, London|Cancer Research UK|Imperial College London|National Cancer Imaging Translational Accelerator	F	UK/EU	UK
University Cologne	F	UK/EU	EU
University Health Network, Toronto|Princess Margaret Hospital, Canada	F	US/Canada	
University Hospital Ghent	F	UK/EU	EU
University Hospital Maastricht	F	UK/EU	EU
University Hospital of Montpellier	F	UK/EU	EU
University Hospital Tuebingen	F	UK/EU	EU
University Hospital, Bordeaux	F	UK/EU	EU
University Hospital, Brest	F	UK/EU	EU
University Hospital, Caen	F	UK/EU	EU
University Hospital, Ghent	F	UK/EU	EU
University Hospital, Ghent|Kom Op Tegen Kanker	F	UK/EU	EU
University Hospital, Tours	F	UK/EU	EU
University Medical Center Groningen	Zr	UK/EU	EU
University Medical Center Groningen, Department of Rheumatology and Clinical Immunology	F	UK/EU	EU
University of Aarhus|Danish Cancer Society	F	UK/EU	EU
University of Aarhus|GCP-unit at Aarhus University Hospital, Aarhus, Denmark|REDCap	F	Location Unknown	
University of Alabama at Birmingham	F	US/Canada	
University of Alberta	F	US/Canada	
University of Alberta|Alberta Health services	F	US/Canada	
University of Alberta|Canadian Urological Association Scholarship Foundation	F	US/Canada	
University of British Columbia|British Columbia Cancer Agency	F	US/Canada	

University of Calgary	F	US/Canada	
University of California, San Francisco	Ga	US/Canada	
University of California, San Francisco|National Cancer Institute (NCI)	F	US/Canada	
University of Cologne	F	UK/EU	EU
University of Edinburgh	F	Worldwide	
University of Iowa|National Cancer Institute (NCI)|National Institutes of Health (NIH)	F	US/Canada	
University of Lausanne Hospitals|Swiss Heart Foundation	Ga	UK/EU	EU
University of Leipzig	F	UK/EU	EU
University of Leuven	F	UK/EU	EU
University of Manitoba|Winnipeg Regional Health Authority	F	US/Canada	
University of Michigan	Ga	US/Canada	
University of North Carolina, Chapel Hill|Eunice Kennedy Shriver National Institute of Child Health and Human Development (NICHD)	F	US/Canada	
University of North Carolina, Chapel Hill|North Carolina Translational and Clinical Sciences Institute	F	US/Canada	
University of Pennsylvania	F	US/Canada	
University of Pennsylvania|Brigham and Women's Hospital|University of Maryland|Yale University|Washington University School of Medicine|The Cardiovascular Medical Research and Education Fund	F	US/Canada	
University of Saskatchewan	Zr	US/Canada	
University of Texas Southwestern Medical Center	F	US/Canada	
University of Utah	F	US/Canada	
University of Washington	Ga	US/Canada	
University of Wisconsin, Madison	F	US/Canada	
University of Wisconsin, Madison|National Cancer Institute (NCI)	F	US/Canada	
VA Greater Los Angeles Healthcare System	F	US/Canada	

Vanderbilt University Medical Center|Vanderbilt Kennedy Center	F	US/Canada	
Vanderbilt-Ingram Cancer Center|National Cancer Institute (NCI)	F	US/Canada	
VU University Medical Center	F	UK/EU	EU
Washington University School of Medicine	F	US/Canada	
Washington University School of Medicine|National Cancer Institute (NCI)	F	US/Canada	
Washington University School of Medicine|St. Louis Children's Hospital	F	US/Canada	
Weill Medical College of Cornell University	Zr, Ga	US/Canada	
Weill Medical College of Cornell University|Cornell University	Ga	US/Canada	
West Virginia University	F, Ga	US/Canada	
Wuerzburg University Hospital|Charite University, Berlin, Germany|Heinrich-Heine University, Duesseldorf|University Hospital, Essen|Johannes Gutenberg University Mainz|Ludwig-Maximilians - University of Munich|Hannover Medical School|University of Leipzig|University of Florence|University of Padova|Cambridge University Hospitals NHS Foundation Trust|University Medical Center Nijmegen|Uppsala University Hospital|Assistance Publique - HÃ´pitaux de Paris|University of Vienna	F	UK/EU	EU
Xiangya Hospital of Central South University	F	ROW	
Xijing Hospital	F, Ga	Location Unknown	
	F	Location Unknown	

Appendix 4. Preclinical studies for Scandium, Rubidium, Oxygen and Nitrogen

The following list includes a total of 43 studies retrieved from Embase (Ovid) that included one of the relevant radionuclides (Sc, Rb, O or N) in title and that were not anaysed using visualisation of similarities.

1. Record no. 1 Ashworth, E. T., Ogawa, R., Vera, D. and Lindholm, P. (2023). **A novel method for tracking nitrogen kinetics in vivo and ex vivo using radioactive nitrogen-13 gas and Positron Emission Tomography.** bioRxiv https://doi.org/https://dx.doi.org/10.1101/2023.06.01.543280.

> Rationale Decompression sickness (DCS) is caused by gaseous nitrogen dissolved in tissues forming bubbles during decompression. To date no method exists to identify nitrogen within tissues, but with advances in PET technology it may be possible to track gaseous radionuclides into tissues. We aimed to develop a method to track nitrogen movement in vivo that could then be used to further our understanding of DCS using nitrogen-13 (13N2) - a radioactive isotope of nitrogen that emits beta+ radiation. Methods A single anesthetized and ventilated Sprague Dawley rat lay supine inside a PET scanner for 30 min. The rat breathed oxygen for the first 2 min, then was switched to a bag containing 13N2 gas mixed with oxygen for 20 min, then breathed oxygen alone for the final 8 min. Gas samples were drawn from the inspiratory line at 5, 15 and 25 min. The PET scanner recorded 13N2 with energy windows of 250-750 keV. Following the scan, a mixed blood sample was taken from the heart, while the brain, liver, femur and thigh muscle were removed to determine organ radioactivity using a gamma counter. Results The gas samples at 5 (5.7 kbq.ml-1) and 15 min (5.3 kbq.ml-1) showed radioactivity in the inspired gas that was absent at 25 min (0.1 kbq.ml-1), when the 13N2 was stopped. The signal intensity in the PET scanner increased from baseline (0.03) to 2-12 min (0.68+/-0.31), and 12-22 min (0.88+/-0.06), before reducing slightly from 22-30 min (0.61+/-0.04). All organs had radioactivity when measured in the gamma counter, with the highest counts in the liver (12593 counts.min-1.g-1) and the lowest in the muscle (2687 counts.min-1.g-1). Principal Conclusions This study successfully demonstrated a quantitative 3D imaging method of tracking nitrogen gas through the body both in vivo and ex vivo using PET.Copyright The copyright holder for this preprint is the author/funder, who has granted bioRxiv a license to display the preprint in perpetuity. It is made available under a CC-BY-NC-ND 4.0 International license.

2. Record no. 507 Benabdallah, N., Zhang, H., Unnerstall, R., Fears, A., Summer, L., Fassbender, M., Rodgers, B. E., Abou, D., Radchenko, V. and Thorek, D. L. J. (2023). **Engineering a modular 44Ti/44Sc generator: eluate evaluation in preclinical models and estimation of human radiation dosimetry.** EJNMMI Research 13(1): 17 https://doi.org/https://dx.doi.org/10.1186/s13550-023-00968-5.

> Background: 44Sc/47Sc is an attractive theranostic pair for targeted in vivo positron emission tomographic (PET) imaging and beta-particle treatment of cancer. The 44Ti/44Sc generator allows daily onsite production of this diagnostic isotope, which

may provide an attractive alternative for PET facilities that lack in-house irradiation capabilities. Early animal and patient studies have demonstrated the utility of 44Sc. In our current study, we built and evaluated a novel clinical-scale 44Ti/44Sc generator, explored the pharmacokinetic profiles of 44ScCl3, [44Sc]-citrate and [44Sc]-NODAGA (1,4,7-triazacyclononane,1-glutaric acid-4,7-acetic acid) in naive mice, and estimated the radiation burden of 44ScCl3 in humans. Method(s): 44Ti/44Sc (101.2 MBq) in 6 M HCl solution was utilized to assemble a modular ZR resin containing generator. After assembly, 44Sc was eluted with 0.05 M HCl for further PET imaging and biodistribution studies in female Swiss Webster mice. Based on the biodistribution data, absorbed doses of 44/47ScCl3 in human adults were calculated for 18 organs and tissues using the IDAC-Dose software. Result(s): 44Ti in 6 M HCl was loaded onto the organic resin generator with a yield of 99.97%. After loading and initial stabilization, 44ScCl3 was eluted with 0.05 M HCl in typical yields of 82.9 +/- 5.3% (N = 16), which was normalized to the estimated generator capacity. Estimated generator capacity was computed based on elution time interval and the total amount of 44Ti loaded on the generator. Run in forward and reverse directions, the 44Sc/44Ti ratio from a primary column was significantly improved from 1038 +/- 440 to 3557 +/- 680 (Bq/Bq) when a secondary, replaceable, ZR resin cartridge was employed at the flow outlet. In vivo imaging and ex vivo distribution studies of the reversible modular generator for 44ScCl3, [44Sc]-citrate and [44Sc]-NODAGA show that free 44Sc remained in the circulation significantly longer than the chelated 44Sc. The dose estimation of 44ScCl3 reveals that the radiation burden is 0.146 mSv/MBq for a 70 kg adult male and 0.179 mSv/MBq for a 57 kg adult female. Liver, spleen and heart wall will receive the highest absorbed dose: 0.524, 0.502, and 0.303 mGy/MBq, respectively, for the adult male. Conclusion(s): A clinical-scale 44Ti/44Sc generator system with a modular design was developed to supply 44ScCl3 in 0.05 M HCl, which is suitable for further radiolabeling and in vivo use. Our data demonstrated that free 44ScCl3 remained in the circulation for extended periods, which resulted in approximately 10 times greater radiation burden than stably chelated 44Sc. Stable 44Sc/47Sc-complexation will be more favorable for in vivo use and for clinical utility.Copyright © 2023, The Author(s).

3. Record no. 225 Biondetti, E., Cho, J. and Lee, H. (2023). **Cerebral oxygen metabolism from MRI susceptibility.** NeuroImage 276: 120189 https://doi.org/https://dx.doi.org/10.1016/j.neuroimage.2023.120189.

This article provides an overview of MRI methods exploiting magnetic susceptibility properties of blood to assess cerebral oxygen metabolism, including the tissue oxygen extraction fraction (OEF) and the cerebral metabolic rate of oxygen (CMRO2). The first section is devoted to describing blood magnetic susceptibility and its effect on the MRI signal. Blood circulating in the vasculature can have diamagnetic (oxyhemoglobin) or paramagnetic properties (deoxyhemoglobin). The overall balance between oxygenated and deoxygenated hemoglobin determines the induced magnetic field which, in turn, modulates the transverse relaxation decay of the MRI signal via additional phase accumulation. The following sections of this review then illustrate the principles underpinning susceptibility-based techniques for quantifying OEF and CMRO2. Here, it is detailed whether these techniques provide global (OxFlow) or local (Quantitative Susceptibility Mapping - QSM, calibrated BOLD - cBOLD, quantitative BOLD - qBOLD, QSM+qBOLD) measurements of OEF or CMRO2, and what signal components

(magnitude or phase) and tissue pools they consider (intravascular or extravascular). Validations studies and potential limitations of each method are also described. The latter include (but are not limited to) challenges in the experimental setup, the accuracy of signal modeling, and assumptions on the measured signal. The last section outlines the clinical uses of these techniques in healthy aging and neurodegenerative diseases and contextualizes these reports relative to results from gold-standard PET.Copyright © 2023

4. Record no. 722 Chen, S. X., Zhang, J., Xue, F., Liu, W., Kuang, Y., Gu, B., Song, S. and Chen, H. (2023). **In situ forming oxygen/ROS-responsive niche-like hydrogel enabling gelation-triggered chemotherapy and inhibition of metastasis.** Bioactive Materials 21: 86-96 https://doi.org/https://dx.doi.org/10.1016/j.bioactmat.2022.08.002.

Though the development of the diverse hypoxia-activated prodrugs (HAPs) has made great progresses in the last several decades, current cancer therapy based on HAPs still suffers many obstacles, e.g., poor therapeutic outcome owing to hard deep reaching to hypoxic region, and the occurrence of metastasis due to hypoxia. Inspired by engineered niches, a novel functional chitosan polymer (CS-FTP) is synthesized for construction of a hydrogel-based bio-niche (CS-FTP-gel) in aiming at remodeling tumor hypoxic microenvironment. The CS-FTP polymers are crosslinked to form a niche-like hydrogel via enzyme-mediated oxygen-consumable dimerization after injected into tumor, in which a HAP (i.e., AQ4N) could be physically encapsulated, resulting in enhanced tumor hypoxia to facilitate AQ4N-AQ4 toxic transformation for maximizing efficacy of chemotherapy. Furthermore, Pazopanib (PAZ) conjugated onto the CS backbone via ROS-sensitive linker undergoes a stimuli-responsive release behavior to promote antiangiogenesis for tumor starvation, eventually contributing to the inhibition of lung metastasis and synergistic action with AQ4N-based chemotherapy for an orthotopic 4T1 breast tumor model. This study provides a promising strategy for hypoxia-based chemotherapy and demonstrates an encouraging clinical potential for multifunctional hydrogel applicable for antitumor treatment.Copyright © 2022 The Authors

5. Record no. 117 Kvitastein, U. A., Kumarananthan, C. P., Fiskeseth, N. G. and Adamsen, T. C. H. (2023). **Production and separation of the PET-radionuclide Ti-45 from a liquid nat-Sc target for ligand complexation.** EJNMMI Radiopharmacy and Chemistry 8(Supplement 1) https://doi.org/https://dx.doi.org/10.1186/s41181-023-00193-4.

Aim: The most common PET-radionuclides are unsuitable for imaging of some physiological processes due to their short (e.g. C-11, Ga-68) or long half-lives (e.g. Zr-89, Cu-64). They either result in insufficient imaging or excessive radiation exposure. Titanium-45 is a promising PET-radionuclide with a half-life of 3.08 h. It has favorable decay characteristics for PET-imaging (85% positron decay) and has previously been produced in a cyclotron via the Sc-45(p,n)Ti-45 reaction by using a solid target [1, 2]. The aim of this study is to optimize the production of Ti-45 using a liquid target. Then isolate Ti-45 from the target material and other impurities formed during irradiation, using solid phase extraction (SPE) and liquid-liquid extraction (LLE) for further complexations with ligands. This to form a foundation for later development of radiopharmaceuticals labeled with Ti-45 for use in PET imaging. Material(s) and

Method(s): The liquid target was prepared by dissolving Sc(NO3)3 3H2O in HNO3. Using a PET Trace 860 cyclotron equipped with a PETtrace 800 68Ga Liquid target, different concentrations (1.0-2.5 M) Sc(NO3)3 were irradiated with a 14.3 MeV proton beam for 60-180 min with a beam-current of 20-30 muA. In the SPE approach the cyclotron product was loaded onto a ZR-resin, then the Sc-species were washed out with HCl, and finally Ti-45 was eluted using a ligand. This method was also automated using the FASTlabTM 2 synthesizer. In the LLE approach a mixture of guaiacol/anisole was used to extract Ti-45 from the aqueous phase into the organic phase. The phases were separated using a centrifuge and isolated. The organic phase was then mixed with different ligand solutions for complexation. The cyclotron product and the separation fractions were analyzed with gamma-ray spectrometry and the formation of the complexes was confirmed with radio-HPLC. A full factorial design was used to optimize the Ti-45 activity. Result(s): Gamma-ray spectrometry revealed EOB activities of Ti-45 ranging from 0.40 to 1.17 GBq in the cyclotron product. Co-production of radionuclidic impurities, i.e. Sc-44, Sc-44 and Mo-93m were found, and trace amounts of Ti-44 were also detected. The radionuclidic purity of the cyclotron product ranged from 85.5 to 99.3 %. Gammaray spectrometry of each separation fraction from the SPEs indicates impurities being washed out with HCl, and most of Ti-45 being eluted out by the ligand solution. For the LLEs the gamma-ray data show higher activity of Ti-45 in the organic phase, compared to the aqueous phase. Radio-HPLC of the [Ti-45]-ligand complexes shows peaks with retention times close to the retention times of cold reference Ti-ligand complexes. Conclusion(s): The productions resulted in Ti-45 activities ranging from 0.40 to 1.17 GBq (EOB) with a radionuclidic purity between 85.5% and 99.3%. Radionuclidic impurities, i.e, Sc-44, Sc-44m and Mo-93m were found, including trace amounts of Ti-44. Using lower currents and irradiation times yielded lower amounts of impurities. A model of the irradiation parameters and Ti-45 activities reveals that a combination of low current and irradiation time, and high concentration of both Sc(NO3)3 and HNO3 yields the highest Ti-45 activities. The complexation of Ti-45 with two different ligands was successfully achieved, utilizing both SPE and LLE for isolation of Ti-45. The SPE was also successfully automated by using the FASTlabTM 2 synthesizer. Further work includes isolating and refining the Ti-45 radiotracer from the complexation process through the use of semi-preparative HPLC. It is also necessary to study the biodistribution of the Ti-45 radionuclide. This is planned in two steps: (1) Ti-45 radiotracer distribution itself in healthy mice (2) biodistribution of a Ti-45 labeled biomolecule in a relevant cancer model.

6. Record no. 392 Pinchuk, A. N., Rampy, M. A., Longino, M. A., Durkee, B. Y., Counsell, R. E. and Weichert, J. P. (2023). **Effect of Polar Head Group Modifications on the Tumor Retention of Phospholipid Ether Analogs: Role of the Quaternary Nitrogen.** Pharmaceutics 15(1): 171 https://doi.org/https://dx.doi.org/10.3390/pharmaceutics15010171.

We have previously described the remarkable capacity of radioiodinated alkyl phospholipids to be sequestered and retained by a variety of tumors in vivo. We have already established the influence of certain structural parameters of iodinated alkyl phospholipids on tumor avidity, such as stereochemistry at the sn-2 carbon of alkylglycerol phosphocholines, meta-or para-position of iodine in the aromatic ring of phenylalkyl phosphocholines, and the length of the alkyl chain in alkyl phospholipids. In order to determine the additional structural requirements for tumor uptake and

retention, three new radioiodinated alkylphospholipid analogs, 2-4, were synthesized as potential tumor imaging agents. Polar head groups were modified to determine structure-tumor avidity relationships. The trimethylammonio group in 1 was substituted with a hydrogen atom in 2, an ammonio group in 3 and a tertiary butyl group in 4. All analogs were separately labeled with iodine-125 or iodine-124 and administered to Walker 256 tumor-bearing rats or human PC-3 tumor-bearing SCID mice, respectively. Tumor uptake was assessed by gamma-camera scintigraphy (for [I-125]-labeled compounds) and high-resolution micro-PET scanning (for [I-124]-labeled compounds). It was found that structural modifications in the polar head group of alkyl phospholipids strongly influenced the tumor uptake and tissue distribution of these compounds in tumor-bearing animals. Phosphoethanolamine analog 3 (NM401) displayed a very slight accumulation in tumor as compared with phosphocholine analog 1 (NM346). Analogs 2 (NM400) and 4 (NM402) lacking the positively charged nitrogen atom failed to display any tumor uptake and localized primarily in the liver. This study provided important insights regarding structural requirements for tumor uptake and retention. Replacement of the quaternary nitrogen in the alkyl phospholipid head group with non-polar substituents resulted in loss of tumor avidity.Copyright © 2023 by the authors.

7. Record no. 28 Trencsenyi, G. and Kepes, Z. (2023). **Scandium-44: Diagnostic Feasibility in Tumor-Related Angiogenesis.** International Journal of Molecular Sciences 24(8): 7400 https://doi.org/https://dx.doi.org/10.3390/ijms24087400.

Angiogenesis-related cell-surface molecules, including integrins, aminopeptidase N, vascular endothelial growth factor, and gastrin-releasing peptide receptor (GRPR), play a crucial role in tumour formation. Radiolabelled imaging probes targeting angiogenic biomarkers serve as valuable vectors in tumour identification. Nowadays, there is a growing interest in novel radionuclides other than gallium-68 (68Ga) or copper-64 (64Cu) to establish selective radiotracers for the imaging of tumour-associated neo-angiogenesis. Given its ideal decay characteristics (Ebeta + average: 632 KeV) and a half-life (T1/2 = 3.97 h) that is well matched to the pharmacokinetic profile of small molecules targeting angiogenesis, scandium-44 (44Sc) has gained meaningful attention as a promising radiometal for positron emission tomography (PET) imaging. More recently, intensive research has been centered around the investigation of 44Sc-labelled angiogenesis-directed radiopharmaceuticals. Previous studies dealt with the evaluation of 44Sc-appended avb3 integrin-affine Arg-Gly-Asp (RGD) tripeptides, GRPR-selective aminobenzoyl-bombesin analogue (AMBA), and hypoxia-associated nitroimidazole derivatives in the identification of various cancers using experimental tumour models. Given the tumour-related hypoxia- and angiogenesis-targeting capability of these PET probes, 44Sc seems to be a strong competitor of the currently used positron emitters in radiotracer development. In this review, we summarize the preliminary preclinical achievements with 44Sc-labelled angiogenesis-specific molecular probes.Copyright © 2023 by the authors.

8. Record no. 373 Unak, P., Yasakci, V., Tutun, E., Karatay, K. B., Walczak, R., Wawrowicz, K., Zelechowska-Matysiak, K., Majkowska-Pilip, A. and Bilewicz, A. (2023). **Multimodal Radiobioconjugates of Magnetic Nanoparticles Labeled with 44Sc and 47Sc for Theranostic Application.** Pharmaceutics 15(3): 850

https://doi.org/https://dx.doi.org/10.3390/pharmaceutics15030850.

This study was performed to synthesize multimodal radiopharmaceutical designed for the diagnosis and treatment of prostate cancer. To achieve this goal, superparamagnetic iron oxide (SPIO) nanoparticles were used as a platform for targeting molecule (PSMA-617) and for complexation of two scandium radionuclides, 44Sc for PET imaging and 47Sc for radionuclide therapy. TEM and XPS images showed that the Fe3O4 NPs have a uniform cubic shape and a size from 38 to 50 nm. The Fe3O4 core are surrounded by SiO2 and an organic layer. The saturation magnetization of the SPION core was 60 emu/g. However, coating the SPIONs with silica and polyglycerol reduces the magnetization significantly. The obtained bioconjugates were labeled with 44Sc and 47Sc, with a yield higher than 97%. The radiobioconjugate exhibited high affinity and cytotoxicity toward the human prostate cancer LNCaP (PSMA+) cell line, much higher than for PC-3 (PSMA-) cells. High cytotoxicity of the radiobioconjugate was confirmed by radiotoxicity studies on LNCaP 3D spheroids. In addition, the magnetic properties of the radiobioconjugate should allow for its use in guide drug delivery driven by magnetic field gradient.Copyright © 2023 by the authors.

9. Record no. 134 Waddle, S. L., Garza, M., Ying, C., Davis, L. T., Jordan, L. C., An, H. and Donahue, M. J. (2023). **Vascular space occupancy asymmetric spin echo (VASO-ASE) for non-invasive quantification of cerebral oxygen extraction fraction.** Magnetic Resonance in Medicine 90(1): 211-221 https://doi.org/https://dx.doi.org/10.1002/mrm.29618.

Purpose: Asymmetric spin echo (ASE) MRI is a method for measuring regional oxygen extraction fraction (OEF); however, extravascular tissue models have been shown to under-estimate OEF. The hypothesis investigated here is that the addition of a vascular-space-occupancy (VASO) pre-pulse will more fully suppress blood water signal and provide global OEF values more consistent with physiological expectation and 15O positron emission tomography (PET)-validated T2-relaxation-under-spin-tagging (TRUST) OEF measures. Method(s): Healthy adults (n = 14; age = 27.7 +/- 5.2 y; sex = 7/7 male/female) were scanned at 3.0T. Multi-echo ASE without inter-readout refocusing (ASERF-), multi-echo ASE with inter-readout refocusing (ASERF+), and single-echo VASO-ASE were acquired twice each with common spatial resolution = 3.44 x 3.44 x 3.0 mm and tau = 0-20 ms (interval = 0.5 ms). TRUST was acquired twice sequentially for independent global OEF assessment (tauCPMG = 10 ms; effective TEs = 0, 40, 80, and 160 ms; spatial resolution = 3.4 x 3.4 x 5 mm). OEF intraclass-correlation-coefficients (ICC), summary statistics, and group-wise differences were assessed (Wilcoxon rank-sum; significance: two-sided $p < 0.05$). Result(s): ASERF+ (OEF = 36.8 +/- 1.9%) and VASO-ASE (OEF = 34.4 +/- 2.3%) produced OEF values similar to TRUST (OEF = 36.5 +/- 4.6%, human calibration model; OEF = 32.7 +/- 4.9%, bovine calibration model); however, ASERF- yielded lower OEF (OEF = 26.1 +/- 1.0%; $p < 0.01$) relative to TRUST. VASO-ASE (ICC = 0.61) yielded lower ICC compared to other ASE variants (ICC >0.89). Conclusion(s): VASO-ASE and TRUST provide similar OEF values; however, VASO-ASE spatial coverage and repeatability improvements are required.Copyright © 2023 International Society for Magnetic Resonance in Medicine.

10. Record no. 671 Bentsen, S., Bang, L. E., Hasbak, P., Kjaer, A. and Ripa, R. S. (2022). **Amiodarone attenuates cardiac Rubidium-82 in consecutive PET/CT scans in a rodent model.**

Journal of Nuclear Cardiology 29(6): 2853-2862 https://doi.org/https://dx.doi.org/10.1007/s12350-021-02785-6.

Background: Risk stratification and diagnosis using Rubidium-82 (82Rb) positron emission tomography (PET) is a routine clinical approach in coronary artery disease (CAD). Various drugs are used to treat CAD; however, whether any of them change the uptake of 82Rb in the heart has not been investigated. The aim of this study is to determine whether drugs used in treatment of CAD affect the uptake of 82Rb in the heart in healthy rats. Method(s): Seventy-seven Sprague-Dawley rats were included in the cross-sectional study. All rats underwent baseline 82Rb PET/CT and divided into eleven groups treated with different drugs. One group was control group (no treatment), eight groups were treated with monotherapy (amiodarone, acetylsalicylic acid (ASA), clopidogrel, ticagrelor, atorvastatin, enalapril, amlodipine, metoprolol succinate), and two groups were treated with polypharmacy (ASA, ticagrelor, atorvastatin, amlodipine or ASA, clopidogrel, atorvastatin, amlodipine). Once a day, they were administered pharmacological therapy through oral gavage, and on day seven, follow-up scanned with 82Rb PET/CT. Result(s): In the control group without pharmacological treatment, no difference in the standard uptake value (SUV) ratio between heart and muscle from baseline to follow-up (5.8 vs 7.0, P = .3) was found. The group treated with amiodarone had a significantly reduced SUV ratio from baseline to follow-up (5.8 vs 5.1, P = .008). All other drugs investigated had no difference in SUV ratio from baseline to follow-up. Conclusion(s): In this study, we showed that drugs normally used to treat CAD do not affect the uptake of 82Rb. However, amiodarone result in a significantly lowered 82Rb uptake, compared to control. This information about amiodarone would probably not change the size assessment of a myocardial perfusion defect in a clinical setting. However, it could change the kinetic parameters when assessing absolute myocardial blood flow in patients treated with amiodarone.Copyright © 2021, American Society of Nuclear Cardiology.

11. Record no. 1238 Csupasz, T., Szucs, D., Kalman, F. K., Holloczki, O., Fekete, A., Szikra, D., Toth, E., Toth, I. and Tircso, G. (2022). **A New Oxygen Containing Pyclen-Type Ligand as a Manganese(II) Binder for MRI and 52Mn PET Applications: Equilibrium, Kinetic, Relaxometric, Structural and Radiochemical Studies.** Molecules (Basel, Switzerland) 27(2) https://doi.org/https://dx.doi.org/10.3390/molecules27020371.

A new pyclen-3,9-diacetate derivative ligand (H23,9-OPC2A) was synthesized possessing an etheric O-atom opposite to the pyridine ring, to improve the dissociation kinetics of its Mn(II) complex (pyclen = 3,6,9,15-tetraazabicyclo(9.3.1)pentadeca-1(15),11,13-triene). The new ligand is less basic than the N-containing analogue (H23,9-PC2A) due to the non-protonable O-atom. In spite of its lower basicity, the conditional stability of the [Mn(3,9-OPC2A)] (pMn = -log(Mn(II)), cL = cMn(II) = 0.01 mM. pH = 7.4) remains unaffected (pMn = 8.69), compared to the [Mn(3,9-PC2A)] (pMn = 8.64). The [Mn(3,9-OPC2A)] possesses one water molecule, having a lower exchange rate with bulk solvents (kex298 = 5.3 +/- 0.4 x 107 s-1) than [Mn(3,9-PC2A)] (kex298 = 1.26 x 108 s-1). These mild differences are rationalized by density-functional theory (DFT) calculations. The acid assisted dissociation of [Mn(3,9-OPC2A)] is considerably slower (k1 = 2.81 +/- 0.07 M-1 s-1) than that of the complexes of diacetates or bisamides of various 12-membered macrocycles and the parent H23,9-PC2A. The [Mn(3,9-OPC2A)]

is inert in rat/human serum as confirmed by 52Mn labeling (nM range), as well as by relaxometry (mM range). However, a 600-fold excess of EDTA (pH = 7.4) or a mixture of essential metal ions, propagated some transchelation/transmetalation in 7 days. The H23,9-OPC2A is labeled efficiently with 52Mn at elevated temperatures, yet at 37 degreeC the parent H23,9-PC2A performs slightly better. Ultimately, the H23,9-OPC2A shows advantageous features for further ligand designs for bifunctional chelators.

12. Record no. 919 Huang, L., Fang, J., Hong, S., Liu, H., Zhu, H., Feng, L., Zhuang, R., Zhao, X., Guo, Z. and Zhang, X. (2022). **MicroPET imaging of bacterial infection with nitroreductase-specific responsive 18F-labelled nitrogen mustard analogues.** European Journal of Nuclear Medicine and Molecular Imaging 49(8): 2645-2654 https://doi.org/https://dx.doi.org/10.1007/s00259-022-05710-2.

Purpose: Bacterial infection and antibiotic resistance are serious threats to human health. This study aimed to develop two novel radiotracers, 18F-NTRP and 18F-NCRP, that possess a specific nitroreductase (NTR) response to image deep-seated bacterial infections using positron emission tomography (PET). This method can distinguish infection from sterile inflammation. Method(s): 18F-NTRP and 18F-NCRP were synthesized via a one-step method; all the steps usually involved in tracer radiosynthesis were successfully adapted in the All-In-One automated module. After the physiochemical properties of 18F-NTRP and 18F-NCRP were characterized, their specificity and selectivity for NTR were verified in E. coli and S. aureus. The ex vivo biodistribution of the tracers was evaluated in normal mice. MicroPET-CT imaging was performed in mouse models of bacterial infection and inflammation after the administration of 18F-NTRP or 18F-NCRP. Result(s): Fully automated radiosynthesis of 18F-NTRP and 18F-NCRP was achieved within 90-110 min with overall decay-uncorrected, isolated radiochemical yields of 21.24 +/- 4.25% and 11.3 +/- 3.78%, respectively. The molar activities of 18F-NTRP and 18F-NCRP were 320 +/- 40 GBq/mumol and 275 +/- 33 GBq/micromol, respectively. In addition, 18F-NTRP and 18F-NCRP exhibited high selectivity and specificity for NTR response. PET-CT imaging in bacteria-infected mouse models with 18F-NTRP or 18F-NCRP showed significant radioactivity uptake in either E. coli- or S. aureus-infected muscles. The uptake for E. coli-infected muscles, 2.4 +/- 0.2%ID/g with 18F-NTRP and 4.05 +/- 0.49%ID/g with 18F-NCRP, was up to three times greater than that for uninfected control muscles. Furthermore, for both 18F-NTRP and 18F-NCRP, the uptake in bacterial infection was 2.6 times higher than that in sterile inflammation, allowing an effective distinction of infection from inflammation. Conclusion(s): 18F-NTRP and 18F-NCRP are worth further investigation to verify their potential clinical application for distinguishing bacterial infection from sterile inflammation via their specific NTR responsiveness.Copyright © 2022, The Author(s), under exclusive licence to Springer-Verlag GmbH Germany, part of Springer Nature.

13. Record no. 950 Jensen, M., Bentsen, S., Clemmensen, A., Jensen, J. K., Madsen, J., Rossing, J., Laier, A., Hasbak, P., Kjaer, A. and Ripa, R. S. (2022). **Feasibility of positron range correction in 82-Rubidium cardiac PET/CT.** EJNMMI Physics 9(1): 51 https://doi.org/https://dx.doi.org/10.1186/s40658-022-00480-0.

Background: Myocardial perfusion imaging (MPI) using positron emission tomography (PET) tracers is an essential tool in investigating diseases and treatment responses in cardiology. 82Rubidium (82Rb)-PET imaging is advantageous for MPI due to its short half-life, but cannot be used for small animal research due to the long positron range. We aimed to correct for this, enabling MPI with 82Rb-PET in rats. Method(s): The effect of positron range correction (PRC) on 82Rb-PET was examined using two phantoms and in vivo on rats. A NEMA NU-4-inspired phantom was used for image quality evaluation (%standard deviation (%SD), spillover ratio (SOR) and recovery coefficient (RC)). A cardiac phantom was used for assessing spatial resolution. Two rats underwent rest 82Rb-PET to optimize number of iterations, type of PRC and respiratory gating. Result(s): NEMA NU-4 metrics (no PRC vs PRC): %SD 0.087 versus 0.103; SOR (air) 0.022 versus 0.002, SOR (water) 0.059 versus 0.019; RC (3 mm) 0.219 versus 0.584, RC (4 mm) 0.300 versus 0.874, RC (5 mm) 0.357 versus 1.197. Cardiac phantom full width at half maximum (FWHM) and full width at tenth maximum (FWTM) (no PRC vs. PRC): FWTM 6.73 mm versus 3.26 mm (true: 3 mm), FWTM 9.27 mm versus 7.01 mm. The in vivo scans with respiratory gating had a homogeneous myocardium clearly distinguishable from the blood pool. Conclusion(s): PRC improved the spatial resolution for the phantoms and in vivo at the expense of slightly more noise. Combined with respiratory gating, the spatial resolution achieved using PRC should allow for quantitative MPI in small animals.Copyright © 2022, The Author(s).

14. Record no. 918 Narciso, L., Ssali, T., Liu, L., Jesso, S., Hicks, J. W., Anazodo, U., Finger, E. and St Lawrence, K. (2022). **Noninvasive Quantification of Cerebral Blood Flow Using Hybrid PET/MR Imaging to Extract the [15O]H2O Image-Derived Input Function Free of Partial Volume Errors.** Journal of Magnetic Resonance Imaging 56(4): 1243-1255 https://doi.org/https://dx.doi.org/10.1002/jmri.28134.

Background: Quantification of cerebral blood flow (CBF) with [15O]H2O-positron emission tomography (PET) requires arterial sampling to measure the input function. This invasive procedure can be avoided by extracting an image-derived input function (IDIF); however, IDIFs are sensitive to partial volume errors due to the limited spatial resolution of PET. Purpose(s): To present an alternative hybrid PET/MR imaging of CBF (PMRFlowIDIF) that uses phase-contrast (PC) MRI measurements of whole-brain (WB) CBF to calibrate an IDIF extracted from a WB [15O]H2O time-activity curve. Study Type: Technical development and validation. Animal Model: Twelve juvenile Duroc pigs (83% female). Population: Thirteen healthy individuals (38% female). Field Strength/Sequences: 3 T; gradient-echo PC-MRI. Assessment: PMRFlowIDIF was validated against PET-only in a porcine model that included arterial sampling. CBF maps were generated by applying PMRFlowIDIF and two previous PMRFlow methods (PC-PET and double integration method [DIM]) to [15O]H2O-PET data acquired from healthy individuals. Statistical Tests: PMRFlow and PET CBF measurements were compared with regression and correlation analyses. Paired t-tests were performed to evaluate differences. Potential biases were assessed using one-sample t-tests. Reliability was assessed by intraclass correlation coefficients. Statistical significance: (Formula presented.) = 0.05. Result(s): In the animal study, strong agreement was observed between PMRFlowIDIF (average voxel-wise CBF, 58.0 +/- 16.9 mL/100 g/min) and PET (63.0 +/- 18.9 mL/100 g/min). In the human study, PMRFlowDIM (y = 1.11x - 5.16, R2 = 0.99 +/- 0.01) and PMRFlowPC-PET (y = 0.87x + 3.82, R2 = 0.97 +/-

0.02) performed similarly to PMRFlowIDIF, and CBF was within the expected range (eg, 49.7 +/- 7.2 mL/100 g/min for gray matter). Data Conclusion(s): Accuracy of PMRFlowIDIF was confirmed in the animal study with the primary source of error attributed to differences in WB CBF measured by PC MRI and PET. In the human study, differences in CBF from PMRFlowIDIF, PMRFlowDIM, and PMRFlowPC-PET were due to the latter two not accounting for blood-borne activity. Level of Evidence: 2. Technical Efficacy Stage: 1.Copyright © 2022 International Society for Magnetic Resonance in Medicine.

15. Record no. 1189 Phipps, M., Cingoranelli, S., Lewis, J., Lapi, S., Cutler, C., Francesconi, L. and Deri, M. (2022). **Evaluation of 3,4,3-LI(1,2-HOPO) as a chelator for radioscandium based radiopharmaceuticals.** Nuclear Medicine and Biology 108-109(Supplement): S155-S156 https://doi.org/https://dx.doi.org/10.1016/S0969-8051%2822%2900331-6.

Objectives: A few different radioscandium nuclides, including 43Sc (t1/2 = 3.89 h, beta+ max = 1.20 MeV, BRbeta+ = 70.9%), 44Sc (t1/2 = 3.97 h, beta+ max = 1.47 MeV, BRbeta+ = 94.3%), and 47Sc (t1/2 = 3.35 d, beta- max = 0.6 MeV, BRbeta- = 100%, gamma = 157 keV, BRgamma = 68%) have decay properties that are suitable for use in radiopharmaceuticals.1 Both 43Sc and 44Sc are suited for use in positron emission tomography (PET) imaging, and 47Sc has emissions suitable for single photon emission computed tomography (SPECT) imaging as well as targeted radiotherapy. In the pursuit of designing constructs for use with these nuclides, an optimized ligand is desired. 3,4,3-LI(1,2-HOPO) (referred to as HOPO) is an octadentate ligand with oxygen donor groups that has demonstrated high affinity and fast formation kinetics for hard positively charged (+3, +4) metal ions.2,3,4 Methods: HOPO was synthesized as previously reported with minor adjustments.4 Macroscopic Sc-HOPO was characterized by X-ray crystallography, mass spectrometry, 1H-NMR, and 45Sc-NMR. Radiolabeling of HOPO or DOTA was performed with either 43Sc, 44Sc, or 47Sc and verified by ITLC and HPLC. 47Sc-HOPO was evaluated with an in vitro EDTA challenge study and an in vivo biodistribution study in healthy Balb/c female mice. Biodistribution with free 47Sc was also performed. 43Sc-HOPO was used for PET imaging in healthy mice over 90 min p/i with biodistribution being performed immediately after the end of the PET scan. Result(s): Non-radioactive, macroscopic Sc-HOPO has been characterized thoroughly. All nuclides of radioscandium used here radiolabeled HOPO with > 95% radiochemical yield after 1 h at 37degreeC. Synthesis of the desired complex was verified by HPLC coinjection with a macroscopic standard. In vitro EDTA challenge against 47Sc-radiolabeled constructs showed comparable stability of 47Sc-HOPO and 47Sc-DOTA with both having > 90% stability at 7d. Biodistribution with either 47Sc-HOPO or 43Sc-HOPO showed high in vivo stability with rapid hepatobiliary excretion. In 47Sc-HOPO, < 1% ID/g remained in any organ at 24 h. Conclusion(s): Macroscopic Sc-HOPO has been thoroughly characterized. Radioscandium complexes of HOPO have been synthesized using 43Sc, 44ScSc, and 47Sc at 37degreeC. 43Sc-HOPO and 47Sc-HOPO exhibited high in vivo stability. Future work will expand to the use of bifunctional HOPO variants to evaluate radiolabeled bioconjugates of radioscandium and HOPO in diseased mouse models using an appropriate biological targeting molecule. Acknowledgements: Supported by the Tow Foundation Graduate Fellowship from the MSKCC Center for Molecular Imaging and Nanotechnology, DOE IP# ST5001020, DESC0020197, NSF-DGE

0965983, and the National Institute of General Medical Sciences of the National Institutes of Health under Award Number SC2GM130464

16. Record no. 647 Shimochi, S., Ihalainen, J., Parikka, V., Kokkomaki, E., Forsback, S., Tolvanen, T., Yatkin, E., Gronroos, T. J. and Iida, H. (2022). **Longitudinal Assessment of Cerebral Oxygen Metabolism in a Rat Model of Neonatal Hypoxic-Ischemic Encephalopathy using PET with Spontaneous Inhalation of 15O-Labeled Oxygen Gases.** European Journal of Nuclear Medicine and Molecular Imaging 49(Supplement 1): S429 https://doi.org/https://dx.doi.org/10.1007/s00259-022-05924-4.

Aim/Introduction: Perinatal hypoxic-ischemic encephalopathy (HIE) is the leading cause of irreversible brain damage resulting in serious neurological dysfunction with high interindividual variability. Hypothermia is well-established therapy but has limited clinical benefits. The present study aimed to evaluate the feasibility of the PET imaging methodology with spontaneous inhalation of 15O-labeled gases (15O-PET), which provides cerebral oxygen metabolic parameters, to assess the pathophysiological progression of cerebral tissue damage in a rat model of neonatal HIE. Material(s) and Method(s): HIE was induced in nine-day-old rats with permanent ligation of the left common carotid artery followed by hypoxia (8% oxygen) for 120min. PET imaging was carried out essentially as reported by Temma et al.[1], except for the sophisticated radio-gas scavenging system implemented in the animal holder. Sequential 15O-PET scans were performed on days 1, 2, 7, and 14 after the insult in HIE (n=5) and normal pups without any insult (n=4). In each scan, a series of 15O-labeled gases were inhaled spontaneously and cerebral oxygen metabolic parameters including cerebral blood flow (CBF) and cerebral metabolic rate for oxygen (CMRO2) were calculated from the functional parametric images. After the last PET scan, brains were removed and histologically examined with H&E and Iba1 staining. Result(s): The implemented system succeeded in the efficient supply of 15O-labeled gases mixed with isoflurane to the animals and allowed the evacuation of excess 15O-gas around the body. CBF and CMRO2 in the ipsilateral side brains of HIE pups decreased remarkably on day 2 after the insult to 72.7+/-7.4% and 51.1+/-9.1% respectively compared to the contralateral sides, and then gradually recovered over 14 days in line with the increasing trend of those values in normal pups according to their natural aging process, while microglial activation was present around the infarct tissues in histology. The increasing trend in CMRO2 after the insult could be attributed to the development of neuronal cells and the increased neurotransmitter function in growing infants. Conclusion(s): The present 15O-PET system enabled sequential evaluations of progressive cerebral tissue damage and the recovery process associated with an early developmental period of the immature brain after hypoxic-ischemic insult in rat neonates. This completely noninvasive imaging strategy without the need for tracheostomy or blood sampling could be of value for assessing new supportive therapeutics which could potentially enhance the neuroprotective effects of hypothermia in neonatal HIE with highly individualized in vivo follow-up.

17. Record no. 673 Werner, R. A., Rowe, S. P. and Higuchi, T. (2022). **No major impact of prescribed CAD drugs on myocardial perfusion uptake derived by [82]rubidium PET.** Journal of Nuclear Cardiology 29(6): 2863-2865 https://doi.org/https://dx.doi.org/10.1007/s12350-

021-02786-5.

18. Record no. 1478 Ding, D., Feng, Y., Qin, R., Li, S., Chen, L., Jing, J., Zhang, C., Sun, W., Li, Y., Chen, X. and Chen, H. (2021). **Mn3+-rich oxide/persistent luminescence nanoparticles achieve light-free generation of singlet oxygen and hydroxyl radicals for responsive imaging and tumor treatment.** Theranostics 11(15): 7439-7449 https://doi.org/https://dx.doi.org/10.7150/THNO.59056.

X-ray excited persistent luminescence (XEPL) imaging has attracted increasing attention in biomedical imaging due to elimination of autofluorescence, high signal-to-noise ratio and repeatable activation with high penetration. However, optical imaging still suffers from limited for high spatial resolution. Method(s): Herein, we report Mn3+-rich manganese oxide (MnOx)-coated chromium-doped zinc gallogermanate (ZGGO) nanoparticles (Mn-ZGGOs). Enhanced XEPL and magnetic resonance (MR) imaging were investigated by the decomposition of MnOxshell in the environment of tumors. We also evaluated the tumor cell-killing mechanism by detection of reactive oxygen (ROS), lipid peroxidation and mitochondrial membrane potential changes in vitro. Furthermore, the in vivo biodistribution, imaging and therapy were studied by U87MG tumor-bearing mice. Result(s): In the tumor region, the MnOxshell is quickly decomposed to produce Mn3+and oxygen (O2) to directly generate singlet oxygen (1O2). The resulting Mn2+transforms endogenous H2O2into highly toxic hydroxyl radical (OH) via a Fenton-like reaction. The Mn2+ions and ZGGOs also exhibit excellent T1-weighted magnetic resonance (MR) imaging and ultrasensitive XEPL imaging in tumors. Conclusion(s): Both the responsive dual-mode imaging and simultaneous self-supplied O2for the production of 1O2and oxygen-independent OH in tumors allow for more accurate diagnosis of deep tumors and more efficient inhibition of tumor growth without external activation energy.

19. Record no. 1443 Fang, H., Gai, Y., Wang, S., Liu, Q., Zhang, X., Ye, M., Tan, J., Long, Y., Wang, K., Zhang, Y. and Lan, X. (2021). **Biomimetic oxygen delivery nanoparticles for enhancing photodynamic therapy in triple-negative breast cancer.** Journal of Nanobiotechnology 19(1): 81 https://doi.org/https://dx.doi.org/10.1186/s12951-021-00827-2.

Background: Triple-negative breast cancer (TNBC) is a kind of aggressive breast cancer with a high rate of metastasis, poor overall survival time, and a low response to targeted therapies. To improve the therapeutic efficacy and overcome the drug resistance of TNBC treatments, here we developed the cancer cell membrane-coated oxygen delivery nanoprobe, CCm-HSA-ICG-PFTBA, which can improve the hypoxia at tumor sites and enhance the therapeutic efficacy of the photodynamic therapy (PDT), resulting in relieving the tumor growth in TNBC xenografts. Result(s): The size of the CCm-HSA-ICG-PFTBA was 131.3 +/- 1.08 nm. The in vitro 1O2 and ROS concentrations of the CCm-HSA-ICG-PFTBA group were both significantly higher than those of the other groups (P < 0.001). In vivo fluorescence imaging revealed that the best time window was at 24 h post-injection of the CCm-HSA-ICG-PFTBA. Both in vivo 18F-FMISO PET imaging and ex vivo immunofluorescence staining results exhibited

that the tumor hypoxia was significantly improved at 24 h post-injection of the CCm-HSA-ICG-PFTBA. For in vivo PDT treatment, the tumor volume and weight of the CCm-HSA-ICG-PFTBA with NIR group were both the smallest among all the groups and significantly decreased compared to the untreated group (P < 0.01). No obvious biotoxicity was observed by the injection of CCm-HSA-ICG-PFTBA till 14 days. Conclusion(s): By using the high oxygen solubility of perfluorocarbon (PFC) and the homologous targeting ability of cancer cell membranes, CCm-HSA-ICG-PFTBA can target tumor tissues, mitigate the hypoxia of the tumor microenvironment, and enhance the PDT efficacy in TNBC xenografts. Furthermore, the HSA, ICG, and PFC are all FDA-approved materials, which render the nanoparticles highly biocompatible and enhance the potential for clinical translation in the treatment of TNBC patients. [Figure not available: see fulltext.].Copyright © 2021, The Author(s).

20. Record no. 1641 Ferini, G., Valenti, V., Tripoli, A., Illari, S. I., Molino, L., Parisi, S., Cacciola, A., Lillo, S., Giuffrida, D. and Pergolizzi, S. (2021). **Lattice or oxygen-guided radiotherapy: What if they converge? possible future directions in the era of immunotherapy.** Cancers 13(13): 3290 https://doi.org/https://dx.doi.org/10.3390/cancers13133290.

Palliative radiotherapy has a great role in the treatment of large tumor masses. However, treating a bulky disease could be difficult, especially in critical anatomical areas. In daily clinical practice, short course hypofractionated radiotherapy is delivered in order to control the symptomatic disease. Radiation fields generally encompass the entire tumor mass, which is homogeneously irradiated. Recent technological advances enable delivering a higher radiation dose in small areas within a large mass. This goal, previously achieved thanks to the GRID approach, is now achievable using the newest concept of LATTICE radiotherapy (LT-RT). This kind of treatment allows exploiting various radiation effects, such as bystander and abscopal effects. These events may be enhanced by the concomitant use of immunotherapy, with the latter being ever more successfully delivered in cancer patients. Moreover, a critical issue in the treatment of large masses is the inhomogeneous intratumoral distribution of well-oxygenated and hypo-oxygenated areas. It is well known that hypoxic areas are more resistant to the killing effect of radiation, hence the need to target them with higher aggressive doses. This concept introduces the "oxygen-guided radiation therapy" (OGRT), which means looking for suitable hypoxic markers to implement in PET/CT and Magnetic Resonance Imaging. Future treatment strategies are likely to involve combinations of LT-RT, OGRT, and immunotherapy. In this paper, we review the radiobiological rationale behind a potential benefit of LT-RT and OGRT, and we summarize the results reported in the few clinical trials published so far regarding these issues. Lastly, we suggest what future perspectives may emerge by combining immunotherapy with LT-RT/OGRT.Copyright © 2021 by the authors. Licensee MDPI, Basel, Switzerland.

21. Record no. 1659 Gertsenshteyn, I., Giurcanu, M., Vaupel, P. and Halpern, H. (2021). **Biological validation of electron paramagnetic resonance (EPR) image oxygen thresholds in tissue.** Journal of Physiology 599(6): 1759-1767 https://doi.org/https://dx.doi.org/10.1113/JP278816.

Measuring molecular oxygen levels in vivo has been the cornerstone of understanding the effects of hypoxia in normal tissues and malignant tumors. Here we discuss the

advances in a variety of partial pressure of oxygen ((Formula presented.)) measurements and imaging techniques and relevant oxygen thresholds. A focus on electron paramagnetic resonance (EPR) imaging shows the validation of treating hypoxic tumours with a threshold of (Formula presented.) <= 10 Torr, and demonstrates utility for in vivo oxygen imaging, as well as its current and future role in cancer studies. (Figure presented.).Copyright © 2020 The Authors. The Journal of Physiology © 2020 The Physiological Society

22. Record no. 1399 Ghiani, S., Hawala, I., Szikra, D., Trencsenyi, G., Baranyai, Z., Nagy, G., Vagner, A., Stefania, R., Pandey, S. and Maiocchi, A. (2021). **Synthesis, radiolabeling, and pre-clinical evaluation of [44Sc]Sc-AAZTA conjugate PSMA inhibitor, a new tracer for high-efficiency imaging of prostate cancer.** European Journal of Nuclear Medicine and Molecular Imaging 48(8): 2351-2362 https://doi.org/https://dx.doi.org/10.1007/s00259-020-05130-0.

Purpose: The aim of this work was to demonstrate the suitability of AAZTA conjugated to PSMA inhibitor (B28110) labeled with scandium-44 as a new PET tracer for diagnostic imaging of prostate cancer. Background(s): Nowadays, scandium-44 has received significant attention as a potential radionuclide with favorable characteristics for PET applications. A polyaminopolycarboxylate heptadentate ligand based on a 1,4-diazepine scaffold (AAZTA) has been thoroughly studied as chelator for Gd3+ ions for MRI applications. The excellent results of the equilibrium, kinetic, and labeling studies led to a preliminary assessment of the in vitro and in vivo behavior of [44Sc][Sc-(AAZTA)]- and two derivatives, i.e., [44Sc][Sc (CNAAZTA-BSA)] and [44Sc][Sc (CNAAZTA-cRGDfK)]. Result(s): B28110 was synthesized by hybrid approach, combining solid-phase peptide synthesis (SPPS) and solution chemistry to obtain high purity (97%) product with an overall yield of 9%. Subsequently, the radioactive labeling was performed with scandium-44 produced from natural calcium target in cyclotron, in good radiochemical yields (RCY) under mild condition (pH 4, 298 K). Stability study in human plasma showed good RCP% of [44Sc]Sc-B28110 up to 24 h (94.32%). In vivo PET/MRI imaging on LNCaP tumor-bearing mice showed high tracer accumulation in the tumor regions as early as 20 min post-injection. Ex vivo biodistribution studies confirmed that the accumulation of 44Sc-PSMA-617 was two-fold lower than that of the radiolabeled B28110 probes. Conclusion(s): This work demonstrated the suitability of B28110 for the complexation with scandium-44 at room temperature and the high performance of the resulting new tracer based on AAZTA chelator for the diagnosis of prostate cancer using PET.Copyright © 2021, Springer-Verlag GmbH Germany, part of Springer Nature.

23. Record no. 1585 Gronman, M., Tarkia, M., Stark, C., Vahasilta, T., Kiviniemi, T., Lubberink, M., Halonen, P., Kuivanen, A., Saunavaara, V., Tolvanen, T., Teuho, J., Teras, M., Savunen, T., Pietila, M., Yla-Herttuala, S., Roivainen, A., Knuuti, J. and Saraste, A. (2021). **Assessment of myocardial viability with [15O]water PET: A validation study in experimental myocardial infarction.** Journal of Nuclear Cardiology 28(4): 1271-1280 https://doi.org/https://dx.doi.org/10.1007/s12350-019-01818-5.

Background: Assessment of myocardial viability is often needed in patients with chest pain and reduced ejection fraction. We evaluated the performance of reduced resting MBF, perfusable tissue fraction (PTF), and perfusable tissue index (PTI) in the

assessment of myocardial viability in a pig model of myocardial infarction (MI). Methods and Results: Pigs underwent resting [15O]water PET perfusion study 12 weeks after surgical (n = 16) or 2 weeks after catheter-based (n = 4) occlusion of the proximal left anterior descending coronary artery. MBF, PTF, and PTI were compared with volume fraction of MI in matched segments as assessed by triphenyl tetrazolium chloride staining of LV slices. MBF and PTF were lower in infarcted than non-infarcted segments. Segmental analysis of MBF showed similar area under the curve (AUC) of 0.85, 0.86, and 0.90 with relative MBF, PTF, and PTI for the detection of viable myocardium defined as infarct volume fraction of < 75%. Cut-off values of relative MBF of >= 67% and PTF of >= 66% resulted in accuracies of 90% and 81%, respectively. Conclusion(s): Our results indicate that resting MBF, PTF, and PTI based on [15O]water PET perfusion imaging are useful for the assessment of myocardial viability.Copyright © 2019, The Author(s).

24. Record no. 1868 Haberska, L., Paisey, S., Watkins, A. and Marshall, C. (2021). **Optimisation of Cyclotron Production of [13N] Ammonia.** Nuclear Medicine Communications 42(10): 1170 https://doi.org/https://dx.doi.org/10.1097/MNM.0000000000001479.

Purpose: Cardiff University PET Imaging Centre (PETIC) introduced routine [13N]Ammonia production for pre-clinical research in 2018. However, the process proved problematic due to low yields, radioactive gas releases and repeated target rinses to unload the product. The aim of this project was to optimise the IBA Cyclone 18/9 cyclotron production of [13N]Ammonia to minimise the release of radioactive gases and maximise the final yield of [13N]Ammonia in order to facilitate pre-clinical research at PETIC. Method(s): [13N]Ammonia is produced by proton irradiation of a natural water target by the 16O(p, alpha)13N nuclear reaction. In order to improve production yields, modification of several cyclotron operating parameters was investigated: target current (10- 38 microA), volume of target solution (1.2- 1.8 ml) and helium transfer pressure (1 - 5 mbar) were optimised. Result(s): In result of this project, optimal production parameters have been established: target current of 15-20 microA, target volume of 1.6 ml, and helium transfer pressure of 2.5 mbar. The final product yield has increased from 1 GBq to 6 GBq and gaseous stack emissions have been reduced to less than 50 MBq. In addition, it is no longer necessary to undertake a target rinse post-production to deliver the final product to the hot cells. Conclusion(s): The implementation of the optimised parameters has increased the final product yield, reduced gaseous emissions and removed the requirement for multiple target rinses.

25. Record no. 1584 Kamani, C. H. and Prior, J. O. (2021). **Assessment of myocardial viability using a [15O]-water perfusion PET: Towards a one-stop shop?** Journal of Nuclear Cardiology 28(4): 1281-1283 https://doi.org/https://dx.doi.org/10.1007/s12350-019-01838-1.

26. Record no. 1883 Liu, Z., Thorn, S., Wu, J., Guo, X., De Rubio Cruz, P. G., Carson, R., Sinusas, A. and Liu, C. (2021). **Assessment of lower extremities flow using dynamic Rb-82 PET: Acquisition protocols and quantification methods.** Journal of Nuclear Medicine 62(SUPPL 1).

Background: Quantitative assessment of lower extremity skeletal muscle flow is critical for managing patients withdiabetes and peripheral arterial disease (PAD). However,

reliable quantitative methods are not well established. Inthis study, we aim to investigate and optimize data acquisition protocols and quantitative data processing methods for dynamic Rb-82 PET imaging in an established porcine model of PAD through tracer kinetic modeling. Method(s): Dynamic Rb-82 PET imaging was performed in five pigs following acute unilateral femoral arteryocclusion using a 4-ring Siemens Biograph mCT scanner with continuous bed motion (CBM) and Jubilant Rb-82generator, with additional pig and human studies ongoing. Rb-82 (518+/-37 MBq) was delivered using a constantactivity delivery protocol over 45 seconds per injection. In each study, multiple sequential dynamic PET scans wereacquired using several acquisition protocols that employed both a single bed position and/or CBM. With ongoinganalysis for all protocols, we focus on reporting 3 protocols: 1) 7-min single bed position dynamic scan of the heart to derive input function from left ventricle (LV) blood pool (35 frames, 5s/frame for the first 90s, then 30s/frame); 2)7-min single bed position dynamic scan of the legs (the same as above); and 3) 1.5-min single position scan(5s/frame x 24 frames) of the lower abdominal aorta (AA) followed by 5.5-min CBM scans (30s/frame x11 frames)between AA and the legs, with input function derived from AA. Protocols 1 and 2 were performed under stableresting conditions, while acquisition protocol 3 was performed both at rest and during adenosine-inducedvasodilation. Arterial blood activity was continuously sampled using an automated blood counter, and these data were used as the gold standard input function for each scan. A one-tissue compartmental model with blood volumeterm was used to quantify K . Image derived arterial input functions from LV and AA were compared with thoseobtained through the continuous input function using IDL 8.0 and MatLAB 2020b. Result(s): High quality voxel-by-voxel parametric K images of the legs were generated. K values for skeletal musclederived from Protocol 2 data using LV input function from Protocol 1 and 2 scans across the five pigs are0.070+/-0.041 mL/min/cm and 0.030+/-0.012 mL/min/cm for the sample ROIs in the non-ischemic legs and ischemiclegs, respectively ($p<0.05$). The image-derived input functions (IDIF) from LV are consistent with those of arterialblood samples. The peak input function derived from AA was consistently 60.0+/-0.3 % of the LV for all pigs, withlower terminal activity from AA, likely due to partial volume effect. The AA input functions from stress scans havesimilar peaks compared to those of the rest scans, but with slightly higher residual terminal activity. Furtherinvestigation is ongoing to quantify K based on data acquired on other acquisition protocols. Conclusion(s): It is feasible to quantify skeletal muscle blood flow in the lower extremities using dynamic Rb-82 PET.Optimal data acquisition protocols that take advantage of CBM, constant activity infusion, and an image derivedinput function, and tracer kinetic modeling methods need to be established to ensure accurate and reproduciblequantification of lower extremities flows in setting of PAD.

27. Record no. 1894 Narciso, L., Ssali, T., Liu, L., Biernask, H., Butlen, J., Morrison, L., Hadway, J., Corsaut, J., Hicks, J., Langham, M., Wehrlis, F., Iida, H. and St Lawrence, K. (2021). **A non-invasive hybrid PET/MR method for imaging thecerebral metabolic rate of oxygen.** Journal of Nuclear Medicine 62(SUPPL 1).

Introduction: Positron emission tomography (PET) is the gold standard for imaging the cerebral metabolic rate ofoxygen (CMRO); however, the technique is invasive as it requires arterial sampling and complex due to the need tocorrect for recirculating

[15O]H2O and blood-borne activity [1]. We propose a non-invasive hybrid PET/ magneticresonance imaging (MRI) method (PMROx) that uses MRI measurements of whole-brain (WB) CMRO to calibrate[15O]O2-PET. With PMROx, cerebral blood flow (CBF) images are obtained with a similar non-invasive PET/MRIapproach combining [15O]H2O PET with phase-contrast MRI [2]. Alternatively, PET imaging can be reduced to just[15O]O2inhalation by incorporating the MRI-based perfusion method, arterial spin labeling (PMROx) [3]. Here wepresent a comparison between PMROx and PMROx in animal experiments that also incorporated an establishedPET-alone method for validation [4]. The sensitivity of PMROx to altered metabolism was investigated byincreasing the anesthetics. Method(s): [15O]H2O and [15O]O2PET data were acquired in a hybrid PET/MR scanner (3 T Siemens BiographmMR), together with simultaneous MRI oximetry (OxFlow [5]) and perfusion (ASL), from juvenile pigs (n = 8).Animals were anesthetized with 3% isoflurane and 6 mL/kg/h propofol. Arterial sampling was performed for PET-alone measurements. Cerebral metabolism was reduced by increasing the propofol infusion to 20 mL/kg/h. Result(s): Significant correlations were found between regional CMRO measurements from PET and each of thePMROx methods (i.e. using either [15O]water or ASL to image CBF) with no significant differences between averageCMRO from the three techniques: 1.89 +/- 0.16 (PMROx), 1.88 +/- 0.24 (PMROx) and 1.81 +/- 0.10 mLO /100g/min(PET). Moreover, PMROx and PMROx were sensitive to propofol-induced reduction in CMRO (Fig. 1). Conclusion(s): This study provides an initial validation of a non-invasive PET/MRI technique that circumvents manyof the complexities of PET-only CMRO imaging. PMROx not only avoids arterial sampling, but can reduce the PETimaging procedure to [15O]O2by incorporating ASL-CBF images. Future studies in humans are required to validatethis approach.

28. Record no. 526 Narciso, L., Ssali, T., Liu, L., Biernaski, H., Butler, J., Morrison, L., Hadway, J., Corsaut, J., Hicks, J. W., Langham, M. C., Wehrli, F. W., Iida, H. and Lawrence, K. S. (2021). **A Noninvasive Method for Quantifying Cerebral Metabolic Rate of Oxygen by Hybrid PET/MRI: Validation in a Porcine Model.** Journal of Nuclear Medicine 62(12): 1789-1796 https://doi.org/https://dx.doi.org/10.2967/JNUMED.120.260521.

The gold standard for imaging the cerebral metabolic rate of oxygen (CMRO2) is PET; however, it is an invasive and complex procedure that also requires correction for recirculating 15O-H2O and the blood-borne activity. We propose a noninvasive reference-based hybrid PET/MRI method that uses functional MRI techniques to calibrate 15O-O2 PET data. Here, PET/MRI of oxidative metabolism (PMROx) was validated in an animal model by comparison to PET-alone measurements. Additionally, we investigated if the MRI perfusion technique arterial spin labeling (ASL) could be used to further simplify PMROx by replacing 15O-H2O PET, and if the PMROx was sensitive to anesthetic-induced changes in metabolism. Method(s): 15O-H2O and 15O-O2 PET data were acquired using a hybrid PET/MR scanner, together with simultaneous functional MRI (OxFlow and ASL), from juvenile pigs (n 5 9). Animals were anesthetized with 3% isoflurane and 6 mL/kg/h propofol for the validation experiments, and arterial sampling was performed for PET-alone measurements. PMROx estimates were obtained using whole-brain (WB) CMRO2 from OxFlow and local cerebral blood flow (CBF) from either noninvasive 15O-H2O PET or ASL (PMROxASL). Changes in metabolism were investigated by increasing the propofol infusion to 20 mL/kg/h.

Result(s): Good agreement and correlation were observed between regional CMRO2 measurements from PMROx and PET alone. No significant differences were found between OxFlow and PET-only measurements of WB oxygen extraction fraction (0.30 6 0.09 and 0.31 6 0.09) and CBF (54.1 6 16.7 and 56.6 6 21.0 mL/100 g/min), or between PMROx and PET-only CMRO2 estimates (1.89 6 0.16 and 1.81 6 0.10 mLO2/100 g/min). Moreover, PMROx and PMROxASL were sensitive to propofol-induced reduction in CMRO2. Conclusion(s): This study provides initial validation of a noninvasive PET/MRI technique that circumvents many of the complexities of PET CMRO2 imaging. PMROx does not require arterial sampling and has the potential to reduce PET imaging to 15O-O2 only; however, future validation involving human participants are required.Copyright © 2021 by the Society of Nuclear Medicine and Molecular Imaging.

29. Record no. 1793 Narciso, L., Ssali, T., Liu, L., Biernaski, H., Butler, J., Morrison, L., Hadway, J., Hicks, J. W., Langham, M. C., Wehrli, F. W., Iida, H. and St Lawrence, K. (2021). **Validation of a non-invasive hybrid PET/MRI method for imaging the cerebral metabolic rate of oxygen (#209).** Journal of Cerebral Blood Flow and Metabolism 41(1 Supplement): 249-250 https://doi.org/https://dx.doi.org/10.1177/0271678X211061050.

Introduction: PET is the gold standard for imaging the cerebral metabolic rate of oxygen (CMRO2) in humans; however, the procedure requires multiple 15O-tracers and arterial blood sampling. Hybrid PET/MR offers a means of simplifying the procedure by using MRI-based measurements of whole-brain (WB) CMRO2 as a reference to calibrate dynamic 15O-oxygen-PET data.1 This hybrid approach eliminates the need for invasive arterial sampling, only requires PET images of 15O-oxygen, and reduces the total duration to 5 min. It is also predicted to be insensitive to errors related to blood-borne activity and recirculating water because they do not affect MRI CMRO2 measurements.2 In this study, we present initial validation of the approach conducted in a large animal model that enabled arterial sampling for measurement of CMRO2 by a previously validated PET method. Method(s): PET and MRI data were obtained from juvenile pigs (n=9, 18.9+/-2.1 kg) under two metabolic conditions on a 3T Siemens Biograph mMR system. MR imaging included arterial spin labelling (ASL) and Oxflow to measure regional cerebral blood flow (CBF) and WB CMRO2, respectively.3 Concurrent PET imaging involved 5-min list-mode acquisitions after injecting 500 MBq of 15O-water, followed by inhaling 2200 MBq of 15O-oxygen. Arterial sampling was obtained using an MR-compatible system (Swisstrace). CT images were acquired post-mortem for attenuation correction. Dynamic PET images were reconstructed into 48 time-frames (30x3s, 6x5s, 6x10s and 6x20s). CMRO2 images were generated from the PET data alone4 and by the hybrid PET/MR procedure. Result(s): Results from the hybrid PET/MR approach (n=6, Figure 1) presented mean CMRO2 within the expected range, for both baseline (1.88+/-0.24mL/100 g/min) and lower metabolic conditions (1.20+/-0.33mL/100 g/min; 36% reduction, p<0.01). Conclusion(s): Initial WB CMRO2 results obtained with the hybrid PET/MR approach were within the expected range, further reinforcing our previous assessments.1 These results suggest that quantitative measurements of CMRO2 can be obtained without the need for arterial blood sampling. The complete analysis of our experiments can be found in Narciso et al.2.

30. Record no. 1809 Phipps, M., Cingoranelli, S., Ferdous, J., Bhupathiraju, N. V. S. D., Lapi,

S., Lewis, J., Francesconi, L. and Deri, M. (2021). **Evaluation of [47Sc]Sc-HOPO toward radioscandium based radiopharmaceuticals.** Nuclear Medicine and Biology 96-97(Supplement): S91-S92 https://doi.org/https://dx.doi.org/10.1016/S0969-8051%2821%2900416-9.

Objectives: Scandium-44 (44Sc) (t1/2 = 4 h, E x = 1.47 MeV, BR^ = 94.3%) and 47Sc (t1/2 = 3.3 d, E x = 0.6 MeV, BR = 100%) are a potential matched pair of radionuclides for developing theranostic agents for positron emission tomography (PET) imaging and targeted radio-immunotherapy. 47Sc has a gamma emission (Ey = 159 keV) suitable for use in single photon emission computed tomography (SPECT) imaging. DOTA is a standard chelator for many radiometals and has been radiolabeled with 44Sc [1]. However, DOTA may not be the optimal chelator for radioscandium, so there is interest in developing better Sc chelators [2]. 3,4,3-LI(1,2-HOPO) (referred to as HOPO) can form octadentate constructs through its oxygen donors and demonstrates high affinity and fast kinetics with hard positive ions at the macroscopic and tracer scales [3-5]. (Figure Presented) Methods: Before radioactive work, stable 45Sc-HOPO was characterized by methods including IR, 1H-NMR, 45Sc-NMR, HPLC, mass spectrometry, and crystallography. 47Sc was produced via cyclotron at the University of Alabama at Birmingham. Radiochemically pure 47Sc was produced from an enriched 50TiO2 target by the 50Ti(p,a)47Sc reaction and separated adapting methods from Loveless et al. [6]. Targets were irradiated at 24 MeV on the UAB TR24 cyclotron. 47Sc was extracted using BDGA resin, isolated in 0.1 M HCl, and shipped to Memorial Sloan Kettering Cancer Center. The radiolabeling of HOPO and DOTA with 47Sc at 37degreeC was optimized and compared. Stability studies, including EDTA challenge at various pH values (5, 6, 7, 8), metal ion challenge (with Fe3+, Mg2+, Cu2+, Zn2+), and human serum stability were evaluated for 47Sc-DOTA and 47Sc-HOPO. Radiolabeling and stability studies were monitored by ITLC using 50 mM EDTA at pH 5. Biodistribution and SPECT imaging with free 47Sc and 47Sc constructs in healthy mice are underway. Result(s): Radiolabeling optimization resulted in 90% and >99% RCY at 37degreeC for 47Sc-DOTA and 47Sc-HOPO respectively. Formation of (Figure Presented) 47Sc-HOPO was verified by HPLC coinjection with a nonradioactive, well-characterized 45Sc-HOPO standard. 47Sc-DOTA and 47Sc-HOPO had comparable performance in stability studies. Conclusion(s): 47Sc-HOPO has been synthesized and has demonstrated high stability under various conditions. Its in vivo behavior is being investigated as well. This work will be followed by the evaluation of the bifunctional analogue p-SCN-Bn-HOPO as well as HOPO-antibody conjugates formed with the bifunctional ligand. In addition, analogous HOPO chelators such as 3,3,3-LI(1,2-HOPO) will be investigated.Copyright 2021 Elsevier Inc. All rights reserved.

31. Record no. 1804 Wyatt, N., Hogan, L., Pellegrini, P., Roberts, M., Hall, A., Smith, N., Hemzal, E., Hill, L., Howell, N., Middleton, R., Safavi-Naeini, M., Rendina, L. and Fraser, B. (2021). **Scandium-47 and lutetium-177 radiolabelling and stability studies of 1st and 2nd generation DOTA-triphenylphosphonium ligands - potential radionuclide theranostics for treatment of glioblastoma multi-forme.** Nuclear Medicine and Biology 96-97(Supplement): S93-S94 https://doi.org/https://dx.doi.org/10.1016/S0969-8051%2821%2900420-0.

Scandium-47 has emerged as a promising radioisotope for targeted radionuclide tumor therapy [1]. This is due, to a significant extent, from the combination of low energy /

short range p- emission, the availability of a "perfect theranostic pair" with Sc-44 for companion PET imaging, the potential to form highly stable radiometal complexes, and the availability of suitable y emissions for companion SPECT imaging [1,2]. Sc-47 also has a shorter half-life (3.35 d) than the chemically similar Lu-177 (6.7 d) which is significant given recent in vitro research that suggests longer lived isotopes require more intial radioactivity to have the same effect upon cell viability [3]. The shorter half-life of Sc-47 also suggests it may be more suitable for smaller biolgical vectors (with shorter biolgical half-lives) such as small molecules and low MW peptides. One area of clinical treatment where Sc-47 can have impact and where improvments in patient outcomes and survival rates remain stubbornly low is glioblastoma multiforme (GBM) [2]. GBM is the most common and aggressive form of malignant brain tumor and represents around 60% of all adult brain tumors with a global incidence of <10 per 100,000 persons [2,4]. The prognosis for GBM patients is poor with a -ear survival rate of 37%, 5 year rate of 5% and a median survival (Figure Presented) time of 10 months [5]. The current standard of treatment is resection of the tumor followed by radiation therapy and chemotherapy [6,7]. Given this poor prognosis there is a clear and unmet need for improved classes of treatment. Although significant progress has been made towards bringing GBM targeted radionuclide therapies to the clinic [8], the efforts to date have not included utilizing Sc-44/ Sc-47. Given this we are developing and evaluating Sc-44/Sc-47 and Lu-177/Ga-68 radiolabelled triphenylphosphonium (TPP) functional-ised DOTA ligands (1st and 2nd generation) as potential theranostics for GBM. Described herein is our work on comparing the radiolabel-ling efficiency (Sc-47 vs. Lu-177) and stability studies (PBS pH 7.4, rat plasma) for our 1st and 2nd generation DOTA-TPP ligands [9]. The presence of an additional carbonyl group in the 2nd generation DOTA-TPP ligand was anticipated to increase the number of donor atoms around the radiometal and affect radiolabelling reaction conditions and, more importantly, increase radiometal complex stabilityCopyright 2021 Elsevier Inc. All rights reserved.

32. Record no. 1472 Zhou, M., Liu, Y., Su, Y. and Su, Q. (2021). **Plasmonic Oxygen Defects in MO3- x (M = W or Mo) Nanomaterials: Synthesis, Modifications, and Biomedical Applications.** Advanced Healthcare Materials 10(23): 2101331 https://doi.org/https://dx.doi.org/10.1002/adhm.202101331.

Nanomedicine is a promising technology with many advantages and provides exciting opportunities for cancer diagnosis and therapy. During recent years, the newly developed oxygen-deficiency transition metal oxides MO3- x (M = W or Mo) have received significant attention due to the unique optical properties, such as strong localized surface plasmon resonance (LSPR), tunable and broad near-IR absorption, high photothermal conversion efficiency, and large X-ray attenuation coefficient. This review presents an overview of recent advances in the development of MO3- x nanomaterials for biomedical applications. First, the fundamentals of the LSPR effect are introduced. Then, the preparation and modification methods of MO3- x nanomaterials are summarized. In addition, the biological effects of MO3- x nanomaterials are highlighted and their applications in the biomedical field are outlined. This includes imaging modalities, cancer treatment, and antibacterial capability. Finally, the prospects and challenges of MO3- x and MO3- x-based nanomaterial for fundamental studies and clinical applications are also discussed.Copyright © 2021

Wiley-VCH GmbH

33. Record no. 2348 Almeida, A. G. (2020). **Myocardial oxygenation assessment at myocardial blood oxygen level-dependent MRI: A fresh look at an old promise.** Radiology 295(1): 94-95 https://doi.org/https://dx.doi.org/10.1148/radiol.2020200163.

34. Record no. 299 Guehl, N. J., Pelletier-Galarneau, M., Wooten, D. W., Guerrero, J. L., Kas, A., Normandin, M. D., Fakhri, G. E. and Alpert, N. M. (2020). **Preclinical Validation of a Single-Scan Rest/ Stress Imaging Technique for 13N-Ammonia Positron Emission Tomography Cardiac Perfusion Studies.** Circulation: Cardiovascular Imaging 13(1): E009407 https://doi.org/https://dx.doi.org/10.1161/CIRCIMAGING.119.009407.

BACKGROUND: We previously proposed a technique for quantitative measurement of rest and stress absolute myocardial blood flow (MBF) using a 2-injection single-scan imaging session. Recently, we validated the method in a pig model for the long-lived radiotracer 18F-Flurpiridaz with adenosine as a pharmacological stressor. The aim of the present work is to validate our technique for 13NH3. METHOD(S): Nine studies were performed in 6 pigs; 5 studies were done in the native state and 4 after infarction of the left anterior descending artery. Each study consisted of 3 dynamic scans: a 2-injection rest-rest single-scan acquisition (scan A), a 2-injection rest/stress single-scan acquisition (scan B), and a conventional 1-injection stress acquisition (scan C). Variable doses of adenosine combined with dobutamine were administered to induce a wide range of MBF. The 2-injection single-scan measurements were fitted with our nonstationary kinetic model (MGH2). In 4 studies, 13NH3 injections were paired with microsphere injections. MBF estimates obtained with our method were compared with those obtained with the standard method and with microspheres. We used a modelbased method to generate separate rest and stress perfusion images. RESULT(S): In the absence of stress (scan A), the MBF values estimated by MGH2 were nearly the same for the 2-radiotracer injections (mean difference: 0.067+/-0.070 mL.min-1.cc-1, limits of agreement: [-0.070 to 0.204] mL.min-1.cc-1), showing good repeatability. Bland-Altman analyses demonstrated very good agreement with the conventional method for.Copyright © 2020 Lippincott Williams and Wilkins. All rights reserved.

35. Record no. 2467 Hashem, M., Zhang, Q., Wu, Y., Johnson, T. W. and Dunn, J. F. (2020). **Using a multimodal near-infrared spectroscopy and MRI to quantify gray matter metabolic rate for oxygen: A hypothermia validation study.** NeuroImage 206: 116315 https://doi.org/https://dx.doi.org/10.1016/j.neuroimage.2019.116315.

Non-invasive quantitative imaging of cerebral oxygen metabolism (CMRO2) in small animal models is crucial to understand the role of oxidative metabolism in healthy and diseased brains. In this study, we developed a multimodal method combining near-infrared spectroscopy (NIRS) and MRI to non-invasively study oxygen delivery and consumption in the cortex of mouse and rat models. The term CASNIRS is proposed to the technique that measures CMRO2 with ASL and NIRS. To determine the reliability of this method, CMRO2 values were compared with reported values measured with other techniques. Also, the sensitivity of the CASNIRS technique to detect changes in CMRO2 in the cortex of the animals was assessed by applying a reduction in core

temperature, which is known to reduce CMRO2. Cerebral blood flow (CBF) and CMRO2 were measured in five mice and five rats at a core temperature of 37 degreeC followed by another measurement at 33 degreeC. CMRO2 was 7.8 +/- 1.8 and 3.7 +/- 0.9 (ml/100 g/min, mean +/- SD) in mice and rats respectively. These values are in good agreement with reported values measured by 15O PET, 17O NMR, and BOLD fMRI. In hypothermia, we detected a significant decrease of 37% and 32% in CMRO2 in the cortex of mice and rats, respectively. Q10 was calculated to be 3.2 in mice and 2.7 in rats. In this study we showed that it is possible to assess absolute values of metabolic correlates such as CMRO2, CBF and oxygen extraction fraction (OEF) noninvasively in living brain of mice and rats by combining NIRS with MRI. This will open new possibilities for studying brain metabolism in patients as well as the many mouse/rat models of brain disorders.Copyright © 2019 The Authors

36. Record no. 519 Toramatsu, C., Mohammadi, A., Wakizaka, H., Seki, C., Nishikido, F., Sato, S., Kanno, I., Takahashi, M., Karasawa, K., Hirano, Y. and Yamaya, T. (2020). **Biological washout modelling for in-beam PET: rabbit brain irradiation by 11C and 15O ion beams.** Physics in medicine and biology 65(10): 105011 https://doi.org/https://dx.doi.org/10.1088/1361-6560/ab8532.

Positron emission tomography (PET) has been used for dose verification in charged particle therapy. The causes of washout of positron emitters by physiological functions should be clarified for accurate dose verification. In this study, we visualized the distribution of irradiated radioactive beams, 11C and 15O beams, in the rabbit whole-body using our original depth-of-interaction (DOI)-PET prototype to add basic data for biological washout effect correction. Time activity curves of the irradiated field and organs were measured immediately after the irradiations. All data were corrected for physical decay before further analysis. We also collected expired gas of the rabbit during beam irradiation and the energy spectrum was measured with a germanium detector. Irradiated radioactive beams into the brain were distributed to the whole body due to the biological washout process, and the implanted 11C and 15O ions were concentrated in the regions which had high blood volume. The 11C-labelled 11CO2 was detected in expired gas under the 11C beam irradiation, while no significant signal was detected under the 15O beam irradiation as a form of C15O2. Results suggested that the implanted 11C ions form molecules that diffuse out to the whole body by undergoing perfusion, then, they are incorporated into the blood-gas exchange in the respiratory system. This study provides basic data for modelling of the biological washout effect.

37. Record no. 2512 Toyohara, J., Kakiuchi, T., Ohba, H., Kanazawa, M., Tago, T., Sakata, M. and Harada, N. (2020). **Head to head comparison of [15O]H2O and [11C]MMP in non-human primates; tracers for measuring regional cerebral blood flow.** European Journal of Nuclear Medicine and Molecular Imaging 47(SUPPL 1): S667-S668 https://doi.org/https://dx.doi.org/10.1007/s00259-020-04988-4.

Aim/Introduction: Increases in fasting plasma glucose (PG) levels lead to a decrease in [18F]FDG uptake, especially in the precuneus, resulting in an Alzheimer's disease (AD)-like pattern. Therefore, patients with higher PG levels, such as those with diabetes, can be erroneously diagnosed with AD when PET imaging is done using [18F]FDG, due to

reduced uptake of [18F]FDG in the precuneus. To help avoid an erroneous diagnosis of AD due to differences in glucose metabolism, evaluating cerebral blood flow (CBF) in the brain is useful. However, current techniques such as SPECT and 15O-water PET have limitations in early diagnosis of AD because the images of they produce are of low resolution. Recently, we developed N-isopropyl-p-[11C] methylamphetamine ([11C]MMP) as a carbon-11-labeled alternative of the standard CBF SPECT tracer N-isopropyl-p-[123I]iodoamphetamine. In this study, we evaluated the brain kinetics of [11C]MMP in the non-human primate. Head-tohead comparison with [15O]H2O was also evaluated. Material(s) and Method(s): Two successive PET measurements with [15O] H2O and [11C]MMP under vehicle and acetazolamide (AZM: 10 mg/kg or 20 mg/kg) loading conditions were performed in 3 conscious state male monkeys (Macaca mulatta) with arterial blood sampling. Metabolite-corrected plasma and whole-blood time-activity curves were used as an input function for pharmacokinetic modeling of [11C]MMP. The preferred model was chosen according to the Akaike Information Criterion (AIC) and were used to calculate the influx constant (K1). Moreover, standardized uptake values (SUV) were estimated using different time intervals. Result(s): The preliminary kinetic analysis of the comparison of AIC (paired t test, $P < 0.05$) in all regions investigated showed that 1-tisue-compartment model provided significantly better AIC scores than the 2-tissue-compartment model ($n = 3$). The regional K1 values of [11C]MMP in vehicle treated monkey were well correlated with that in rCBF (Pearson $r = 0.9230$, $p < 0.0001$). Furthermore, short duration scan (0-10 min) of SUV showed good correlation with rCBF ($r = 0.9042$, $p < 0.0001$), too. The data suggest that [11C]MMP probably detect changes of rCBF in the low to normal range of flows. However, this correlation was decreased at higher flow range under AZM-loading (10 mg/kg: $r = 0.6581$, $p = 0.0041$; 20 mg/kg: $r = 0.7510$, $p = 0.0005$), due to the underestimation of rCBF at higher flows. Conclusion(s): The K1 and early phase SUV (0-10 min) of [11C]MMP well reflect rCBF in vehicle treated non-human primate, but that in higher flow region after AZM-loading did not.

38. Record no. 2067 van der Meulen, N. P., Hasler, R., Talip, Z., Grundler, P. V., Favaretto, C., Umbricht, C. A., Muller, C., Dellepiane, G., Carzaniga, T. S. and Braccini, S. (2020). **Developments toward the Implementation of 44Sc Production at a Medical Cyclotron.** Molecules (Basel, Switzerland) 25(20) https://doi.org/https://dx.doi.org/10.3390/molecules25204706.

44Sc has favorable properties for cancer diagnosis using Positron Emission Tomography (PET) making it a promising candidate for application in nuclear medicine. The implementation of its production with existing compact medical cyclotrons would mean the next essential milestone in the development of this radionuclide. While the production and application of 44Sc has been comprehensively investigated, the development of specific targetry and irradiation methods is of paramount importance. As a result, the target was optimized for the 44Ca(p,n)44Sc nuclear reaction using CaO instead of CaCO3, ensuring decrease in target radioactive degassing during irradiation and increased radionuclidic yield. Irradiations were performed at the research cyclotron at the Paul Scherrer Institute (~11 MeV, 50 microA, 90 min) and the medical cyclotron at the University of Bern (~13 MeV, 10 microA, 240 min), with yields varying from 200 MBq to 16 GBq. The development of targetry, chemical separation as well as the practical issues and implications of irradiations, are analyzed and discussed. As a proof-

of-concept study, the 44Sc produced at the medical cyclotron was used for a preclinical study using a previously developed albumin-binding prostate-specific membrane antigen (PSMA) ligand. This work demonstrates the feasibility to produce 44Sc with high yields and radionuclidic purity using a medical cyclotron, equipped with a commercial solid target station.

39. Record no. 2265 Wang, J., Mpharm, S. L., Liu, T. W., Zhang, J. M., Chen, Y., Li, J. M. and Xu, W. G. (2020). **Preliminary and Comparative Experiment Study Between 18F-Flurpiridaz and 13N-NH3.H2O Myocardial Perfusion Imaging With PET/CT in Miniature Pigs.** Molecular Imaging 19 https://doi.org/https://dx.doi.org/10.1177/1536012120947506.

Objectves: To comparatively explore the differences between 18F-Flurpiridaz and 13N-NH3.H2O PET/CT myocardial perfusion imaging in miniature pigs. Method(s): Ten Bama minipigs were divided into normal group and myocardial infarction group. The changes of the ratio of left ventricular myocardium to main organs with time were calculated and the best imaging time was confirmed for 18F-Flurpiridaz imaging in normal group. The image quality score, summed rest score(SRS), Extend, total perfusion deficit(TPD) and left ventricle ejection fraction(LVEF) were respectively compared for 18F-Flurpiridaz and 13N-NH3.H2O in infarction group. Result(s): 18F-Flurpiridaz was rapid distributed in myocardium, and the background counts of cardiac cavity were very low, and no obvious interference extracardiac radioactivity was observed. The radioactive ratio of the left ventricular myocardium to cardiac blood pool and adjacent liver were high. Compared with 13N-NH3.H2O, there were no significant differences in functional parameters, including SRS, Extend, TPD and LVEF. Conclusion(s): The results preliminaryly show that 18F-Flurpiridaz is a promising positron MPI agent with good image quality, ability of accurately evaluating cardiac function, and also convenience for application.Copyright © The Author(s) 2020.

40. Record no. 2016 Yamamoto, K., Brender, J. R., Seki, T., Kishimoto, S., Oshima, N., Choudhuri, R., Adler, S. S., Jagoda, E. M., Saito, K., Devasahayam, N., Choyke, P. L., Mitchell, J. B. and Krishna, M. C. (2020). **Molecular imaging of the tumor microenvironment reveals the relationship between tumor oxygenation, glucose uptake, and glycolysis in pancreatic ductal adenocarcinoma.** Cancer Research 80(11): 2087-2093 https://doi.org/https://dx.doi.org/10.1158/0008-5472.CAN-19-0928.

Molecular imaging approaches for metabolic and physiologic imaging of tumors have become important for treatment planning and response monitoring. However, the relationship between the physiologic and metabolic aspects of tumors is not fully understood. Here, we developed new hyperpolarized MRI and electron paramagnetic resonance imaging procedures that allow more direct assessment of tumor glycolysis and oxygenation status quantitatively. We investigated the spatial relationship between hypoxia, glucose uptake, and glycolysis in three human pancreatic ductal adenocarcinoma tumor xenografts with differing physiologic and metabolic characteristics. At the bulk tumor level, there was a strong positive correlation between18F-FDG-PET and lactate production, while pO2 was inversely related to lactate production and18F-2-fluoro-2-deoxy-D-glucose (18F-FDG) uptake. However, metabolism was not uniform throughout the tumors, and the whole tumor results masked different localizations that became apparent while imaging.18F-FDG uptake

negatively correlated with pO2 in the center of the tumor and positively correlated with pO2 on the periphery. In contrast to pO2 and18F-FDG uptake, lactate dehydrogenase activity was distributed relatively evenly throughout the tumor. The heterogeneity revealed by each measure suggests a multimodal molecular imaging approach can improve tumor characterization, potentially leading to better prognostics in cancer treatment.Copyright © 2020 American Association for Cancer Research.

41. Record no. 2000 Yan, R., Li, X., Song, J., Guo, M., Cai, H., Wu, Z., Wu, P., Li, L., Yang, M., Wang, Y. and Li, S. (2020). **Metabolic changes precede radiation-induced cardiac remodeling in beagles: Using noninvasive18f-fdg (18f-fludeoxyglucose) and13n-ammonia positron emission tomography/computed tomography scans.** Journal of the American Heart Association 9(18): e016875 https://doi.org/https://dx.doi.org/10.1161/JAHA.120.016875.

BACKGROUND: This study was performed to characterize the metabolic, functional, and structural cardiac changes in a canine model of radiation-induced heart disease by serial in vivo imaging and ex vivo analyses. METHODS AND RESULTS: Thirty-six dogs were randomly assigned to control or irradiated groups at 3 time points (months 3, 6, and 12 after radiation; each group comprised 6 dogs). The left anterior myocardium of dogs in irradiated groups was irradiated locally with a single dose of 20-Gy X-ray. The irradiated myocardial regions showed increased myocardial uptake of18F-FDG (18F-fludeoxyglucose) in the irradiated beagles, but the increased uptake area decreased at months 6 and 12 compared with month 3 after radiation. Abnormality of myocardial perfusion and cardiac function were detected at month 6 after radiation. Compared with the control groups, the protein expression of GLUT4 (glucose transporter 4) was upregulated in the irradiated groups, correlating with significantly decreased CPT1 (carnitine acyltransferase 1) expression. Mitochondria degeneration, swelling, and count reduction in the irradiated groups were observed. The difference in CD68 of macrophage markers and the inflammatory cytokines (IL-6 [interleukin 6], TNF-alpha [tumor necrosis factor alpha]) between the irradiation and control groups was not significant. Furthermore, the progressive aggravation of apoptosis and fibrosis was displayed. CONCLUSION(S): Elevated18F-FDG uptake occurred after irradiation and subsequently led to ventricular perfusion defects and dysfunction. The process was associated with myocardial metabolic substrate remodeling, cardiac muscle cell apoptosis, and myocardial fibrosis rather than inflammation.Copyright © 2020 The Authors.

42. Record no. 1927 Yokell, D. L., Rice, P. A., Neelamegam, R. and El Fakhri, G. (2020). **Development, validation and regulatory acceptance of improved purification and simplified quality control of [13N] Ammonia.** EJNMMI Radiopharmacy and Chemistry 5(1): 11 https://doi.org/https://dx.doi.org/10.1186/s41181-020-00097-7.

Background: [13N]Ammonia is a cyclotron produced myocardial perfusion imaging agent. With the development of high-yielding [13N]ammonia cyclotron targets using a solution of 5 mM ethanol in water, there was a need to develop and validate an automated purification and formulation system for [13N]ammonia to be in a physiological compatible formulation of 0.9% sodium chloride since there is no widely available commercial system at this time. Due to its short half-life of 10 min, FDA and USP regulations allow [13N]ammonia to be tested in quality control (QC) sub-batches

with limited quality control testing performed on the sub-batches for patient use. The current EP and the original USP method for the determination of the radiochemical purity and identity of [13N]ammonia depended on an HPLC method using a conductivity detector and a solvent free of other salts. This HPLC method created issues in a modern cGMP high volume PET manufacturing facility where the HPLC is used with salt containing mobile phase buffers for quality control analysis of other PET radiopharmaceuticals. Flushing of the HPLC system of residual salt buffers which may interfere with the [13N]ammonia assay can take several hours of instrument time. Since there are no mass limits on [13N]ammonia, a simplified TLC assay to determine radiochemical identity and purity could be developed to simplify and streamline QC. Result(s): We have developed and validated a streamlined automated synthesis for [13N]ammonia which provides the drug product in 8 mL of 0.9% sodium chloride for injection. A novel radio-TLC method was developed and validated to demonstrate feasibility to quantitate [13N]ammonia and separate it from all known radiochemical impurities. Conclusion(s): The process for automated synthesis of [13N]ammonia simplifies and automates the purification and formulation of [13N]ammonia in a cGMP compliant manner needed for high-throughput manufacture of [13N]ammonia. The novel radio-TLC method has simplified [13N]ammonia quality control (QC) and now enables it to be tested using the same QC equipment as [18F]fludeoxyglucose (FDA/USP recognized name for 2-[18F]fluoro-2-deoxy-D-glucose). Both the streamlined automated synthesis of [13N]ammonia and the novel radio-TLC method have been accepted and approved by the US Food and Drug Administration (FDA) for the cGMP manufacture of [13N]ammonia.Copyright © 2020, The Author(s).

43. Record no. 2230 Yu, W., Su, X., Zhang, D., Qiao, F., Wang, H., Jiang, J. and Xu, H. (2020). **Dual-Tracer Assessment of Dynamic Changes in Reoxygenation and Proliferation Decrease During Fractionated Radiotherapy in Murine Tumors.** Frontiers in Oncology 10: 1046 https://doi.org/https://dx.doi.org/10.3389/fonc.2020.01046.

Objective: The present work aimed to assess reoxygenation and tumor inhibition during fractionated radiotherapy (FRT) in murine tumors using 18F-fluoromisonidazole (18F-FMISO) and 18F-fluorothymidine (18F-FLT) based micro positron emission tomography/computed tomography (PET/CT). Material(s) and Method(s): A nude mouse xenograft model was established with the head and neck squamous carcinoma cell (FaDu), followed by administration of FRT. Imaging was carried out with both 18F-FMISO and 18F-FLT PET/CT, prior to FRT (Pre-FRT, 0 Gy), during FRT (Inter-FRT, 21 Gy), and after FRT (Post-FRT, 40 Gy). The maximum standardized uptake (SUVmax) and tumor-to-normal muscle ratio (TNR) were determined in regions of interest (ROIs) in 18F-FMISO and 18F-FLT PET/CT images. Then, hypoxic (HV) and proliferative tumor (PTV) volumes obtained by PET/CT were analyzed. Immunohistochemistry was performed to analyze the changes of hypoxia-inducible factor- (HIF)-1alpha, carbonic anhydrase 9 (CAIX), Ki67 and proliferating cell nuclear antigen (PCNA). Associations of the levels of these biomarkers with PET/CT parameters were analyzed. Result(s): 18F-FMISO PET/CT demonstrated markedly elevated reduction rates of SUVmax (30.3 vs. 14.5%, p = 0.012), TNR (27.9 vs. 18.3%, p = 0.032) and HV (85.0 vs. 71.4%, p = 0.047) from Pre-FRT to Inter-FRT compared with values from Inter-FRT to Post-FRT. Meanwhile, PTV reduction rate in 18F-FLT PET/CT from Pre-FRT to Inter-FRT was significantly decreased compared with that from Inter-FRT to Post-FRT (21.2 vs. 82.7%,

p = 0.012). Tumor HIF-1alpha, CAIX, Ki67, and PCNA amounts were continuously down-regulated during radiotherapy. TNR (FMISO) showed significant correlations with HIF-1alpha (r = 0.692, p = 0.015) and CAIX (r = 0.801, p = 0.006) amounts in xenografts, while associations of SUVmax (FMISO) with hypoxia markers were weak (r = 0.418, p = 0.041 and r = 0.389, p = 0.037, respectively). SUVmax (FLT) was significantly correlated with Ki67 (r = 0.792, p = 0.003) and PCNA (r = 0.837, p = 0.004). Conclusion(s): Tumor reoxygenation occurs early during radiotherapy, while inhibition of cell proliferation by tumoricidal effects mainly takes place gradually with the course of radiotherapy. 18F-FMISO and 18F-FLT PET/CT are sensitive and non-invasive tools for the monitoring of tumor reoxygenation and proliferation during radiotherapy.

Appendix 5: Radiopharmaceutical pipelines for various therapeutic areas

During the meeting held on 16th November 2023, the WHSSC team requested additional analysis regarding specific indications in clinical development. A list of 28 categories was shared with the IO which included, adrenocortical, amyloid, anal, bladder, breast, cardiac conditions, cervical, choline, colorectal, cancer of unknown origin (cuo), endometrial cancer, euronet, gynaecological conditions, head & neck, lung, lymphoma, myeloma, neuroendocrine, oesophageal, other, ovary, pancreas, PSMA, PUO, SABR, sarcoma, thyroid, and vasculitis. An analysis of 17 of these categories was provided by the IO, which is presented below.

Regulatory status
Licensed
Not licensed

Amyloid

Radionuclides	Radiopharmaceuticals	Conditions	Regulatory status	Regulatory authority	Number of clinical trials
F	Florbetaben	Cardiac Amyloidosis	Not licensed	N/A	1
		Cardiac Amyloidosis|AL Amyloidosis|ATTR Amyloidosis	Not licensed	N/A	1
		Cerebral Amyloid Angiopathy Related Inflammation	Licensed	MHRA	1
	Flutemetamol	Amyloid pathology	Licensed	MHRA	1
		Cerebral Amyloidosis	Licensed	MHRA	1
	Florbetapir	Cerebral Amyloid Angiopathy|Intracerebral Hemorrhage	Not licensed	N/A	1
		Cerebral Amyloid Angiopathy|Intracranial Hemorrhages|..	Not licensed	N/A	1
	Flutematamol	Cardiac Amyloid	Not licensed	N/A	1

0 1
Number of clinical trials

Bladder cancer

Radionuclides	Radiopharmaceuticals	Regulatory status	Regulatory authority	Number of clinical trials
F	Fluorodeoxyglucose	Not licensed	N/A	2
	Choline	Not licensed	N/A	1
Ga	NOTA-AE105	Not licensed	N/A	1

0 1 2 3
Number of clinical trials

Cardiovascular conditions

Radionuclides	Radiopharmaceuticals	Regulatory status	Regulatory authority	Number of clinical trials
Cu	Thiosemicarbazone	Not licensed	N/A	1
	Fluorodeoxyglucose	Licensed	MHRA	1
	Dotatate	Licensed	MHRA	1
F	Flurpiridaz	Not licensed	N/A	4
	Sodium fluoride	Not licensed	N/A	3
	Fluorodeoxyglucose	Not licensed	N/A	3
	Florbetaben	Not licensed	N/A	2
	XTR004	Not licensed	N/A	1
	XTR003	Not licensed	N/A	1
	Water	Not licensed	N/A	1
	Triphenylphosphonium	Not licensed	N/A	1
	GP1	Not licensed	N/A	1
	FSPG	Not licensed	N/A	1
	Flutemetamol	Licensed	MHRA	1
	Flutematamol	Not licensed	N/A	1
	Fluorocholine	Not licensed	N/A	1
	FCPHA	Not licensed	N/A	1
	Choline	Not licensed	N/A	1
Ga	Edotreotide	Not licensed	N/A	1
O	Water	Not licensed	N/A	2
Ru	Chloride	Licensed	MHRA	1

0 1 2 3 4 5

Number of clinical trials

Choline

Radionuclides	Radiopharmaceuticals	Therapeutic area	Cancer/Non-cancer	Regulatory status	Regulatory authority	Number of clinical trials
F	Fluorocholine	Blood and bone marrow cancers	Yes	Not licensed	N/A	2
		Breast cancer	Yes	Not licensed	N/A	1
		Cardiovascular conditions	No	Not licensed	N/A	1
		Diabetes, other endocrinal, nutritional, metabolic conditions	No	Not licensed	N/A	5
		Liver cancer	Yes	Not licensed	N/A	2
		Metastases	Yes	Not licensed	N/A	2
		Multiple conditions	Both	Not licensed	N/A	2
		Prostate cancer	Yes	Not licensed	N/A	13
		Thyroid cancer	Yes	Not licensed	N/A	2
	Choline	Bladder cancer	Yes	Not licensed	N/A	1
		Brain cancer	Yes	Not licensed	N/A	1
		Cardiovascular conditions	No	Not licensed	N/A	1
		Diabetes, other endocrinal, nutritional, metabolic conditions	No	Not licensed	N/A	1
		Multiple cancers	Yes	Not licensed	N/A	1
		Prostate cancer	Yes	Not licensed	N/A	5
	Fluoroethylcholine	Prostate cancer	Yes	Not licensed	N/A	4

0 5 10 15

Number of clinical trials

Cervical cancers

Radionuclides	Radiopharmaceuticals	Regulatory status	Regulatory authority	Number of clinical trials
F	Fluorodeoxyglucose	Not licensed	N/A	4
	HX4	Not licensed	N/A	1
	Fluoromisonidazole	Licensed	EMA	1
	Fluoroerytronitroimidazole	Not licensed	N/A	1

0 1 2 3 4 5

Number of clinical trials

Colorectal cancers

Radionuclides	Radiopharmaceuticals	Regulatory status	Regulatory authority	
Cu	ATSM	Not licensed	N/A	1
F	Fluorodeoxyglucose	Licensed	MHRA	1

0 1 2

Number of clinical trials

Endometrial cancer

Radionuclides	Radiopharmaceuticals	Regulatory status	Regulatory authority	
F	Fluorodeoxyglucose	Not licensed	N/A	1
Ga	NOTA-Anti-HER2 VHH1	Not licensed	N/A	1

0 1 2

Number of clinical trials

Gynaecological conditions

Radionuclides	Radiopharmaceuticals	Regulatory status	Regulatory authority	
F	Fluorodeoxyglucose	Not licensed	N/A	2
	Fluorofuranylnorprogeste..	Not licensed	N/A	1
	Fluoroestradiol	Licensed	EMA	1

0 1 2 3

Number of clinical trials

Head and neck cancers

Radionuclides	Radiopharmaceuticals	Regulatory status	Regulatory authority	
F	Fluorodeoxyglucose	Licensed	MHRA	3
	Fluciclatide	Not licensed	N/A	3
	HX4	Not licensed	N/A	2
	ML-10	Not licensed	N/A	1
	Fluorothymidine	Not licensed	N/A	1
	Fluoromisonidazole	Licensed	EMA	1
	EF5	Not licensed	N/A	1
Ga	Dotatate	Licensed	MHRA	1
	Dota-E-(cRGDfK)2	Not licensed	N/A	1
Zr	Panitumumab	Not licensed	N/A	1
	Girentuximab	Not licensed	N/A	1

0 1 2 3 4

Number of clinical trials

Lung cancer and other respiratory conditions

Radionuclides	Radiopharmaceuticals	Cancer/Non-cancer	Regulatory status	Regulatory authority	Number of clinical trials
F	Fluorodeoxyglucose	No	Licensed	MHRA	1
			Not licensed	N/A	4
		Yes	Licensed	MHRA	9
	Fluoromisonidazole	Yes	Licensed	EMA	2
	FSPG	Yes	Licensed	MHRA	1
	Fluorothymidine	Yes	Not licensed	N/A	1
	Fludeoxyglucose	Yes	Licensed	EMA	1
	FAZA	Yes	Not licensed	N/A	1
	Dota-noc	No	Not licensed	N/A	1
	Arabinosyl guanine	Yes	Not licensed	N/A	1
Ga	MAA	Yes	Not licensed	N/A	1
	Gozetotide	Yes	Licensed	MHRA	1
	FAPI-46	Yes	Not licensed	N/A	1
N	Ammonia	No	Not licensed	N/A	1
Zr	Pembrolizumab	Yes	Licensed	MHRA	1
	Durvalumab	Yes	Licensed	MHRA	1

0 2 4 6 8 10
Number of clinical trials

Breast cancer

Radionuclides	Radiopharmaceuticals	Regulatory status	Regulatory authority	Number of clinical trials
Cu	Dota-trastuzumab	Not licensed	N/A	1
F	Fluoroestradiol	Not licensed	N/A	11
	Fluorodeoxyglucose	Licensed	MHRA	8
	Fluorothymidine	Not licensed	N/A	4
	DPA-714	Not licensed	N/A	2
	MFES	Not licensed	N/A	1
	Flutemetamol	Licensed	MHRA	1
	Fluorthanatrace	Not licensed	N/A	1
	Fluorofuranylnorprogeste..	Licensed	MHRA	1
	Fluorocholine	Not licensed	N/A	1
	FDHT	Not licensed	N/A	1
Ga	NeoB	Not licensed	N/A	1
Zr	Trastuzumab	Licensed	MHRA	1
	Girentuximab	Not licensed	N/A	1

0 2 4 6 8 10 12
Number of clinical trials

Oesophageal cancer

Radionuclides	Radiopharmaceuticals	Conditions	Regulatory status	Regulatory authority	Number of clinical trials
F	Fluorodeoxyglucose	Esophageal Cancer|Lung Can..	Licensed	MHRA	1
Ga	ABY-025	Esophageal Neoplasms|Gast..	Not licensed	N/A	1
Zr	Girentuximab	Cervical Cancer|Colorectal C..	Not licensed	N/A	1

0 1 2
Number of clinical trials

Regulatory status
Licensed
Not licensed

Prostate cancer

Radionuclides	Radiopharmaceuticals	Regulatory status	Regulatory authority	Number of clinical trials
Cu	Copper chloride	Licensed	MHRA	3
	SAR-Bombesin	Not licensed	N/A	2
F	Piflufolastat	Licensed	EMA	21
	PSMA-1007	Not licensed	N/A	13
	Fluorocholine	Not licensed	N/A	13
	Fluciclovine	Licensed	MHRA	12
	rhPSMA-7.3	Not licensed	N/A	7
	PSMA	Not licensed	N/A	5
	Choline	Not licensed	N/A	5
	Fluoroethylcholine	Not licensed	N/A	4
	Gozetotide	Not licensed	N/A	3
	Fluoromisonidazole	Not licensed	N/A	2
	CTT1057	Not licensed	N/A	2
	PSMA-617	Not licensed	N/A	1
	JK-PSMA-7	Not licensed	N/A	1
	Fluorochlorine	Not licensed	N/A	1
	Florastamin	Not licensed	N/A	1
Ga	Gozetotide	Licensed	MHRA	19
	HBED-CC PSMA	Not licensed	N/A	10
	RM2	Not licensed	N/A	1
	PSMA-617	Not licensed	N/A	1
	PSMA	Not licensed	N/A	1
	NeoB, PSMA-R2	Not licensed	N/A	1
Zr	DF-IAB2M	Not licensed	N/A	2

Regulatory status: Licensed, Not licensed

0 5 10 15 20 25

Number of clinical trials

Ovarian cancer

Radionuclides	Radiopharmaceuticals	Regulatory status	Regulatory authority	Number of clinical trials
F	Fluoroestradiol	Not licensed	N/A	2
	PEG folate	Not licensed	N/A	1
	Fluorodeoxyglucose	Licensed	MHRA	1
Ga	FAPI-04	Not licensed	N/A	1

Regulatory status: Licensed, Not licensed

0 1 2 3

Number of clinical trials

Pancreatic cancer

Radionuclides	Radiopharmaceuticals	Regulatory status	Regulatory authority	Number of clinical trials
F	Piflufolastat	Not licensed	N/A	1
	Fluorothymidine	Not licensed	N/A	1
Ga	FAPI-46	Not licensed	N/A	2

Regulatory status: Not licensed

0 1 2 3

Number of clinical trials

Thyroid cancer

Radionuclides	Radiopharmaceuticals	Regulatory status	Regulatory authority	Number of clinical trials
F	Gozetotide	Not licensed	N/A	2
	Fluorodopa	Licensed	EMA	1
		Not licensed	N/A	1
	Fluorocholine	Not licensed	N/A	2
	HBED-CC PSMA	Not licensed	N/A	1
	Fluorodeoxyglucose	Licensed	MHRA	1
Ga	Dotatate	Not licensed	N/A	2

Regulatory status: Licensed, Not licensed

Blood and bone marrow cancers

Radionuclides	Radiopharmaceuticals	Regulatory status	Regulatory authority	Number of clinical trials
F	Fluorodeoxyglucose	Licensed	MHRA	5
		Not licensed	N/A	3
	Fluorothymidine	Not licensed	N/A	3
	Sodium fluoride	Not licensed	N/A	2
	Fluorocholine	Not licensed	N/A	2
	FTC 146	Not licensed	N/A	1
Ga	Dota-SSTR	Not licensed	N/A	1
Zr	Rituximab	Not licensed	N/A	1
	Ofatumumab	Not licensed	N/A	1
	Daratumumab	Licensed	MHRA	1
	Atezolizumab	Not licensed	N/A	1

Regulatory status: Licensed, Not licensed

Acknowledgements and Disclaimers

This study/project is funded by the National Institute for Health Research (NIHR) [NIHRIO/project reference HSRIC-2016-10009]. The views expressed are those of the author(s) and not necessarily those of the NIHR or the Department of Health and Social Care.

We would like to thank our project partners at All Wales PET Radiopharmaceutical Workstream who provided invaluable expertise, guidance, and input at various stages of this report